University of Alberta

Leukotrienes in Rat Lung Development

by

Stephen William Alexander Reynolds

A thesis submitted to the Faculty of Graduate Studies and Research
in partial fulfillment of the requirements for the degree of

Master of Science

Department of Physiology

Edmonton, Alberta
Fall 2007

Your file Votre référence
ISBN: 978-0-494-33333-4
Our file Notre référence
ISBN: 978-0-494-33333-4

Abstract

Hyperoxia (>95% oxygen) is a potent inhibitor of lung alveolarization. It replicates features of human newborn chronic lung disease. Previous studies demonstrated a role for leukotrienes (LTs) in this process. The main foci of this study were to elucidate the roles of the LT receptors (BLT_1, BLT_2, $CysLT_1$, and $CysLT_2$) in normal and hyperoxic alveolarization and develop a model for increasing LTs in lung development.

We found that during lung development BLT_1 and $CysLT_2$ mRNA expression increased while BLT_2 decreased and $CysLT_1$ was unchanged. Exposure to hyperoxia during this period resulted in decreased BLT_2 and $CysLT_1$ expression and no change in BLT_1 and $CysLT_2$. There were significant differences between mRNA and protein expression.

The development of a model increasing LT synthesis specifically during alveolarization demonstrated mixed results. Although the virus was successfully delivered to the lung of neonatal rat pups, it failed to significantly alter lung maturation.

Acknowledgements

I would like to thank my supervisor, David Olson, and my committee members, Bernard Thebaud and Marek Duszyk, for their support and guidance during my project. A special thanks to Dean Zaragoza and Sheena Fang for their friendship and assistance over the past four years. To all my friends who have been there with me through this experience, I could not have done it without you. And finally to my mom and dad, thank you for your love and support through the good times and the bad.

Table of Contents

List of Figures

Tables

List of Abbreviations

°C	Degrees Celsius
5-HPETE	5-hydroxyeicosatetraenoic acid
5LO	5-lipoxygenase
12LO	12-lipoxygenase
AA	Arachidonic acid
Ad5LO	5-lipoxygenase adenovirus
AdGFP	Green fluorescent protein adenovirus
Adv	Adenovirus
AEC	Airway epithelial cell
Ang	Angiopoietin
Ang-1	Angiopoietin 1
ANOVA	Analysis of variance
ASM	Airway smooth muscle cell
B	Blank
B_o	Total bound
bp	Base pair
BCA	Bicinchorinic acid
BLT_1	Leukotriene B_4 receptor 1
BLT_2	Leukotriene B_4 receptor 2
BPD	Bronchopulmonary dysplasia
BSA	Bovine serum albumin
Ca^{2+}	Calcium

cDNA	Complementary deoxyribonucleic acid
CLD	Chronic lung disease
CMV	Cytomegalovirus
CO_2	Carbon dioxide
COX	Cyclooxygenase
CPE	Cytopathic effects
$cPLA_2$	Cytosolic phospholipase A_2
cpm	Counts per minute
CVL	Crude viral lysate
cyc	Cyclophilin
CysLT	Cysteinyl leukotriene
$CysLT_1$	Cysteinyl leukotriene receptor 1
$CysLT_2$	Cysteinyl leukotriene receptor 2
d	Day
Da	Daltons
ddH_2O	De-ionized distilled water
DEPC	Diethylpyrocarbonate
DNA	Deoxyribonucleic acid
EDTA	Ethylenediaminetetraacetic acid
e.g.	Exempli gratia (for example)
EIA	Enzyme immunoassay
ELISA	Enzyme-linked immunosorbent assay
et al.	Et alii (and others)

EtOH	Ethanol
FBS	Fetal bovine serum
FGF	Fibroblast growth factor
FGFR	Fibroblast growth factor receptor
FiO_2	Fraction of inhaled oxygen
FLAP	5-lipoxygenase activating protein
g	Grams
g	Gravity
G_i	Pertussis toxin sensitive G protein
G_q	Pertussis toxin insensitive G Protein
GFP	Green fluorescent protein
GGL	γ-glutamyl leukotrienase
GGT	γ-glutamyl transpeptidase
GOI	Gene of interest
GPCR	G protein coupled receptor
GSH	Glutathione
h	Hour
H_2O	Water
H_2O_2	Hydrogen peroxide
h5LO	Human 5-lipoxygenase
H&E	Hematoxylin and eosin
HEK	Human embryonic kidney
HRP	Horseradish peroxidase

HUVEC	Human umbilical vein endothelial cell
i.e.	Id est (that is)
IgG	Immunoglobulin G
IL	Interleukin
i.p.	Intraperitoneal
LT	Leukotriene
LTA_4	Leukotriene A_4
LTB_4	Leukotriene B_4
LTC_4	Leukotriene C_4
LTD_4	Leukotriene D_4
LTE_4	Leukotriene E_4
MAP	Mitogen-activated protein
MAPK	Mitogen-activated protein kinase
MEM	Minimal essential media
MK	Montelukast/Singulair®
MK-591	[3 tert butyl thio (4 chlorobenzyl) 5 (2 quinolinylmethoxy) 2 indoyl] 2, 2 dimethylpropionic acid
MK-571	3 [2 methoxy 4 [(2 methylbenzene sulphonyl) carbamoyl]] benzyl methyl indole 5 carbamic acid cyclopentyl ester
min	Minutes
MLI	Mean linear intercept
MMP	Matrix metalloproteinase
MOI	Multiplicity of infection

mRNA	Messenger ribonucleic acid
MRP1	Multi-drug resistance associated protein
n	Number of replications
NSB	Non-specific binding
NTP	Nucleotide triphosphate
O_2	Oxygen
O_2^-	Superoxide anion
OD	Optical density
OH^-	Hydroxyl
p	Probability
PAGE	Polyacrylamide gel electrophoresis
PBS	Phosphate buffered saline
PCR	Polymerase chain reaction
PDGF	Platelet-derived growth factor
pfu	Plaque forming units
PG	Prostaglandin
PGE_2	Prostaglandin E_2
PGHS	Prostaglandin H synthase
PHT	Pulmonary hypertension
PKC_α	Protein kinase C alpha
PMSF	Phenylmethylsulphonofluoride
PN	Postnatal
PPARα	Peroxisome proliferator-activated receptor alpha

r5LO	Rat 5-lipoxygenase
RDS	Respiratory distress syndrome
RNA	Ribonucleic acid
ROS	Reactive oxygen species
rpm	Revolutions per minute
RT	Reverse transcription
s.c.	Subcutaneous
SDS	Sodium dodecyl sulphate
SEM	Standard error of the mean
SPE	Solid phase extraction
SRS-A	Slow reacting substance of anaphylaxis
TA	Total activity
TBS	Tris-buffered saline
TEMED	N,N,N',N'-tetramethylethylenediamine
VEGF	Vascular endothelial growth factor
VEGFR	Vascular endothelial growth factor receptor
VEGFR1	Vascular endothelial growth factor receptor 1
VEGFR2	Vascular endothelial growth factor receptor 2
wk	Week
Wy-50295	Alpha methyl 6(2 quinomethoxy) 2 naphylacetic acid
x	Multiplied by

CHAPTER 1 - INTRODUCTION

Introduction

Lung development is a complex process that is essential for postnatal life. Any disruption may lead to severe diseases that significantly impact quality of life. Leukotrienes (LTs) are inflammatory mediators known to participate in pulmonary hypersensitivity reactions. They have also been shown to be involved in lung damage associated with hyperoxia. Hyperoxia (>95% oxygen) in newborn rats is a potent inhibitor of alveolarization, the final stage of lung developments. This animal model replicates many of the features of human newborn chronic lung disease or bronchopulmonary dysplasia (BPD). Recent studies in our laboratory have demonstrated a role for LTs in the hyperoxia-mediated arrest of lung development. Different LTs have been shown to both stimulate and inhibit lung maturation. The studies in this thesis were carried out to determine the effects of hyperoxia on the LT receptors and to develop a new, more specific model to investigate the roles of LTs in the lungs of newborn rats.

Lung Development

The process of lung development in humans occurs in five stages and is based on a histological description (Figures 1.1 & 1.2) [1-6]. The first is the embryonic stage that occurs during the first 7 weeks of gestation. The trachea and larynx differentiate from the primitive foregut endoderm, and the lung buds invade the splanchnic mesenchyme beginning on embryonic day 26 [7]. The lung buds then elongate, forming the two major bronchi, which continue branching to form the airway tree [7, 8]. At this time, the epithelium is multi-layered and composed of undifferentiated cells [7, 8].

The second stage is the pseudoglandular phase that extends from weeks 7 to 16. Dichotomous branching forms airways to the level of the terminal bronchioles. Differentiation of respiratory epithelial cells and cartilage occurs, and pulmonary blood vessel development begins via vasculogenesis [7]. Airway divisions are complete by the end of this phase, but the epithelial tubes have not yet developed lumens.

The third stage is the canalicular phase that takes place from week 16 until approximately weeks 26 to 28. During this phase, terminal bronchioles divide into respiratory bronchioles, which further subdivide into alveolar ducts. The peripheral epithelial lining becomes cuboidal and distinct from the bronchiolar epithelium. Also, differentiation of the cuboidal cells into type II, and later type I, epithelial cells begins. During this stage, the lung tubules have a relatively small lumen and the mesenchyme remains prominent. Additionally, development of the distal pulmonary circulation by vasculogenesis occurs as endothelial cells invade the thinning mesenchyme, with capillaries being present by week 20 [7, 8]. Moreover, interstitial tissue undergoes thinning in the regions that are to become the future gas exchange units [5, 7, 8].

The fourth stage of human lung development is the saccular phase, which commences between weeks 26 and 28 and terminates approximately at weeks 32 to 36. This period is identifiable by the formation of the terminal sacs or primitive alveoli. Capillaries also establish close contacts with the epithelium via angiogenesis. Furthermore, type I and II cells are now identifiable and surfactant is being produced [8, 9].

The fifth and final stage is the alveolar phase (alveolarization). The alveolar phase begins between weeks 32 and 36, but occurs primarily after birth with more than 90% of alveoli being formed postnatally in humans, completing at approximately age two years. The saccules mature into alveoli through a process known as septation, which involves the outgrowth of the septal crests and the elongation of the septal walls to form individual alveoli. The capillaries, which formed a double capillary layer during the late saccular and early alveolar phases, are remodelled to form a single capillary layer via angiogenesis, apoptosis, and other processes. The rapidity with which alveolarization occurs, and the fact that the process of septation requires unfolding and growth of capillary layers within the septa, are two examples that suggest highly complex interactions between endothelial and epithelial cells [10, 11]. The lungs of preterm babies are different from those born at term because they complete development in an external setting and not *in utero* [12]. Infants born in the saccular phase produce little surfactant and therefore require artificial surfactant to survive. However, this and other treatments provided, such as oxygen, inhibit septation and alveolarization leading to long-term complications [13, 14].

During lung development, blood vessel growth is of particular importance. The airspace must be in close contact with the blood in order to facilitate gas exchange. Angiogenesis is essential to this process and provides for close epithelial and endothelial association. After differentiation of the initial endothelial cells from mesenchymal precursors (vasculogenesis), angiogenesis, the sprouting of new blood vessels from pre-existing ones, develops the capillary network necessary for respiration [15]. Capillaries proliferate

during the pseudoglandular and canalicular stages of lung development [16-19]. The capillary network matures throughout the saccular and alveolar stages to a level where the endothelial barrier is only a single cell thick at the gas exchanging regions [7, 16, 17]. Any disruption of angiogenesis before and/or after birth can affect the ability of the lung to oxygenate the blood and can lead to severe developmental lung problems, such as BPD.

Alveogenesis is the production of alveoli by the subdivision of the terminal airway saccules, a process also known as septation [16, 17]. Septation involves the outgrowth of the septal crests and the elongation of the septal walls to form individual alveoli [16, 17]. Septation is advantageous because it allows for an increase in surface area without a proportional increase in lung volume [16, 17]. There is tremendous variation among species in the timing of septation [16, 17]. In humans, the process of septation begins near birth and continues until approximately 2 years of age [16, 17, 20]. Concurrent with septation, the alveolar wall becomes thinner and its cellular composition changes, promoting formation of gas exchange surfaces [16, 17]. Also, the capillaries, which form double capillary layers in the immature gas exchange regions, are remodelled to form a single capillary layer [16, 17]. Together with angiogenesis, alveogenesis provides highly efficient gas exchange structures that develop during this final phase of lung development.

The processes of angiogenesis and alveogenesis are extensively intertwined and essential for human life. Therefore, disruption of these processes and/or the interactions between

them can have severe consequences for lung development. Research has shown that there are parallel increases in vascular and alveolar growth, which are closely synchronized [20]. However, the molecules that link the distal airspace growth with angiogenesis are uncertain [20]. Vascular endothelial growth factor (VEGF), an angiogenic factor, has been shown to play a central role in vascular development [20, 21]. It is synthesized by epithelial cells and has receptors on both epithelial and endothelial cells, suggesting it has regulatory functions for both cell types and acts as a link between blood vessels and airway cells [7, 15, 20, 22, 23].

Vascular Development

New blood vessels are formed by two processes: vasculogenesis and angiogenesis, which are characterized by the source of their endothelial precursor cells [24]. Vasculogenesis is the differentiation of the initial endothelial cells from mesenchymal precursors [15, 16]. Angiogenesis is defined above. There are two main types of angiogenesis: sprouting and non-sprouting [25, 26]. Sprouting angiogenesis involves the process of proteolytic degradation of the extracellular matrix, followed by the chemotactic migration and proliferation of endothelial cells, formation of a lumen, and functional maturation of the endothelium [26]. Non-sprouting angiogenesis, has two subtypes: (1) intussusception, a process of splitting pre-existing vessels by the formation of transcapillary pillars or posts from the extracellular matrix, and (2) bridging, a process where endothelial cells subdivide the vessel [26-30]. The type of angiogenesis that occurs in a given tissue may depend on the number of blood vessels already present when the organ begins to grow rapidly [26]. For example, sprouting angiogenesis occurs in the brain, which lacks

angioblasts and thus has few pre-existing vessels. Conversely non-sprouting angiogenesis is prolific in the lung, which is extensively vascularized by vasculogenesis early in development [26, 28, 31]. The control of angiogenesis is important to prevent over or under growth of blood vessels into tissues; thereby, ensuring the metabolic demands of cells are adequately met. Many factors are known to regulate angiogenesis in the lung, the most important of which are VEGF and angiopoietins. The formation of new blood vessels via angiogenesis is vital for normal lung development and is necessary for alveolarization to occur. Development of the airways and vasculature must occur in tandem as inhibition of one will result in the inhibition of both [32].

Airway and vascular development are closely related processes that rely on interactions with each other to occur properly. The lung vasculature is divided into the pulmonary and the bronchial systems [11]. The pulmonary vessels form an extensive capillary network at the level of the respiratory bronchioles and alveoli, and are chiefly responsible for gas exchange [5, 11]. The bronchial system is responsible for supplying the lung tissue with nutrients and perfusing the capillary beds within the bronchi and perihilar region [5, 11]. This two-tiered circulatory system requires a complex pattern of development in concert with the branched airways.

Alveolar Development

By the fourth week of gestation in humans, the newly formed lung bud is surrounded by mesenchyme that contains numerous endothelial cells [33]. By the fifth week, a capillary network is present around each future bronchus and circulating blood cells can be

detected, corresponding with the late embryonic phase of lung development [33, 34]. These early vessels are formed by vasculogenesis, as endothelial cells coalesce to create capillaries, which merge to form small blood vessels along the airways [5]. As each new airway buds into the mesenchyme, a new plexus forms and adds to the developing vessels [5]. This system of vessel formation continues until the end of the pseudoglandular stage [5].

In the canalicular phase, the division of airways to the level of respiratory bronchioles and acini is accompanied by the start of angiogenesis and the initial formation of close contacts between the epithelial and endothelial cells [5, 33, 34]. By the end of this third phase of lung development, at 25 weeks gestation, the blood-gas barrier has thinned to the same level as an adult and the gas exchange area is sufficient to support premature infants [5]. Recent data show that interfering with angiogenesis results in abnormal lung development [11, 20, 32, 35-38]. Therefore, angiogenic growth factors are likely to play a role during normal and abnormal lung maturation.

Regulation of Alveolarization

The regulation of alveolarization is a complex process involving both blood vessel development (angiogenesis) and subdivision of the saccular compartments into alveoli (alveogenesis). Processes involved in angiogenesis are discussed above. Control of alveogenesis is known to involve fibroblast growth factor (FGF) and platelet derived growth factor (PDGF) signalling pathways [39]. The downstream targets of these pathways remain unknown, but some of the factors in early lung morphogenesis, such as

Hnf-3, GATA6, and Nkx2.1, are involved [39]. Retinoids and glucocorticoids are also able to affect alveogenesis [39]. Retinoids alter the expression of Hox genes in developing lung mesenchyme, thus affecting epithelial morphogenesis [39]. The role of glucocorticoids in lung development is also not well understood. Deletion of glucocorticoid receptors results in postnatal death from respiratory insufficiency [40]. The mechanisms through which these compounds exert their effects remain unclear. The maturation of type II alveolar epithelial cells to type I is another critical component of alveolar formation; yet, the processes governing the switch remain unknown. Type I cells are thin and flat and comprise 95% of the alveolar surface in a mature lung [41]. Type II cells are large cuboidal cells that are important in the production of surfactant and host defence [41]. Type II cells act as progenitor cells for type I [41]. This is important in hyperoxic lung damage because hyperoxia selectively kills type I cells, which are repopulated by differentiating type II cells [41]. This recovery process, while restoring alveolar structure, can lead to fibrosis and lung damage [41]. This disruption is evident in BPD, where hyperoxia results in an arrest of lung development [41]. Hyperoxia also disrupts type II cell proliferation and organization, further inhibiting alveogenesis [23]. Interference with type II cell activity (e.g. hyperoxia) can also inhibit angiogenesis as type II cells are a source of VEGF [42]. Clearly, more needs to be learned about the regulation of alveolarization and its disruption in hyperoxia.

Rat Lung Development

In rats, lung development occurs in the same five stages as in humans, but obviously at a much accelerated rate. The embryonic phase occurs from days 0-13 of gestation [43]. The

pseudoglandular stage begins on the 14th day of gestation and is complete by day 18 [43]. The canalicular phase is the last step that occurs completely *in utero*, from days 19-20 [43]. The saccular stage straddles birth, taking place from gestational day 21 until postnatal day 3. Therefore, rats are born while their lungs are in the saccular period, similar to pre-term human infants and before the start of alveolarization, making them an excellent model for studying the final step in lung development [43]. The alveolar phase occurs in rats primarily between days 4-14 post-natal (PN), peaking on day 7, and complete by the third PN week [44]. The lungs continue to grow in size until maturity.

Tropoelastin

Due to the complexity of lung formation, biochemical markers, such as elastin and tropoelastin, are useful in characterizing the developmental stage. Elastin is a connective tissue protein that conveys elastic properties and allows tissues to resume their shape after stretching or contracting. It is made by covalently linking many soluble tropoelastin protein molecules together in a reaction catalyzed by lysyl oxidase, to make a massive, insoluble, durable cross-linked array [45, 46]. Elastic fibres are thought to provide structural support for secondary septa as the lung undergoes the transition from the saccular to the alveolar stage [45, 46]. In rats, the synthesis of the soluble precursor of elastin, tropoelastin, occurs during a finite developmental period [46]. Tropoelastin gene expression is up-regulated late in gestation. After birth, tropoelastin is down-regulated to day 6 postnatal [46]. During alveolarization, tropoelastin levels are increased further supporting that it is important in septation [46]. Exposure to >95% oxygen, when initiated on postnatal day 2 or 3 and continued until day 11, significantly diminished the

developmental increase in tropoelastin mRNA normally seen on days 9-11; indicating that the postnatal up-regulation of tropoelastin gene expression is inhibited by hyperoxic exposure in the early postnatal period [46]. Macrophage and neutrophil proteinases released during hyperoxia also damage lung elastin, disrupting alveolar epithelium and filling alveoli with inflammatory exudates [45]. Alveolar collapse and regional hypoxia occur. Regional hypoxia limits lung elastin repair following protease injury, at least in part, by inhibiting elastin gene expression [45]. Tropoelastin can therefore be used as a measure of lung development.

Bronchopulmonary Dysplasia (BPD)

BPD, a chronic lung disease of infancy, is the result of ventilator and oxygen therapy for acute respiratory distress syndrome (RDS) [23, 47, 48]. Northway *et al.* first described BPD in 1967 in premature infants treated for severe RDS who developed a new type of chronic lung disease after being treated with intermittent positive pressure mechanical ventilation and oxygen supplementation [49]. Although these treatments increased survival in infants with RDS, the resulting BPD presented new clinical difficulties [48, 50, 51]. The pathology of BPD was characterized by injury and repair affecting both the parenchyma and the airways, with alteration of normal growth and development of the lung [48-52]. Great advances in the prognosis of RDS have been made since the introduction of surfactant and antenatal steroid treatment, and it is no longer the leading cause of mortality in premature infants [48, 51]. However, the incidence of BPD, since its identification 35 years ago, has not decreased and may actually be on the rise today [48, 51].

Traditionally, BPD was marked by fibrosis and cellular proliferation [23, 47, 48]. However, due to medical advances, infants with BPD are now far less mature, have markedly lower birth weights, and present with arrested lung development in the form of impaired vascular and alveolar growth [13, 23, 47-50, 52]. Infants born during the late canalicular stage (at 24-27 weeks gestation) have disrupted lung development, resulting in alveolar simplification and dysmorphic vascular growth [13, 23, 47, 49, 50, 52]. In addition to its changing epidemiology, the pathological signs of BPD have also changed, in that the signs of severe chronic lung injury (fibrosis and cellular proliferation) are much less common [20, 48]. In fact, decreased alveolarization and abnormal vascular growth are the hallmarks of the "new BPD" [13, 20, 50-53]; however, mechanisms that inhibit lung growth in premature infants with BPD remain poorly understood [13, 20].

Animal experiments have shown that alveolar development can be delayed by hypoxia, hyperoxia, glucocorticoids, or poor nutrition [13]. Hyperoxia and glucocorticoids are used in the treatment of RDS, and it is thought they are involved in the arrested lung development observed in infants with BPD [13, 15, 22, 52, 54]. In fact, postnatal glucocorticoid therapy is no longer recommended due to the relative lack of benefit and the long-term complications resulting from steroid-induced alterations in brain development [55]. This has led to the search for alternate treatments to reduce the inflammation associated with BPD while also avoiding the negative effects of steroid therapy. One possibility is administration of exogenous VEGF as proposed by Compernolle *et al.* [56]. They found that VEGF treatment was as effective as perinatal

steroid treatment but avoided the acute side effects [56]. Recently, Thebaud *et al.* administered combined VEGF and Ang-1 gene transfer to rat pups prior to exposure to hyperoxia [57]. They found that this therapy helped protect the lungs from hyperoxic damage and prevented the arrest in development [57]. This is exciting in that it may lead to a potential therapy in humans. The long-term effects however, must be investigated before it can be considered as a viable therapeutic option. The effects of gene therapy must also be explored before this type of therapy becomes viable in humans. These findings serve to enhance the understanding that VEGF is important to lung maturation. Whether disruption of VEGF signalling impairs lung vascular growth and contributes to the pathogenesis of BPD remains uncertain.

Hyperoxia

In the lung, hyperoxia impairs development by inhibiting septation [53, 58, 59]. Prolonged exposure to high oxygen levels in rats leads to intra-alveolar edema and morphologic changes [60, 61]. High oxygen concentrations have long been known to be harmful to cells due to the increase in toxic by-products (reactive oxygen species; ROS) produced [62, 63]. ROS, such as superoxide anion (O_2^-) and hydrogen peroxide (H_2O_2), are produced in normal cellular reactions (e.g. oxidation reduction) [62]. Normally, the lung uses an antioxidant system of chemicals and enzymes to prevent the formation of, and damage from, ROS [62]. However, in preterm infants this system is not fully matured and therefore a greater number of ROS are active in cells [64, 65]. This problem is exacerbated by the hyperoxic therapy used to treat preterm babies. ROS cause damage to proteins, lipids, and DNA, thus injuring lung epithelial and endothelial cells and

impairing their ability to repair themselves [60, 63, 66, 67]. The exact mechanisms through which ROS damage the lung have not been established but it results in widespread remodelling of the lung [61]. There has been significant research into the effects of hyperoxia on vascular remodelling. It has been shown to inhibit angiogenesis and promote edema which causes fluid leak into the airspaces and further amplifies the damage [66]. Capillary damage leads to a reduction in septation and therefore decreases the surface area for gas exchange [61, 68].

Hyperoxia and Lung Development

It has been demonstrated that exposing newborn animals to hyperoxia can damage the lung and prevent lung septation. Bucher *et al.* exposed newborn rats to greater than 0.95 FiO_2 for up to 12 days [69]. The pups showed microscopic evidence of lung injury and reduced alveolar development [69]. Hyperoxia (>95% O_2) has also been shown to inhibit lung DNA synthesis and increase lung cell apoptosis [70-72]. Exposure to hyperoxia for 7 days has also been shown to arrest alveolarization in rat pups [59]. In our own laboratory, exposure of neonatal rat pups to >95% O_2 resulted in fewer and larger alveoli and alveolar ducts compared with animals exposured to normal air [73].

Hyperoxia and Inflammation

Prolonged exposure to hyperoxia in newborn rats results in inflammatory lung damaged characterized by interstitial and alveolar edema, followed by infiltration of protein, entry of cells, and finally hemorrhage into the alveolar space [74]. This is accompanied by rapid neutrophil infiltration into the lung [75]. Activated neutrophils produce large

quantities of ROS as well as elastase and arachidonic acid (AA) metabolites, which can damage the pulmonary parenchyma [75]. This leads to activation of surrounding cells and recruitment of more inflammatory cells, resulting in further release of inflammatory mediators. One group of AA metabolites, leukotrienes (LTs) and their receptors, were the focus of this research.

Hyperoxia Model of BPD

Exposure to 95% O_2 during the period of alveolar development in the rat causes nearly a complete inhibition of septation [51]. Our laboratory interprets this as a model of inhibited alveolar development rather than a model of BPD. While it replicates the decreased septation seen in human cases of BPD, it fails to produce the dysplastic lesions characteristic of the disease, such as thickened septa. The rat model is also not an ideal model for the human condition. Rats are born with a lung in an immature state of structural development and it is obvious these pups are able to survive outside the womb. This is because the bronchioles are still in close contact with the vasculature at birth allowing ventilation to occur here as well as the immature saccules. Also, antioxidants and surfactant are already abundant at birth in rats [76]. This is one reason such high oxygen concentrations are used in rat BPD models; to appreciably increase the oxidant:antioxidant ratio to overcome the endogenous rat antioxidants and obtain a level more representative of humans. The rat model is widely used to study lung development as rat pups are relatively inexpensive, available in large quantities, and easily manipulated [77-82]. They also develop rapidly allowing us to study the entire alveolarization period (which occurs over a period of approximately 10 days). The

progression of lung development is also similar between rats and humans; yet, the fact that rats undergo alveolarization postnatally negates the need for a model involving preterm birth and its accompanying complications.

Leukotrienes

Leukotrienes are members of the eicosanoid family that includes thromboxanes and prostaglandins. LTs were first identified in 1979 and termed the slow reacting substance of anaphylaxis (SRS-A) [83-86]. Subsequent research determined that SRS-A was actually a group of molecules and were renamed LTs, in recognition that they were first identified as being released by leukocytes and have three conjugated double bonds in a triene ring structure [83-87]. There are two biologically active groups: LTB_4 and the cysteinyl-LTs (LTC_4, LTD_4, and LTE_4).

LTs are inflammatory mediators derived from arachidonic acid by 5-lipoxygenase (5LO) and 5-lipoxygenase activating protein (FLAP) (Figure 1.3). LTs are synthesized in mast cells, alveolar macrophages, and alveolar epithelial cells and act locally [83]. They are synthesized *de novo* upon cell activation by physical or chemical factors and activation of cytosolic phopholipase A_2 ($cPLA_2$) [83, 88, 89]. Cytosolic PLA_2 cleaves and oxidizes AA from phospholipids in the cell membrane [83]. Once cleaved, AA is acted upon by 5LO, the principal enzyme in the LT synthesis pathway [83]. 5LO competes for AA with other enzymes such as prostaglandin H synthase-1 (PGHS-1), PGHS-2, thromboxane-A_2 synthase, and 12-lipoxygenase [83, 86]. 5LO, which is located in either the cytosol or nucleus, depending on cell type, also requires the presence of FLAP, which is located on

the nuclear envelope, for it to act on AA [83, 86]. In the presence of Ca^{2+}, FLAP presents AA to 5LO, which converts it first to 5(*S*)-hydroperoxy-6-*trans*-8,11,14-*cis*-eicosatetranoic acid (5-HPETE), and then to LTA_4, an unstable epoxide [83, 86].

LTA_4 is next metabolized by one of two pathways. The first pathway involves the hydrolysis of LTA_4 to LTB_4 by LTA_4 hydrolase [83, 88, 90]. LTB_4 is then transported out of the cell by an as yet uncharacterized LTB_4 transporter [83, 88]. LTB_4 then binds BLT_1 and BLT_2 receptors on the surface of surrounding cells [83, 88, 90-92]. It can also bind the nuclear receptor PPARα (peroxisome proliferator-activated receptor alpha), which activates the transcription of genes involved in terminating inflammation [83, 88, 90-92]. LTB_4 is involved in inflammatory diseases such as arthritis and leads to the production of superoxide anion, chemotaxis, and leukocyte degranulation [83]. It is chemotactic for neutrophils and less so for eosinophils and is involved in leukocyte communication [83, 84, 93].

The second pathway conjugates LTA_4 to glutathione (GSH, γ-glutamyl-cysteinyl-glycine) via LTC_4 synthase, which is located on the nuclear envelope, to produce LTC_4 [83]. LTC_4 is part of the CysLT family (peptido-LT), which includes LTD_4 and LTE_4, and are so named because a peptide side chain is attached to carbon six [83, 94, 95]. CysLTs are produced by inflammatory cells: basophils, eosinophils, mast cells, and macrophages (alveolar macrophages are the main source in lungs) [83, 96]. LTC_4 is then transported out of the cell by the membrane receptor multi-drug resistance-associated protein-1 (MRP1) where it is either binds to its receptors ($CysLT_1$ and $CysLT_2$ receptors) or is

further metabolized to LTD_4 and LTE_4 [83, 84]. LTC_4 is converted to LTD_4 by γ-glutamyl transpeptidase (GGT) and γ-glutamyl leukotrienase (GGL), which are located on the extracellular membrane and cleave a γ-glutamyl group from the peptide side chain [83, 97, 98]. LTD_4 binds to the same receptors as LTC_4, $CysLT_1$ and $CysLT_2$ [83]. It is an extremely potent bronchoconstrictor [83, 99]. Hyperoxia has been shown to increase GGT expression in rat lungs, and by extrapolation, LTD_4 [100]. LTD_4 is converted to LTE_4 by an extracellular membrane-bound dipeptidase which cleaves the peptide side chain [83]. LTE_4 also binds $CysLT_1$ and $CysLT_2$ receptors but is normally metabolized quickly and excreted in the urine [83, 101, 102]. LTE_4 is 10-100 times less potent than LTD_4 [103].

As a group, LTs increase vascular permeability (leading to edema), stimulate mucous secretion, and trigger bronchoconstriction [83, 89, 104, 105]. LTs also stimulate the migration of endothelial cells, indicating they may be involved in angiogenesis [83, 89, 105]. They also recruit granulocytes into the airways to aid in the propagation of inflammation [101]. The mechanisms through which LTs stimulate cell migration and recruitment remain unknown [83, 89, 105]. LTs can also stimulate airway smooth muscle (as well as other smooth muscle cells) proliferation and tone [105]. Many of these effects are symptoms associated with both asthma and BPD [89, 105, 106].

Leukotriene Receptors

Leukotrienes bind one of four known G protein-coupled receptors (GPCR). GPCRs are located in the plasma membrane and are characterized by seven transmembrane regions.

There are two primary receptors for LTB_4, BLT_1 and BLT_2, and two for the CysLTs, $CysLT_1$ and $CysLT_2$. The LT receptors demonstrate different affinities for the LTs and have different downstream actions in cells [88, 91, 92, 107-115].

LTB_4 Receptors

The two BLT receptors have different affinities for LTB_4. BLT_1 is the high affinity receptor; BLT_2 has lower affinity [88, 91, 92, 115]. Despite this, they have similar downstream signalling pathways [88, 91, 92, 115]. As the main action of LTB_4 is neutrophil chemotaxis, BLT_1 expression is most abundant in neutrophils [83, 112, 115, 116]. It is, however, also present on other leukocytes, with the exception of macrophages and monocytes [83, 88]. BLT_2, the lower affinity receptor, is expressed on most tissues [83, 91]. The BLT receptors have only 26-28% amino acid uniformity with CysLT receptors, indicating a distant evolutionary divergence [91, 114]. In addition to the BLT receptors, LTB_4 is suggested to be able to bind PPARα in the nucleus and participate in the arrest of inflammation [83, 117]. This proposed second receptor system is unique to LTB_4 as the CysLTs have no known equivalent target in the cell [83, 117].

CysLT Receptors

In contrast to the BLT receptors, the two CysLT receptors have several natural agonists with varying affinities. All of the LTs, except LTA_4 which is unstable and not released from cells, can bind both CysLT receptors. Human CysLT receptors are approximately 38% homologous in their amino acid sequence, but over 70% identical to the rat CysLT receptors due to the fact that they bind structurally identical molecules [108, 110, 118].

CysLTs act locally in a paracrine and possibly autocrine manner, and it has been suggested that communication between the two CysLT receptors could promote cell interactions [83, 109, 119].

$CysLT_1$ demonstrates the greatest affinity for LTD_4, 10 times more than for LTC_4, and 10 times again for LTE_4 (LTD_4>>LTC_4>LTE_4>>LTB_4) [83, 107, 108, 111, 114, 118, 120]. $CysLT_1$ is generally thought of as an LTD_4-specific receptor because at physiological concentrations, LTD_4 is its only biologically effective agonist; however, it is capable of responding to the other LTs at higher concentrations [121-123]. $CysLT_1$ is expressed in the lung, spleen, pancreas, macrophages, leukocytes, eosinophils, and monocytes [105, 124]. In the lung, $CysLT_1$ is present on airway smooth muscle cells, where is promotes bronchoconstriction and edema [83, 124]. $CysLT_1$ appears to be the dominant CysLT receptor in the lung as it is expressed in larger amounts [121]. The signal transduction pathway for the $CysLT_1$ receptor is the best understood. When activated, $CysLT_1$ binds a heterotrimeric GTP-binding protein (G-protein), which causes a rise in intracellular Ca^{2+} levels [106, 110, 122, 125, 126]. $CysLT_1$ acts through one of two different G-protein pathways: G_i or G_q [106, 126]. G_i (pertussis toxin sensitive G-protein) is believed to be triggered when LTD_4 binds $CysLT_1$ [106]. G_i then triggers the downstream activation of Ras, another G-protein [106, 126]. G_i also stimulates tyrosine phosphorylation, leading to actin reorganization in airway smooth muscles cells [106]. In contrast, activation of G_q (pertussis toxin insensitive G-protein) causes an increase in cellular Ca^{2+} concentrations via protein kinase C_α (PKC_α) [125]. G_q then acts in concert with Raf-1 (mitogen-activated protein (MAP) kinase kinase) to phosphorylate MAP kinase [125].

Phosphorylated MAP kinase triggers an increase in $cPLA_2$ levels, leading to increased AA release from phosphatidylethanolamine and more LT production [125, 127].

$CysLT_2$ has slightly different affinities for the LTs than $CysLT_1$. $CysLT_2$ binds according to: LTC_4=LTD_4>>LTE_4>>LTB_4, where LTC_4 and LTD_4 are equally potent agonists [83, 110, 114, 118, 128]. LTE_4 is only a partial agonist and LTB_4 has little ability to bind the receptor [83, 114]. $CysLT_2$ was first identified in vascular tissue and is responsible for many of the effects of LTs on blood vessels [83, 108, 110, 129, 130]. $CysLT_2$ has been found in the lung, spleen, heart, adrenal glands, brain, and placenta [83, 130]. In the lung, $CysLT_2$ is most abundant on macrophages, but is also present on pulmonary endothelial cells [83, 108, 110]. The exact roles of $CysLT_2$ remain uncertain, but it appears to be involved in eosinophil recruitment and the lung reaction to allergen exposure [83, 130, 131]). Activation of $CysLT_2$ causes a rise in intracellular Ca^{2+} in a similar manner as $CysLT_1$; but, the signal transduction pathway remains unknown [114, 132].

LT Antagonists

LTs, as potent bronchoconstrictors and inflammatory mediators, are important factors in lung diseases such as asthma and BPD. Because of this, several inhibitors have been developed to antagonize their effects. 5LO and LT receptor inhibitors are commonly used to treat asthma, due to their anti-inflammatory properties [83, 85, 133-139]. In particular, the $CysLT_1$ receptor has been shown to play a critical role in asthma, and receptor antagonists such as montelukast (Singulair®) are highly effective asthma therapies.

Leukotrienes and Lung Development

Recent evidence has led to the idea that LTs are involved in lung development. The first studies examining LT levels in rat pup lungs after exposure to hyperoxia were performed by Dr. Boros in our laboratory. Lungs developing for 10 days in >95% O_2 had increased levels of CysLTs versus control pups [73]. The laboratory was then interested in whether or not this effect could be reduced using specific inhibitors of LT synthesis. Wy-50295 was used to block 5LO and MK-591 was used to inhibit FLAP. Both antagonists caused a reduction in the amount of CysLTs present during exposure to hyperoxia in neonatal rat lungs, *ex vivo* [73]. Interestingly, it was also observed that these inhibitors prevented the arrest of alveolarization usually seen during exposure to hyperoxia [73]. Next, Hosford *et al.* found that 5LO and FLAP protein as well as LTB_4 synthesis levels were all increased in rat lungs exposed to >95% O_2 following birth [96]. These data led to the idea that LTs may be acting as mediators in hyperoxic lung injury. Following these findings, the lab was interested in determining the period of lung development during which the LTs and hyperoxia effects were most significant. Manji *et al.* described a 'critical period', from days 4-9 postnatal, during which exposure to hyperoxia inhibited alveolarization [78, 140]. Exposure from days 1-4 or 9-14 had no significant effects on lung alveolarization [140]. Recently, Shauna McGill in our laboratory studied the effects of individual LTs on alveolarization in rat pups. She found that LTB_4 and LTC_4 inhibited septation when administered between days 4 and 13 postnatal [141]. Interestingly, however, LTD_4 was shown to accelerate alveolarization during this same period [141]. To further test the involvement of LTD_4 in lung development, McGill *et al.* administered a $CysLT_1$ (LTD_4 receptor) antagonist, MK-571, to rat pups exposed to normal air and compared them to

rat lungs exposed to hyperoxia [141]. Morphometric analysis demonstrated that MK-571 arrested alveolarization to a degree similar to hyperoxia [141]. A study by Jouvencel *et al.* looked at whether montelukast (MK; Singulair®), a $CysLT_1$ receptor selective antagonist, reversed hyperoxia-induced (50% O_2) changes in lung structure [142]. They found that MK did not protect the lung against oxygen injury; however, this is likely because LTD_4 was found to promote alveolarization and by blocking its receptor they removed its beneficial effects [141, 142]. These data clearly indicate that LTs play a role in lung development and suggest they can both arrest and accelerate alveolarization.

LTs have been shown to influence other pathological processes in the lung, such as pulmonary hypertension (PHT). PHT, an increase in blood pressure in lung vasculature, is a common co-morbidity in left-sided heart failure and diseases of lung hypoxia (e.g. chronic obstructive pulmonary disease) [143]. Studies examining 5LO have shown a potential role for leukotrienes in the development of PHT [143, 144]. Although over-expressing 5LO in rats did not cause PHT, it caused a marked acceleration in the progression of the disease in animals with PHT [143, 144]. Recently, a study by Caironi *et al.* demonstrated that 5LO deficient mice were partially protected from the damage induced by mechanical ventilation and maintained better systemic oxygenation [145]. The results of these studies and the data from our experiments indicate that LTs play a central role in lung injury.

There are several sources of LTs in the lung and there is evidence to suggest that production is affected by hyperoxia. Studies have shown that AA products of the 5LO

pathway are released during exposure to hyperoxia [146, 147]. In the lung, LTs released by alveolar macrophages exposed to hyperoxia mediate the release of other inflammatory mediators and can lead to tissue damage. [65, 83, 147].

Animal Models

Alveolarization was the focus of these studies and it was important that the results be as applicable to humans as possible. The rat model is commonly used to examine lung development. They have a similar pattern of lung development to humans, occurring in 5 phases [44]. Hyperoxia can be used to replicate oxygen damage induced by ventilation in preterm infants with BPD. When exposed to hyperoxia, newborn rat pups develop changes in lung morphology similar to BPD lungs, as discussed above [59]. Airspaces enlarge and capillaries are altered and reduced in number [61].

The ideal model for studying BPD would be the baboon. When exposed to hyperoxia, they develop edema, airway thickening, and fibrosis similar to human preterm infants with BPD [148]. They also demonstrate arrested alveolarization and alterations in angiogenic factors [23]. However, the difficulty and expense in maintaining a baboon colony and intensive care unit, the long gestation period, and limited number of offspring per mother, make the rat model more feasible for our studies.

Other rodent models, such as mice, have been used to examine the effects of hyperoxia. They have the same period of alveolarization as rats and demonstrate similar changes when exposed to hyperoxia [149, 150]. They also make an excellent model because they

can be genetically manipulated. Knockout mice models have been developed to study lung development. A 5LO knockout mouse has used to establish the role of LTs in infection [151]. Without 5LO, macrophage activity against bacteria was weakened and neutrophil recruitment was inhibited [112, 151]. Unfortunately, none of these studies looked at these mice for changes in alveolarization. Despite these advantages, due to their size, mouse pups are more difficult to manipulate and less tissue is available for study.

For our studies, the rat model was selected for a number of reasons. The model was already established in our laboratory and the cost of purchasing and housing is reasonable. Rats provide adequate litter sizes for testing and have enough lung tissue for experimentation. Their tracheas are large enough for cannulation, which is important for morphometric studies. Most importantly, our previous studies used the rat model allowing for comparisons between those data with our results.

Study Rationale

Leukotrienes are derived from AA and are involved in the mediation of pulmonary hypersensitivity reactions. Their role in asthma is well established as they are involved with bronchial constriction, mucous secretion, and edema. New evidence suggests they play a role in a newborn chronic lung disease, BPD. This condition is common in preterm infants weighing less than 1000g who require ventilation with oxygen, causing damage through hyperoxia and barotrauma. Our laboratory has:

1. Used a hyperoxic (>95% O_2) model in neonatal rats that inhibits alveolarization, replicating certain aspects of BPD [152].
2. Determined that the 'critical period' of hyperoxia-induced arrest of alveolarization is days 4-9 postnatal [140].
3. Found that increases in both LTB_4 and the CysLTs are associated with the inhibition of alveolarization observed in hyperoxia [73, 96, 153].
4. Reversed the arrest of alveolarization in hyperoxia using inhibitors of 5LO and FLAP during the 'critical period', suggesting LTs are mediators of this process during this period [73, 140, 153].
5. Administered exogenous LTs to newborn rats in the absence of hyperoxia and shown that they can arrest (LTB_4) and stimulate (LTD_4) lung alveolarization [141].

Study Aims & Hypotheses

Aim 1

The next step in exploring the role of LTs in normal and hyperoxic lung development is to examine changes in LT receptors that are occurring and to correlate them with the effects of the LTs. To this end, the first specific aim of this study was to study LT receptor expression in neonatal rat lungs in both normoxic and hyperoxic environments. We **hypothesized** that BLT_1 and BLT_2 mRNA abundance would be increased in hyperoxia, $CysLT_1$ mRNA and protein levels would be decreased, and $CysLT_2$ mRNA and protein abundance would show little change (Figure 1.4).

Aim 2

Although an earlier study looked at the effects of increased LTs on lung development, it involved subcutaneous systemic administration of individual LTs [141]. We were interested in a more physiological model that localized an endogenous increase in 5LO and LT concentrations to the lungs in order to examine the effects on alveolarization exclusively. Therefore, the second specific aim was to administer an adenovirus expressing 5LO specifically to the lungs of neonatal rats during the period of alveolarization and examine the changes in LT levels, LT receptor expression, and lung development (morphometry and tropoelastin). We **hypothesized** that administration of 5LO would increase endogenous LTs and replicate the effects of hyperoxia on the arrest of lung alveolarization, morphometry, and LT receptor expression (Figure 1.4). The **goal** of this study was to establish a technique for examining the role of LTs specifically in lung development.

Significance

These studies aim to improve our understanding of the roles of LTs and their receptors in alveolarization and also develop a new model to examine the effects of LTs specifically in the lungs. The significance of these studies is to ultimately extrapolate the results to human lung development and to elucidate the causes and identify possible therapeutic targets and treatments for lung diseases of preterm birth. By identifying the changes in LT receptor expression and establishing a new technique to study LTs in the lung, we hope to discover new therapeutic targets or methods for determining them.

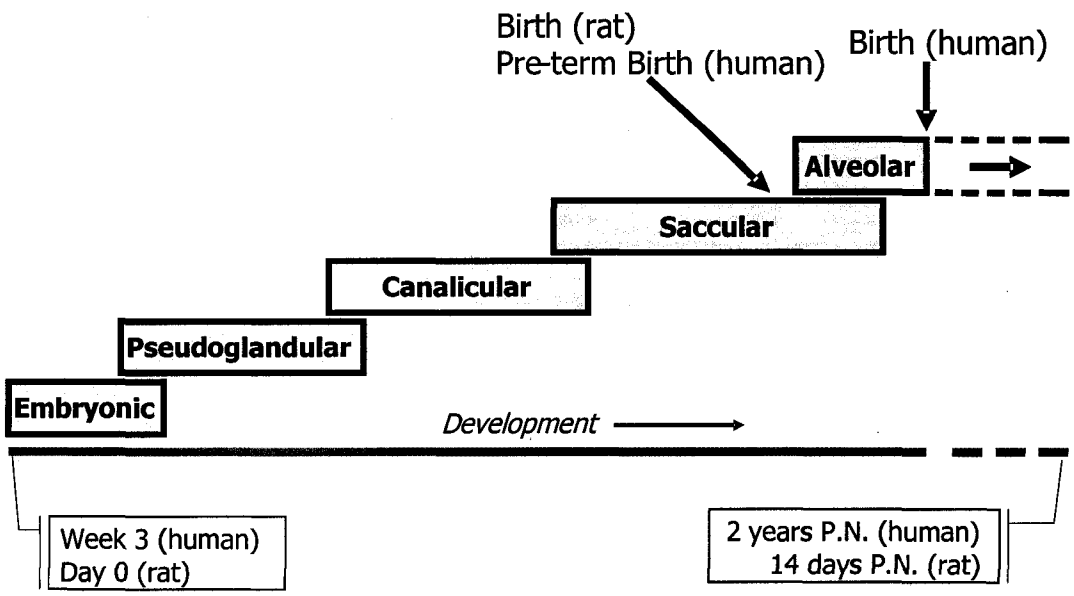

Figure 1.1: Stages of Lung Development

The five stages of lung development are illustrated here as they occur in both humans and rats. The time of birth and human preterm birth are highlighted. Rats born on d21 have lungs developmentally equivalent to human lungs in the saccular stage (26-36 wks gestation). This demonstrates why the rat model is appropriate for studying the premature lung. Modified from [154].

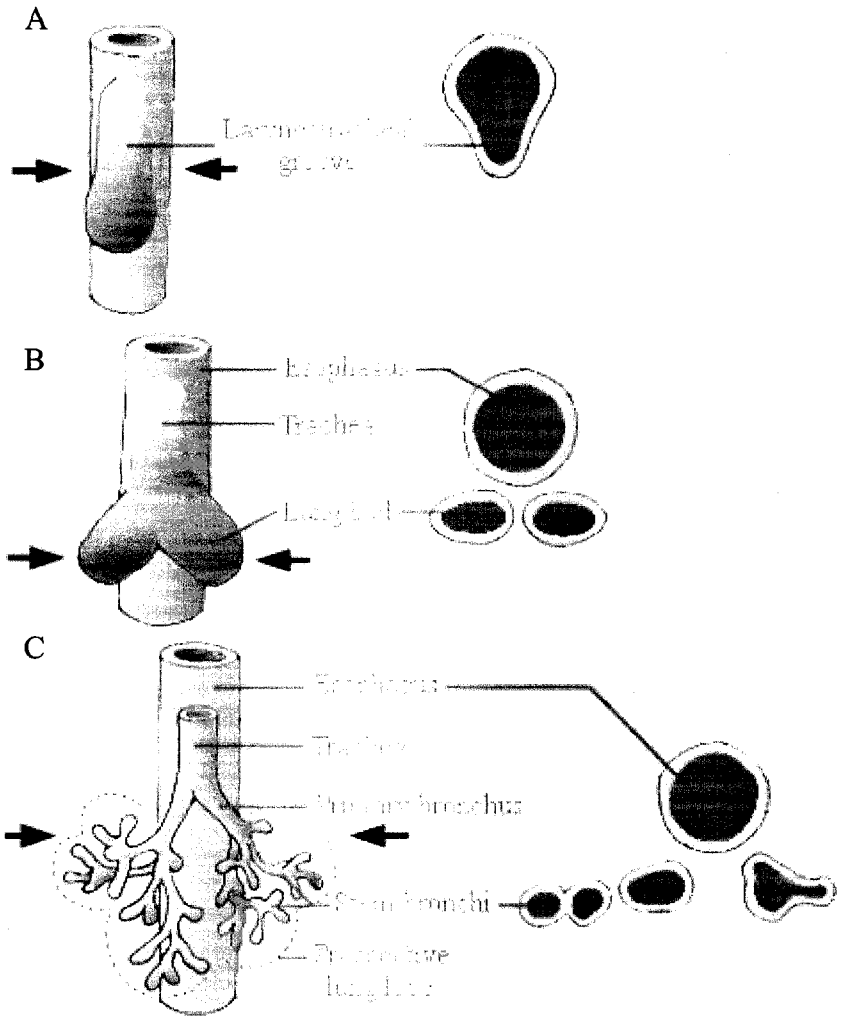

Figure 1.2: Schematic of Lung Development

This figure shows ventral views of the esophagus and developing lungs, accompanied by cross-sectional views through the area between the black arrows. Note how the lung starts as an outgrowth, from the esophogeal endoderm, called the larygotracheal groove (A). As the larygotracheal groove grows, it develops two outcroppings at its caudal end, the lung buds (B). As the lung buds grow, they branch repeatedly forming the primary bronchi and stem bronchi (C) which branch further to form bronchioles, which will eventually develop terminal air sacs (alveoli) to complete the adult lung. Also, note how the trachea, once attached as a ventral groove on the esophagus, has separated to become a distinct tube (C).
Figure modified from: http://www.uoguelph.ca/zoology/devobio/210labs/lung1.html

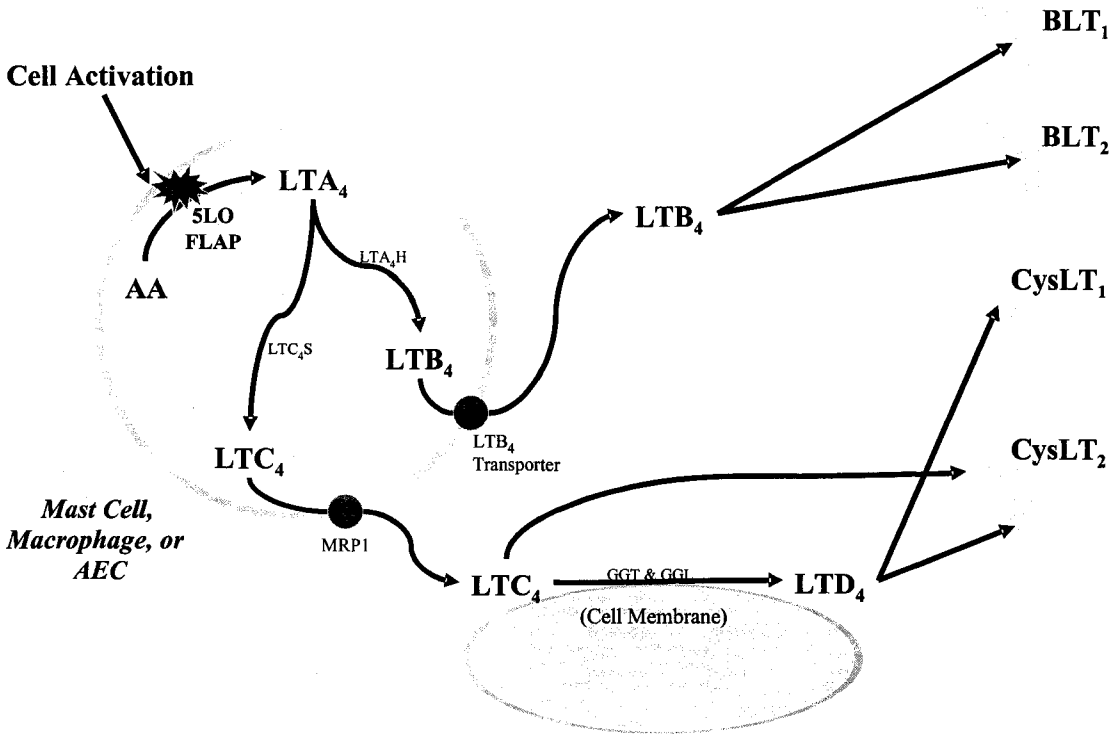

Figure 1.3: Leukotriene Synthesis and Action

This figure illustrates the LT synthesis pathway and their sites of action. In the lung, LTs are made in mast cells, marcropages, and alveolar epithelial cells (AEC). Following cell activation, arachidonic acid is converted to LTA_4, which is further metabolized to LTB_4, LTC_4, LTD_4, and LTE_4. Only LTA_4, LTB_4, and LTC_4 are synthesized intracellularly. The LTs, once secreted, act on their respective receptors. Blue circles represent cells involved in LT synthesis. Yellow semicircles represent LT receptors on their target sites. Modified from [83].

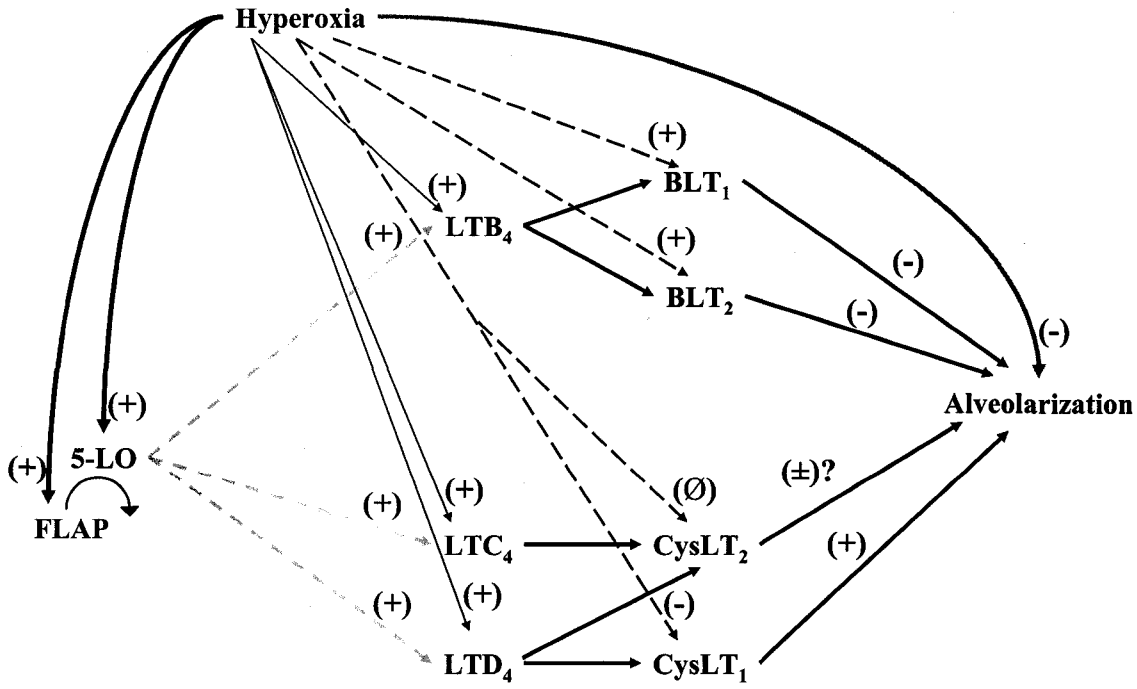

Figure 1.4: Hypothesis Schematic

Our pre-study hypothesis outlining the role LTs and their receptors in alveolarization. Previous work has shown that the synthesis of LTB_4 and the CysLTs are increased in lungs exposed to hyperoxia. The roles of hyperoxia on 5LO and FLAP expression, as well as alveolarization, are indicated. We predicted that BLT_1 and BLT_2 mRNA abundance would be increased in hyperoxia, $CysLT_1$ mRNA and protein levels would be decreased, and $CysLT_2$ mRNA and protein abundance would show little change. According to this hypothesis, increasing 5LO (as with hyperoxia) leads to an increase in leukotriene expression and an inhibition of alveolarization. Dotted lines indicate the effects to be tested in this study (black for Study 1 and green for Study 2). (+) indicates a stimulatory effect. (-) indicates an inhibitory effect. (Ø) indicates no effect. (±)? indicates an undefined effect.

CHAPTER 2 - MATERIALS & METHODS

Animals

All experiments were conducted in accordance with the guidelines of the Canadian Council on Animal Care and with ethical approval from the University of Alberta Health Sciences Animal Policy and Welfare Committee. Sprague-Dawley albino rats (Charles River Breeding Laboratories, St. Constant, QC, Canada) of both sexes were used. The pregnant dams were housed under veterinary supervision in the Health Sciences Laboratory Animal Services Department of the University of Alberta. Rats were maintained on Laboratory Rodent Diet (#5001; Lab Diet, Richmond, IN, USA) pellets and water *ad libitum* and kept on a 12 hour light/dark cycle. Pups were randomized into litters of 10 animals/dam 2 days following delivery. Following randomization, dams were rotated daily between litters to minimize variation. Dams were euthanized 14 days post-partum with an overdose of pentobarbital sodium injected intraperitoneally.

Hyperoxic Exposure

Pups of both genders were randomized into litters of 10 pups 2 days following delivery. They were placed into 0.14 m^3 Plexiglas chambers from days 4-14 PN and exposed to either hyperoxic (>95% O_2) or normoxic (>21% O_2) conditions (Figure 2.1). Oxygen concentrations were monitored daily (Ventronic Oxygen Analyzer, #5517, RDI, Temecula, CA, USA) and the carbon dioxide was filtered using barium hydroxide lime (Baralyme; Chemtron Medical Division, St. Louise, MO, USA). The environment was maintained at 26 °C and 75-80% humidity. The chambers were opened for less than 5 minutes per day to rotate dams, feed and water, clean the cages, and weigh the pups.

Adenovirus

The human 5LO adenovirus (AdV) used was generously provided by Dr. Ying-Yi Zhang (Boston University School of Medicine, Boston, MA, USA). This vector, Ad5LO, contains the cytomegalovirus (CMV) promoter-enhancer and the human 5LO gene, and is replication deficient. It has been established that this vector is expressed, translated, and biologically active in rat epithelial cells *in vitro* and *in vivo* [143, 144, 155-157]. An adenovirus expressing green fluorescent protein (AdGFP), generously provided by Dr. Jason Dyck (University of Alberta), was used as a control.

Adenoviral Propagation

Ad5LO was propagated by the University of Alberta Adenoviral Core Facility. AdGFP was propagated according to the following protocol adapted from Tong-Chuan *et al.* [158]. Human embryonic kidney (HEK) 293A cells (Invitrogen Cat. # R705-07) were grown in minimal essential media ((MEM) with Earle's Salts and 2 mM L-glutamine (Gibco Cat. # 11095-098 (500 mL x 10)), 10% fetal bovine serum (FBS), 1% MEM Non-Essential Amino Acids (Gibco Cat. # 11140-050 (100 mL)), and 1% Pen-Strep; with phenol red) on 175 cm^2 plates or flasks (seeded at 2-3 $\times 10^4$ cells/cm^2 + 25 mL media). When cells reached ~80% confluence (2 days), cells were split at a ratio of 1:5. Twenty-five 175mm^3 flasks were used for amplification of the virus (20 for purification and 5 for storage and later propagations). On the day of infection, cells were at ~80% confluence and were infected with 0.5μL (~12 MOI) of purified GFP adenovirus per flask.

Ten mL of media containing virus were added gently at the corner of each flask. They were incubated 1 h on a rocker to distribute the virus. After the incubation, 15 mL of media (containing 5% horse serum instead of FBS to reduce the growth rate of the cells.) were added to the flasks. Cells were incubated until they started showing cyto-pathic effects (CPE). CPE consist of cell rounding, disorientation, shrinking, swelling, death, detachment, or any other detectable changes in host cells due to viral infection. CPE began to be evident after 24 h and were fully developed after 36-72 h. Cells became rounded and detached from the plate before lysing (blebbing also occurred). GFP-fluorescence was monitored (Leica DM1RB Microscope, Germany) to ensure successful viral infection.

Cells were harvested 48 h after infection (when cells were 80% to 90% lysed). Remaining cells were detached by pipetting up and down with the media and scraping if necessary. Recovered cells were pooled along with the supernatant in 50 mL falcon tubes. Cells were lysed by freezing (liquid nitrogen for 30 min) and thawing (37°C water bath until thawed) 2 times to release the virus. After each freeze/thaw cycle, cells were mixed well for 30 sec. After the final thaw, cell debris was spun at 1000 × *g* for 10 min and the supernatant pooled in a sterile 1 L flask. Powdered $AmSO_4$ was slowly added to this crude viral lysate (CVL; 242.3 g/L) in the fume hood while stirring for 2 h. Contents were then transferred to sterile 50 mL conical tubes and centrifuged at 1000 × *g* for 10 min. Supernatant was discarded and the precipitate was re-suspended in 20 mL of sterile PBS in a 50 mL sterile tube. It was then centrifuged at 2500 rpm (1000×*g*) for 10 min and

the supernatant was collected in a fresh tube. Finally, the adenovirus was purified using a cesium chloride (CsCl) gradient.

Adenoviral Purification

A CsCl (filter sterilized) step gradient was generated in a 30 mL tube (Sorvall ultra bottles, Catalogue # 03719; Sealing Caps, Catalogue # 03614) by first layering 1 mL of 1.5 g/mL, then 6 mL of 1.35 g/mL, then 6 mL of 1.25 g/mL. 10 mL of CVL was overlaid on top of the gradient and spun for 22 h at 45000 rpm in a T-70I rotor (Beckman L8-70M Ultracentrifuge) at 10°C. Adenovirus banded at the junction of the two densest step gradients (approximately 3 cm from the bottom of the tube) and was blue/gray in colour. The immature virus banded in the 1.25g/mL gradient. The 1.5 g/mL band should be and was completely clear (since the spin was successful). The purified virus was harvested using a sterilized 9" Pasteur pipette. Virus was pooled in a 50 mL sterile tube. The density of the purified viral band was 1.33 g/mL, which confirmed viral purity. The virus was transferred to a Pierce Slide-A-Lyzer (10,000 MWCO; gamma irradiated) Cassette (Pearce Catalogue # P66807) using a syringe fitted with an 18 G × 1.5" needle. It was dialyzed for 4 h against 1 L of 10% glycerol in PBS (filter sterilized) and then placed in fresh solution overnight (stirring slowly at 4°C). After dialysis, the virus was aliquotted into 1.5 mL sterile microcentrifuge tubes and stored at 4 °C (stable for 4 years) until needed.

Titre determination by Plaque Assay

The titre assay was run in duplicate. HEK 293A cells were plated (1×10^5/mL) in 6-well plates, and grown at 37°C and 5% CO_2. Serial dilutions (10^2-10^{12}) of purified adenovirus (1 mL) were added to cells when they were around 60% - 70% confluent. Plates were incubated at 37°C for 4 h, after which the virus was removed and the cells were overlaid with 3 mL of 5% horse serum, 0.5% agar, 1 x MEM (no antibiotics). After 5 and 10 d, 2 mL of media were added to sustain the cells for the duration of the titer. Cells were monitored for plaque formation and counted daily. Values from the duplicates were combined and averaged. The titer was calculated as the number of plaques/well × 10^E dilution.

Adenovirus Studies

Expression of AdV in Rat Lung Epithelial L2 Cells

In preliminary studies, the expression of the human 5LO AdV (Ad5LO) and AdGFP was determined *in vitro* in the rat lung epithelial Type II L2 cell line (American Type Culture Collection, Manassas, Virginia, USA). L2 cells were grown in 90% F12K Nutrient Mixture (Gibco, Mississauga, ON, Canada) with 10% fetal bovine serum (FBS; Gibco) and antibiotic-antimycotic (Gibco; 100U penicillin/mL, 100ug streptomycin/mL, and 0.25 μg amphotericin B/mL) at 37 °C in 5% CO_2. Cells were grown in 75 cm^2 flasks and then 1 x 10^5 cells were seeded in each well of a 6 well plate. After 24 h, the media were removed and the cells washed with PBS. Cells were then starved of FBS for 24 h prior to infection with either Ad5LO or AdGFP. Infection was achieved with ~30 copies of each virus (1.5 X 10^7 pfu/well in 2mL of media) per cell. Following a 6 h incubation with the

virus, the media were changed and RNA was extracted from the cells 72 h later using TRIzol© (Invitrogen, Burlington, ON, Canada) to confirm stable expression (Figure 2.2).

Expression of AdV *In Vivo*

Under isoflurane (Halocarbon Laboratories, River Edge, NJ, USA) anaesthesia, 4 day-old rat pups were injected intratracheally (30 gauge needle) with 25 uL of either Ad5LO or AdGFP (both 8.1 x 10^9 pfu/mL), or vehicle (10% glycerol in PBS) control. This technique effectively restricts adenoviral expression to the lungs [155-157]. Vetbond© (3M, St. Paul, MN, USA) was used to adhere tissue together, and pups were then allowed to recover under a lamp on a heating pad. No adverse effects were observed, and once the rat pups had regained consciousness, they were returned to their mothers. Adenoviral delivery of genes directly to the lungs using this technique has been shown to have no effect on mortality, lung toxicity, or inflammation of the lungs [155, 157]. Pups were euthanized with pentobarbital sodium (Euthanyl; 100 mg/kg, Bimeda-Mtc, Cambridge, ON, Canada) at 9 or 14 days PN.

Animal and Tissue Processing

Every animal euthanized in the course of the LT Receptor study was dissected and their brains, hearts, livers, lungs and kidneys removed and weighed on days 4, 6, 9, 12, 14 PN. Organs were blotted dry before weighing to remove excess fluid and blood. Animals in the 5LO Adenoviral study had only the blotted lung weights measured. Lung volumes in both the LT Receptor and 5LO Adenoviral groups were determined as outlined below for animals used in the perfusion studies. For morphometric and GFP fluorescence studies,

tissues were perfusion fixed and processed as outlined below. For RNA, protein, and EIA studies, the lungs were removed, weighed, and snap frozen in liquid nitrogen and tissues were processed as outlined below.

Tissue Fixation

For morphometric and GFP fluorescence studies, pups were euthanized with an intraperitoneal injection of pentobarbital sodium (Euthanyl; 100 mg/kg, Bimeda-Mtc, Cambridge, ON, Canada). A midline laparotomy was performed in the upper abdomen and the internal organs were removed to reveal the diaphragm. The diaphragm was punctured to create a bilateral pneumothorax. An incision was made in the throat area to expose the trachea. Two sutures were placed dorsal to the trachea and a small slit made on the ventral surface. A small catheter was inserted into the slit and tied off with one of the sutures to prevent leakage. Lungs were processed differently from this point depending on what they were used for.

Morphometric Analysis

The lungs were perfused with 4% paraformaldehyde for 5 min at 20 cm of H_2O pressure. After 5 min, the catheter was removed and the trachea tied off with the remaining suture. An incision was made along the left side of the sternum to open the ribcage and the lungs were delicately cut out, taking care not to puncture them. The lungs were placed in 4% paraformaldehyde overnight at 4 °C. All excess tissue was then removed from the lungs. The bronchi were tied off with sutures and the right and left lungs separated. Lungs were weighed in 4% paraformaldehyde to determine their volume. The right lung was

separated into its 4 lobes. The right middle lobe was selected for all lungs and placed into tissue cassettes and washed 3 times for 30 min in PBS. They were then soaked overnight in 0.1M glycine in PBS. Lobes were then dehydrated with 1 h washes in each of 70%, 80%, 90%, 95%, and 3x 100% EtOH and 1x 100% xylene. Lobes were left overnight in paraffin wax at 57°C. Tissues were embedded in wax for slicing by microtome (superior lobe tip oriented towards the bottom of the mould).

Slide Preparation

The right caudal lobe was embedded with the tip against the bottom of the mould in all samples [159]. This ensured that all lungs would be sliced equally and that the sections were representative of the entire lung. Serial step sections were sliced by microtome (Leica RM2135, Germany) at 5 μm along the longitudinal axis of the lobe. The distance between sections was calculated to allow for systematic sampling of the lobe. Sections were mounted on slides (Fisherbrand Superfrost Plus, Fisher Scientific, Pittsburgh, PA, USA), dried overnight at 37 °C, and then stained. Paraffin wax was removed with 2 washes for 5 min in xylene. Slices were re-hydrated by washing for 5 min in each of 100% (x2), 95%, 90%, 70%, 50% ethanol, and ddH_2O. Slides were stained with Harris Hematoxylin (Vector Laboratories, Burlingame, CA, USA) for 15 sec, and then rinsed with warm tap water for 5 min. They were then stained with Eosin Yellowish (Fisher Scientific, Pittsburgh, PA, USA) for 5 min, and then rinsed in ddH_2O for 5 min. Sections were dehydrated by washing for 5 min in each of 70%, 95%, 100% (x2) ethanol, and xylene (x3). Coverslips (Fisher Scientific, Pittsburgh, PA, USA) were mounted with DPX Mountant (Fluka, Switzerland) and dried overnight.

Morphometric Analysis

The right caudal lobe was used for morphometric analysis because previous studies have shown that any lobe of the lung can be used, since no differences were found between them [159, 160]. Slides were first randomized and coded to ensure that the analysis was blinded. The technique was performed using a light microscope (Leica DMLA, Germany) with a motorized stage attached. Sections were imaged with Open Lab© version 3.5 software. A point target was superimposed on the section. The top left and bottom right points were entered into the computer to establish section boundaries and a grid pattern for the microscope to follow. The motorized stage travelled sequentially along this grid. Each parameter the target point landed on was counted using the 40X objective lens. Parameters measured were airspace, septa, bronchi, and vessels. A minimum of 300 points were counted per lung. The mean linear intercept method was used to quantify alveolar structures [161]. Briefly, the volume densities of parenchyma (alveolar airspace, alveolar septa, alveolar ducts, respiratory bronchiolar tissues, blood vessels, and their contents) and non-parenchyma (bronchi and bronchioli >20 μm and larger connective tissue strips) were determined using the whole lobe as a reference space [161]. Absolute volumes were calculated for each animal as the product of volume densities for each variable and the respective lung volume [161].

For Fluorescence Analysis

The lungs were perfused with 0.8 (d9) – 1.0 (d14) mL of Tissue-Tek© O.C.T. Compound (Sakura, Torrance, CA, USA). The right caudal lobe was then tied off with a suture and isolated from the other lobes. It was then embedded in O.C.T. and flash frozen in liquid

nitrogen. Lobes were stored at -80 °C until slicing. Sections of 10 μm were made using a cryostat (Leica CM 1900, Germany). Sections were dried in the dark at room temperature for 1 h and then imaged immediately using an Olympus BX40 Microscope.

RNA Analysis

Principle

Real-Time Reverse Transcription-Polymerase Chain Reaction (RT-PCR) is a technique used for measuring the abundance of mRNA transcripts. RNA cannot act as a template for PCR, so first it must be transcribed into cDNA in a process termed reverse transcription (RT). Random DNA hexamer primers are annealed to the RNA then extended using a reverse transcriptase enzyme. The resulting cDNA can then be used for PCR analysis. The PCR reaction involves the annealing of two oligonucleotide primers specific to the gene of interest followed by the elongation of these primers by a heat-stable DNA polymerase enzyme. The DNA strands are then heated to denature them and cooled so that the primers anneal and extend again in repetitive cycles to amplify the target DNA sequence. Real-Time PCR allows the analysis of the progression of a PCR reaction as it is running. SYBR Green (Applied Biosystems, Foster City, CA, USA) is a molecule which fluoresces at 521 nm when it is bound to double-stranded DNA and excited by a light source at 494 nm. By exposing individual PCR reactions to a beam of light and measuring the fluorescence each time the cycle finishes its primer annealing/DNA extension phase it is possible to measure the amount of double-stranded DNA present. A threshold can then be calculated, above which the reaction is deemed to

have reached its exponential stage. The number of cycles needed before a reaction crosses this threshold is inversely proportional to the amount of cDNA being amplified.

Once the programmed number of PCR cycles has been completed a melt curve of the reaction products is performed. The temperature of the reaction is progressively increased and the fluorescence assessed at each increment. Once the DNA denatures into single strands the amount of fluorescence drops sharply. The temperature at which the DNA denatures depends on the strand length and the sequence of the product. If a single product is formed in the PCR reaction then there should be a single drop in the level of fluorescence. The presence of multiple temperature-dependent drops in fluorescence would suggest non-specific amplification, contamination, or primer dimers.

In order for Real-Time PCR to measure the actual quantity of the target cDNA present it is necessary to first calculate a standard curve. This is achieved by performing PCR reactions with a number of serial dilutions of cDNA. The standard curve calculates both the efficiency of the PCR reaction and the correlation coefficient of the relationship between the amount of cDNA template and the threshold cycle.

RNA

Total RNA was extracted from lung samples using TRIzol™ (Invitrogen, ON, Canada). This reagent works by dissolving the RNA into solution as the tissue is homogenized. One mL of TRIzol was added to approximately 0.1 mg of lung tissue. Addition of 200 μL chloroform separates the homogenate into 3 phases, including an aqueous phase

containing the RNA. This phase was then isolated and the RNA was precipitated with isopropyl alcohol and washed with 1 mL of 75% ethanol. RNA pellets were then re-suspended in 50 uL of sodium citrate (1 mM, pH 6.4). Following extraction, RNA samples were treated with DNAse I (Ambion DNA-free Kit, Ambion, Austin, TX, USA) to remove any DNA that might be remaining. RNA concentration was determined by measuring sample absorbance in a spectrophotometer (Hewlett Packard 8452A). The optical density (OD) was measured at 260 nm and at 280 nm. RNA concentrations were then calculated using the following equation:

RNA concentration (μg/μL) = (OD260nm x 40* x 500**)/1000***

* 1 OD unit for single strand RNA is 40 ng/μL
** RNA dilution
*** Conversion to μL

A 260nm/280nm ratio above 1.8 was used as a cutoff for contamination.

Reverse transcription

Two μL (2000 ng) of RNA was incubated at 65 °C for 5 minutes with 1 μL of random primers (Invitrogen, ON, Canada), 2 μL of 10 mM dNTPs (Invitrogen, ON, Canada) and 19 μL of DEPC treated (RNase/DNase free) water. To this 8 μL of 5× RT Buffer (Invitrogen, ON, Canada), 4 μL of 0.1 M DTT (Invitrogen, ON, Canada) and 2 μL of RNase Out (Invitrogen, ON, Canada) were added. Two μL of either Superscript II Reverse Transcriptase enzyme (Invitrogen, ON, Canada) or 2 μL of DEPC treated water (-RT control) were then added. The reaction was then incubated at 25 °C for 25 min followed by 50 min at 42 °C and then 15 min at 70 °C to inactivate the superscript enzyme. The cDNA was then stored at -20 °C for up to 7 days.

Real-Time Polymerase Chain Reaction

Oligonucleotide primers specific for each gene were designed or obtained as indicated in (Table 2.1). The primer annealing temperature was optimized for each primer set. Correct product formation was confirmed by agarose eletrophoresis and sequencing. All PCR reactions (except human-only 5LO) of 25 μL were run in triplicate and prepared containing 1 μL of cDNA (5 ng/μL), 12.5 μL 2× SYBR Green master mix (Applied Biosystems, CA, USA), 0.25 μL AmpErase® (Applied Biosystems, CA, USA), 200 nM forward and reverse primers and 10.25 μl of water. Human-only 5LO reactions of 25 μL were run in triplicate and prepared with 1 μL of cDNA (5 ng/μL), 10 μL of TaqMan Universal PCR Master Mix (no AmpErase®; Applied Biosystems, CA, USA), 1 μL of 20× assay mix (forward and reverse primers and TaqMan probes; Applied Biosystems, CA, USA), and 8 μL of water. Samples were loaded into 96 well PCR plates and then placed into an *i*Cycler (Bio-rad, ON, Canada). The protocol used during each PCR run was: (1) initial denaturation step (95 °C for 10 min), (2) followed by 40 cycles of a denaturation step (95 °C for 20 sec) and an amplification and quantification step (at each primer's specific annealing temperature for 1 min), (3) followed by a melt curve step where the temperature was gradually increased by 0.5 °C every 12 sec from 55 °C to 95 °C (to confirm product uniformity). Mouse cyclophilin (mCyc) primers for the housekeeping gene cyclophilin, were used as a reference gene for all samples. In addition, a single sample was run on each plate to assess inter-assay variation, which was calculated using the formula below. Variation was found to be less than 10%.

$$\text{Inter-assay coefficient of variation (\%)} = 100 \times \frac{\text{Standard deviation of density of same sample on different plates}}{\text{Mean density of same sample repeated on different plates}}$$

Data analysis

Rat mRNA measurements were normalized to cyclophilin (Cyc) mRNA. Standard curves for each gene of interest (GOI) and cyclophilin were generated by serial dilutions of pooled cDNA samples. The amplification efficiency for each primer set was determined by converting the slope of the standard curve using the algorithm $E = 10^{-1/slope}$. For each GOI, the mean threshold cycle (from triplicate reactions) was corrected for the efficiency of the reaction and expressed relative to a control sample for each experiment [162]. GOI levels were then expressed relative to cyclophilin levels using the following formula:

$$Ratio = \frac{E_{GOI}^{\Delta Ct(Control-Sample)}}{E_{Cyc}^{\Delta Ct(Control-Sample)}}$$

The mean of each treatment group was determined. Results were expressed as a percentage of the sample that was run on all plates. Results for all mRNA measurements were analyzed by a two-way analysis of variance (post-hoc test using the Holm-Sidak method). Significance was achieved at $p < 0.05$.

Protein Analysis

Protein Extraction

Protein was extracted from lung samples by homogenizing 0.1 g of tissue in 1 mL of lysis buffer (50 µL 1 M Tris, 27.4 µL 5 M NaCl, 5 µL 200 mM Na-orthovanadate, 10 µL 0.5 M EDTA, 10 µL Triton X-100 (VWR International, ON, Canada), 5 µL 200 mM phenylmethylsulphonofluoride (PMSF), 10 µL Protease Inhibitor Cocktail (Sigma, ON,

Canada) and 882.6 μL of H_2O) followed by centrifugation at 1000 × *g* for 20 min at 4 °C. The supernatant was then transferred to a fresh tube and stored at -80 °C until needed.

BCA Assay

Principle

Total protein concentration was determined using a Micro BCA™ Protein Assay Reagent Kit (Pierce, IL, USA). This assay is based on the following two reactions:

Reaction (A) Protein (peptide bonds) + Cu^{2+} → tetradentate-Cu^{1+} complex

Reaction (B) Cu^{1+} complex + Bicinchorinic acid (BCA) → BCA-Cu^{1+} complex (purple coloured)

The product of this reaction is purple coloured and absorbs strongly at 562 nm. The intensity of absorption at this wavelength is proportional to the concentration of protein in the sample.

Procedure

Extracted proteins were diluted to concentrations of both 1/75 and 1/150 with the lysis buffer used for protein extraction. These dilutions were then pipetted in triplicate into 96 well plates (Corning Inc., NY, USA) and the BCA reagent solution added. Plates were then covered and incubated at 37 °C for 2 h. The plate was then placed into a plate-reader (Molecular Devices UV Max for receptor ontogeny study; or, BIO-TEK EL808 for adenoviral study) and absorbance measured at 562 nm. Protein concentrations were calculated by comparing the OD to a standard curve of known protein concentrations (bovine serum albumin (BSA)). Triplicate results were averaged and the protein

concentration of the two dilutions compared. Results within 10% of each other were considered to be accurate. For consistency, the concentration value from the 1/75 dilution was used when calculating the volume of sample to load onto gels for Western blotting.

Western Blotting

Principle

The abundance of the protein under investigation was measured using sodium dodecyl sulphate-polyacrylamide gel electrophoresis (SDS-PAGE). SDS denatures proteins by wrapping itself around the polypeptide backbone. It is an anionic detergent so it confers a negative charge to a polypeptide proportional to its length. The SDS-protein complexes can be separated by size using electrophoresis through a polyacrylamide gel, with proteins moving towards the anode at a rate inversely related to their size. The pore size of the gel depends on the concentration of acrylamide and cross-linking bisacrylamide used for its synthesis. In SDS-PAGE, migration is determined by molecular weight, not by electrical charge [163].

Once proteins have been separated by SDS-PAGE they can then be transferred onto a nitrocellulose membrane for analysis and quantification. To detect an antigen on the membrane a specific primary antibody is incubated with the membrane. Unbound antibodies are washed away after the incubation. To detect the presence of the primary antibody an anti-immunoglobulin secondary antibody is incubated with the membrane. This is coupled to a reporter molecule such as the enzyme horseradish peroxidase (HRP). After incubation excess secondary antibody is washed off, and a substrate is added which

emits light upon reaction with the conjugate, showing a visible band where the primary antibody is bound. Band intensity is correlated to antigen abundance. The intensity of this band is then determined by densitometry.

Procedure

Polyacrylamide gels were cast using glass plates and combs with a dual gel caster (BioRad, ON, Canada) and 12% acrylamide. The resolving gel (15 mL resolving gel: 7.25 mL distilled H_2O, 4 mL 30% acrylamide/0.8% bisacrylamide solution, 3.75 mL 4x Tris-Cl/SDS (pH 8.8), 50 μL 10% (w/v) ammonium persulphate and 10 μL N,N,N',N'-tetramethylethylenediamine (TEMED)) was poured between the glass plates at a thickness of 1.5 mm to a level 1.5 cm below the position of the wells. A small amount of de-ionised water was then pipetted over the surface of the gel to ensure a straight edge and to prevent the top of the gel drying during polymerization.

After the gel set (~45 min) the water was removed. Stacking gel (5 mL stacking gel: 3.05 mL distilled H_2O, 0.65 mL 30% acrylamide/0.8% bisacrylamide solution, 1.25 mL 4x Tris-Cl/SDS (pH 6.8), 25 μL 10% (w/v) ammonium persulphate and 5 μL TEMED) was poured over the top of the resolving gel and a 15-well comb inserted to create wells. This comb was then removed after polymerisation and the gels were transferred to a vertical slab electrophoresis unit (Biorad Mini-Protean 3, Biorad, ON, Canada). The wells and chamber were filled with Tris/Glycine/SDS electrophoresis buffer (Bio-Rad, 161-0732, Hercules, CA, USA).

Samples were prepared for loading by the addition of 5 × SDS loading buffer (1 mL 0.5M Tris-Cl, pH 6.8, 1 mL β-mercaptoethanol, 4 mL glycerol, 2 mL 20% SDS, 4 mg bromophenol blue) and water. Samples were denatured at 95 °C for 5 min and 60 μg of protein was loaded into each lane of the gel. Each gel was also loaded with a pre-stained protein ladder (Fermentas, SM0671) as well as a biotinylated ladder that was HRP-conjugated (Bio-Rad, 161-0319, ON, Canada). The same sample was run on a lane of every gel to compare the protein abundance between gels.

Proteins were separated by electrophoresis at 15 mA until the colour in the loading buffer reached the bottom of the gel. Proteins were then transferred to nitrocellulose membranes (Bio-Rad, 161-0115, ON, Canada) using an electroblotting apparatus (Bio-Rad Mini-Protean 3, Biorad, ON, Canada). The gel and the membrane were sandwiched between two layers of blotting paper soaked in transfer buffer (Bio-Rad, 161-0734, Hercules, CA, USA) and supported by two foam pads. These layers were placed into a cassette and inserted into the electroblotter which was then filled with transfer buffer. An ice block was used to prevent overheating. The proteins were then blotted for 60 min at 100 volts in a cold room (4 °C).

The nitrocellulose membranes were incubated for 1 h at room temperature in 50 mL of blocking buffer (7% non-fat milk in TBS-0.1% Tween) in order to reduce non-specific binding of the antibody. The blocking solution was removed by washing 4 times with TBS-0.1% Tween. Membranes were then incubated overnight on a rocker at 4 °C in 4 mL of primary antibody solution (antibody diluted to a concentration of 1:1000 in 5%

non-fat milk in TBS-0.1% Tween). Primary (and secondary) antibody concentrations were optimised by using a series of dilutions on a gel loaded with a single sample. The concentration was selected which gave the strongest band with minimal background. Blots were then washed 4 more times for 15 min in TBS-0.1% Tween to remove any unbound primary antibodies. Membranes were then incubated at room temperature with 20 mL of HRP-conjugated goat anti-rabbit antibodies (Jackson Immunoresearch Laboratories, West Grove, Pennsylvania, USA) at a dilution of 1:4000 in TBS-0.1% Tween containing 5% non-fat milk. Following the incubation with the secondary antibody, membranes were washed 4 times for 5 min with TBS-Tween 0.15%. The bands were visualised by immersion, protein side down, in 2 mL of Enhanced Chemiluminescence Western Blotting Detection Reagents (Amersham Biosciences UK Limited, Buckinghamshire, UK) and agitated for 2 min. Gel images were taken with a Fluor-S Max multi-imager (Bio-Rad, CA, USA) and densitometric analysis was performed using Quantity-One software (Figure 2.3).

Data Analysis

Data were calculated as a percentage of the single reference sample that was run on all gels.

Enzyme Immunoassay Experimental Protocol

Extraction

Leukotrienes were extracted from lung tissue for measurement by enzyme immunoassay (EIA). The protocol was modified from an existing in-laboratory protocol for extracting

prostaglandins in combination with a protocol accompanying LTB_4 (Cat. # 900-068) and CysLT (Cat. # 900-070) EIA kits from Assay Designs (Ann Arbor, MI, USA). EIA kits are extremely sensitive; therefore, all solutions were prepared using ultra-pure Milli-Q water. Samples were kept on ice throughout the extraction procedure to minimize product breakdown.

Tissues were pulverized in liquid nitrogen and 0.05g of tissue was homogenized in 500 uL of 100% ethanol and 50 uL of ^{3}H-PGE_2 (2500 cpm; used to determine extraction recovery percentage) in a 5 mL glass test tube. Two blanks containing only ethanol and ^{3}H-PGE_2 were also homogenized to ensure that the presence of tissue did not affect the recovery values. Following homogenization, 4 mL of 50 mM citrate buffer (pH 3.5) were added to each sample to reduce the ethanol concentration to below 15%, which is necessary for sample purification. Samples were then mixed vigorously and allowed to settle at room temperature for 5 min. They were then centrifuged at 2500 rpm for 10 min. Ninety percent (4.05 mL) of the supernatant was withdrawn for sample purification. The remaining protein pellet was capped and stored at 4 °C and assayed within 24 h using the Micro BCA Protein Assay Reagent Kit (Pierce, Rockford, IL, USA; see BCA protocol above). Protein measurements were used to normalize LT levels, which are expressed as pg/mg protein (see below).

Purification

Samples were purified according to an existing in-laboratory protocol. C-18 solid phase extraction (SPE) Sep-Pak cartridges were attached to 5 mL syringes and activated with

methanol followed by 5 mL of Milli-Q water. The sample was passed slowly through the SPE column. The column was then washed with 5 mL Milli-Q water, followed by 5 mL hexane. The LTs were eluted with 5 mL ethyl acetate containing 1% methanol. The ethyl acetate was evaporated to dryness under a nitrogen stream. Samples were reconstituted by vortexing in 450 μL EIA assay buffer (Assay Designs, Cat. # 80-0011, Ann Arbor, MI, USA). Fifty μL of each sample were used for scintillation counting (to determine recovery percentages). The remaining sample (400 μL) was aliquotted and stored at -80°C until assayed.

Assay Protocol

Leukotriene levels were quantified using an EIA kit specific for LTB_4 or the CysLTs (Assay Designs, Ann Arbor, MI, USA). All EIAs were performed on a 96 well plate. Each well was pre-coated with secondary antibodies. The assays are based on the competition between the LTs contained in a sample/standard and a synthetic LT conjugated to an alkaline phosphatase tracer for a limited number of primary antibody binding sites (LTB_4-specific IgG or $LTC_4/D_4/E_4$-specific IgG). The antibody-LT complex (sample/standard or tracer) binds to the secondary antibody site previously attached to the well. Since the amount of tracer is held constant while the sample concentration varies, the amount of LT in a sample is inversely proportional to the amount of tracer in the well. Following incubation for 2 h at room temperature, the wells were washed to remove any unbound LT-antibody complexes. Substrate was then added to each well and the plate was incubated at 37 °C for 2 h. The reaction was stopped using an acidic "stop solution". The substrate compound gives the solution a yellow colour with a strong absorbance at

405 nm. The intensity of this colour is proportional to the amount of tracer bound to the well and inversely proportional to the amount of sample LT in the well during the incubation.

Samples were assayed in either duplicate or triplicate, depending on plate space. A standard curve and four controls were assayed in duplicate for each plate. The four control assays were as follows: (1) Total Activity (TA) – total possible enzyme activity (maximum absorbance of the tracer), (2) Total Bound (B_o) – total possible binding (tracer and antibody only), (3) Non-Specific Binding (NSB) – non-specific (non-immunological) binding of the tracer to the well (tracer only), and (4) Blank (B) – background absorbance of the substrate reagent. The tracer was not added to the TA well until after the incubation and washing steps. Substrate reagent was added to the blank well after incubation and washing steps. These controls were used to calculate final results talking into account background absorbance and binding.

Assay Characteristics

The detection limits for the LTB_4 and CysLT EIAs are 11.7-3000 pg/mL and 78.1-2500 pg/mL, respectively. The LTB_4 assay exhibits 100% specificity for LTB_4 and <0.2% for the CysLTs. The CysLT assay exhibits 100% specificity for LTC_4, 115.12% for LTD_4, 62.74% for LTE_4, and 1.16% for LTB_4. Therefore, the relative concentrations of the LTs in the sample can cause variation in the results.

Calculation of Final Concentrations

All assay values were calculated against a standard curve of known concentrations (pg/μL). Final concentrations of each sample were expressed as pg/mg protein. The recovery factor is a measure of the effectiveness of the extraction procedure and was calculated for each individual sample. This factor was adjusted to account for the loss of 10% of the supernatant in the extraction procedure. The following formulae were used to calculate the concentration of LTs in a sample:

$$\text{Recovery Factor} = \frac{\text{(Initial Sample Volume)}}{\text{(Recovery Sample Volume)}} \times \frac{\text{(Final cpm} - \text{Background cpm)}}{\text{(Initial cpm} - \text{Background cpm)}} \times 100$$

$$\text{Adjusted Recovery Factor (adjusted for sample loss)} = \frac{\text{Recovery Factor}}{0.90}$$

$$\text{Final Concentration (pg/mg protein)} = \frac{\text{Sample (pg/mg) x Total Initial Sample Volume (μL)}}{\text{Adjusted Recovery Factor}} \Big/ \text{mg protein}$$

Statistical Analysis

A two-way analysis of variance (ANOVA) comparing time with treatment was performed for most experiments using SigmaStat software (Version 3.1, Systat, Point Richmond, CA, USA). A one-way ANOVA was performed on 5LO Adenoviral EIA and morphometry data that compared treatment alone. When a significant F value was detected, the Holm-Sidak post-hoc test was performed to separate the effects. Differences were accepted as significant at $p \leq 0.05$. All data were expressed as mean ± standard error of the mean (SEM).

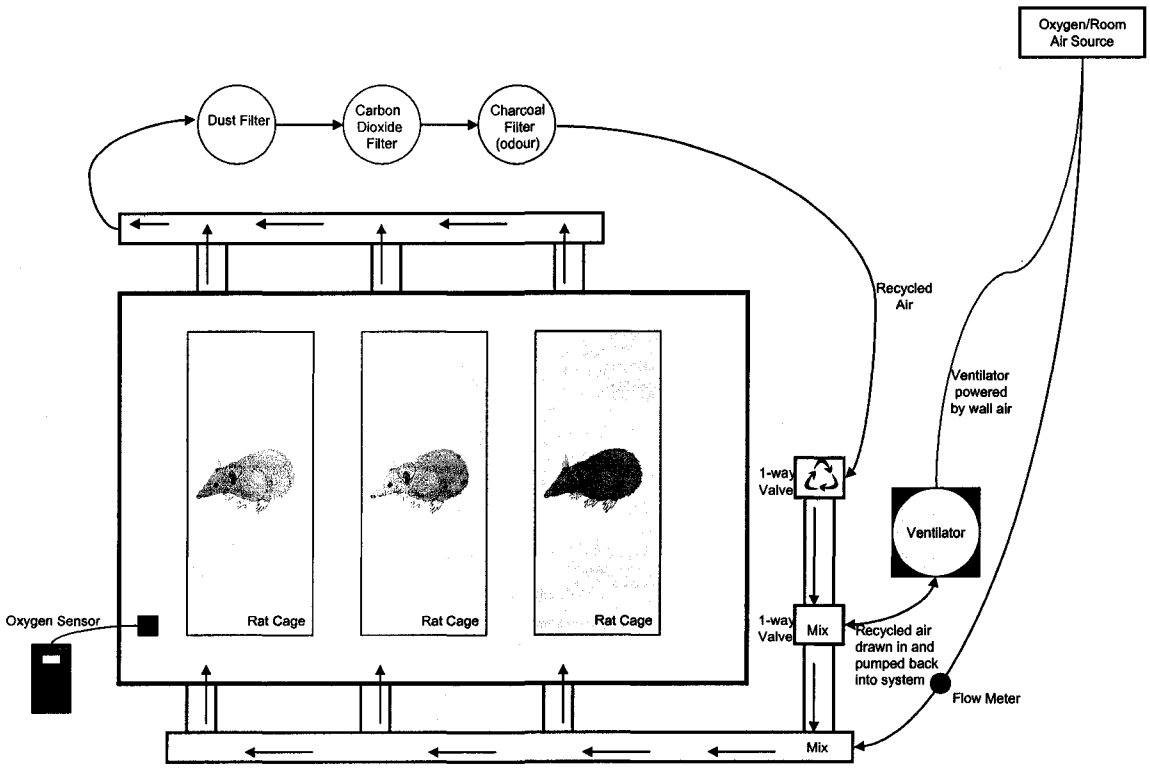

Figure 2.1: Exposure Chambers

This figure illustrates the chambers used to expose pups to either normoxia or hyperoxia. Oxygen levels were monitored with an oxygen sensor and the gases were filtered for dust, carbon dioxide, moisture, and odour. The ventilator attached to the system was not utilized as oxygen levels were maintained at target levels.

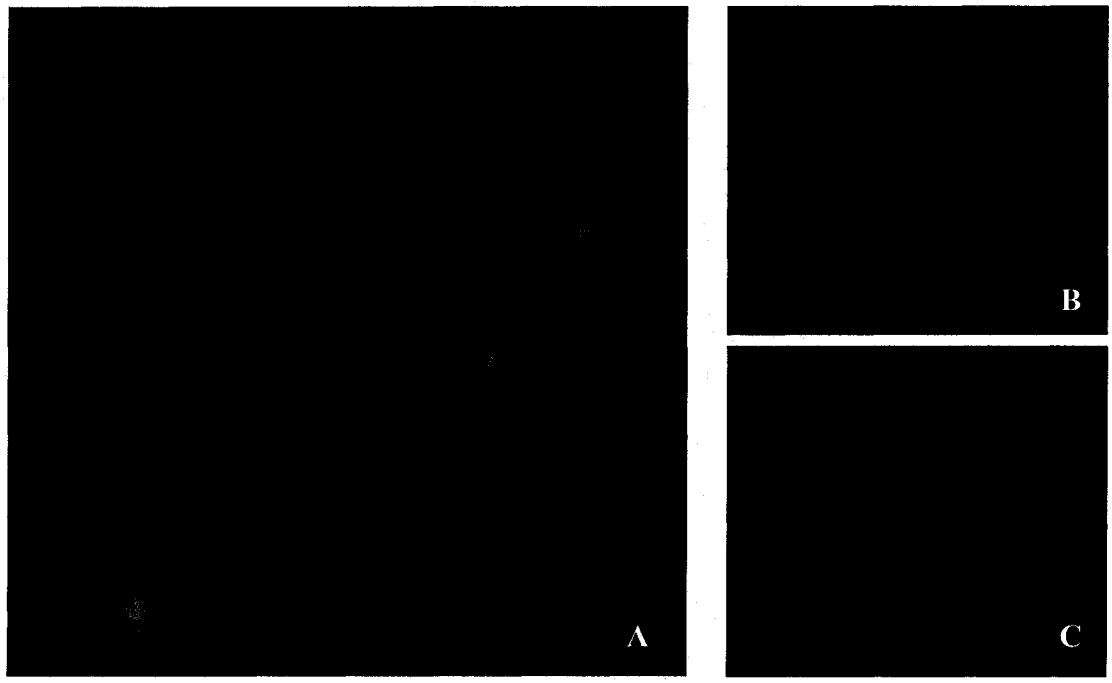

Figure 2.2: Preliminary *In Vitro* Adenoviral Experiments

This figure illustrates viral expression in rat type II epithelial cells during *in vitro* trial experiments. Cells expressing GFP are clearly visible (A), indicating successful viral delivery of the GFP gene. Control (B) and Ad5LO (C) are shown for comparison and to demonstrate that the cells did not autofluoresce.

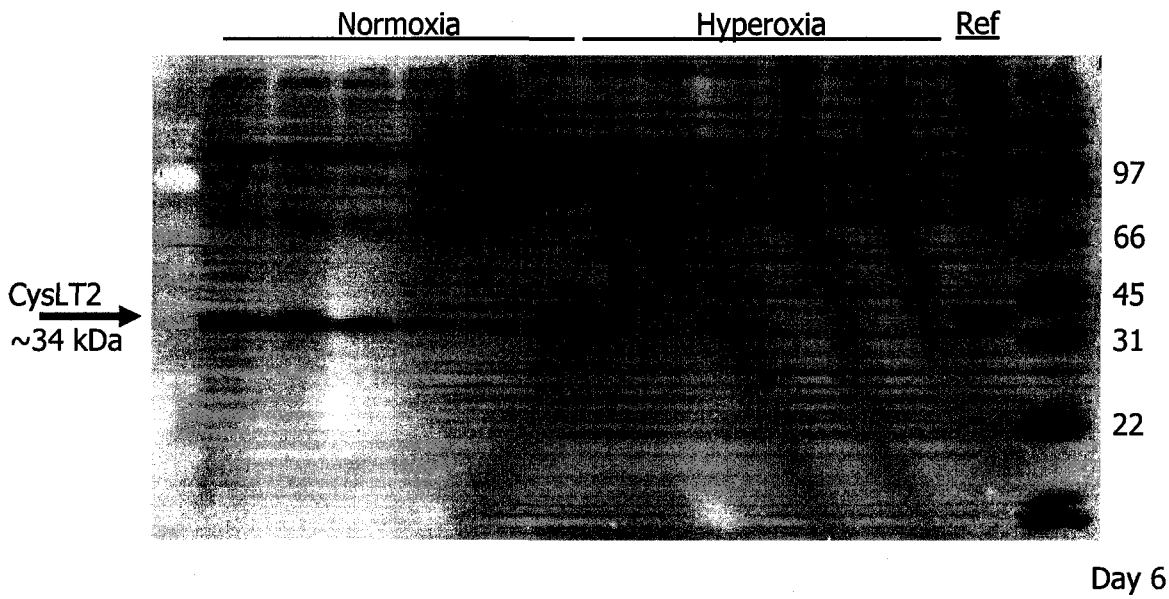

Figure 2.3: Representative Western Blot

A representative Western immunoblot of $CysLT_2$ is shown. The bands for $CysLT_2$ on d6 PN are clearly visible at 34 kDa in normoxic samples, but the signals are markedly weaker in hyperoxic pups. A reference sample, run on all gels, is also shown. The antibody used was insufficiently specific for use in immunohistochemistry studies.

Table 2.1A

Gene	Accession Numbers	Forward Primer	Reverse Primer	Product Size (bp)	Annealing Temp. °C
BLT_1	NM_021656	ATGGCTGCAAACACTAC	GGACAATGGGCAACAGA	76	59
BLT_2	NM_053640	ATGTCTGTCTGCTACCA	ACTCAGCAGCGTCTCATT	45	56
$CysLT_1$	NM_053641	ATGGTTGGAGCTGAAAA	GAAACCCACAACGGAGAT	120	56
$CysLT_2$	NM_133413	GGGCTTCTTGCTTCCATT	CAGAGTGATGACCGTGGC	149	57
r5LO	NM_012822	AAAGGCTGTTCTAGGTGG	GGTTACTAAGCTGGACTGG	134	53
FLAP	NM_017260	AAGAGGCTGTGGGCAATG	ACCCGCTCGAAGGCAAG	151	53
Tropoelastin	J04035	CCTGTCCCTGACTCCCATTA	CAGTGTGAGAAGTCGTCGGA	76	60
GFP	N/A	TCGTGACCACCCTGACCT	GAAGATGGTGCGCTCCTG	119	60
mCyclophilin	M19533	CACCGTGTTCTTCGACATCAC	CCAGTGCTCAGAGCTCGAAAG	114	60

Table 2.1B

Gene	Accession Numbers	Forward Primer	Reverse Primer	TaqMan Probe	Annealing Temp. °C
h5LO	NM_000698	GCACACTGCCAGTCTCACT	GCAGGCTGGAGTCCATCTG	AAGGCCAGCTGCCCC	60

Table 2.1: PCR Primers

A table describing the primer sequences used, for both Sybr Green (2.1A) and TaqMan (2.1B). All were designed and optimized by our lab.

CHAPTER 3 – RESULTS

Study 1: Effects of Hyperoxia on the Leukotrienes and Their Receptors

Lung mRNA & Protein Analysis

The aim of this study was to examine the ontogeny of expression of the LT receptors during lung development in normoxic and hyperoxic conditions. Real-Time RT-PCR analysis and Western immunoblotting (for CysLT receptors) were used to assess receptor expression. The primers used for the Real-Time RT-PCR analysis were designed to amplify a sequence unique for rat BLT_1, BLT_2, $CysLT_1$, or $CysLT_2$. Antibodies were available for $CysLT_1$ and $CysLT_2$ so their protein levels were measured as well.

BLT1

The developmental changes over the first 14 days in total lung mRNA abundance levels for BLT_1 were examined and compared to the effects of hyperoxia. By extrapolating from previous data, we hypothesized that hyperoxia would increase BLT_1 mRNA expression as previous data indicated that LTB_4 inhibits lung alveolarization [141]. Normoxic receptor levels increased from d6-12 and then decreased on d14 ($p < 0.001$) (Figure 3.1A). Exposure to oxygen (>95%) stimulated a sharp increase in BLT_1 receptor mRNA abundance on d6 ($p < 0.001$) and a smaller one on d9, since normoxia BLT_1 mRNA levels were rising, but the hyperoxic mRNA levels were lower later in development on d12 ($p < 0.05$) and d14.

BLT2

We hypothesized that like BLT_1, BLT_2 would be increased by exposure to hyperoxia due to the inhibitory effect of LTB_4 on lung development [141]. BLT_2 mRNA decreased with

time overall ($p = 0.005$), and, in contrast to our predictions, exposure to hyperoxia caused an overall decrease in expression ($p < 0.001$). There was a significant decrease in receptor expression on d6 ($p < 0.05$) due to oxygen exposure (Figure 3.1B).

CysLT1

We hypothesized that since LTD_4 has been shown to enhance lung development, $CysLT_1$ would be reduced in lungs exposed to high oxygen [141]. Although there was no significant effect of time, hyperoxia caused a decrease in receptor expression ($p < 0.001$). Oxygen exposure also caused a significant decrease ($p < 0.001$) in $CysLT_1$ expression on d14 (Figure 3.2A).

In contrast, $CysLT_1$ protein mass decreased over time ($p < 0.001$), but hyperoxia stimulated protein levels ($p < 0.001$). Hyperoxia triggered significant increases in receptor protein overall ($p < 0.001$) and on d6 ($p < 0.05$) and d14 ($p < 0.05$) (Figure 3.2B).

CysLT2

We hypothesized that because $CysLT_2$ plays a relatively minor role in the lung and is acted on equally by LTC_4 and LTD_4, which have opposite effects on lung development, $CysLT_2$ levels would show no significant change when exposed to hyperoxia [141]. There was an overall increase in receptor mRNA expression during development ($p < 0.001$), and a significant increase in hyperoxia ($p < 0.001$). The interaction indicated an increase of expression of lung $CysLT_2$ mRNA on d12 ($p < 0.001$) in animals exposed to

hyperoxia, but this effect was reversed on d14 where hyperoxic animals showed a decrease in expression ($p < 0.05$) (Figure 3.3A).

$CysLT_2$ protein levels also increased with time ($p < 0.001$), but exposure to hyperoxia suppressed this increase ($p < 0.001$). Animals raised in high oxygen had significantly lower levels of $CysLT_2$ on d6 ($p < 0.001$) and d12 ($p < 0.05$) versus normoxic animals (Figure 3.3B).

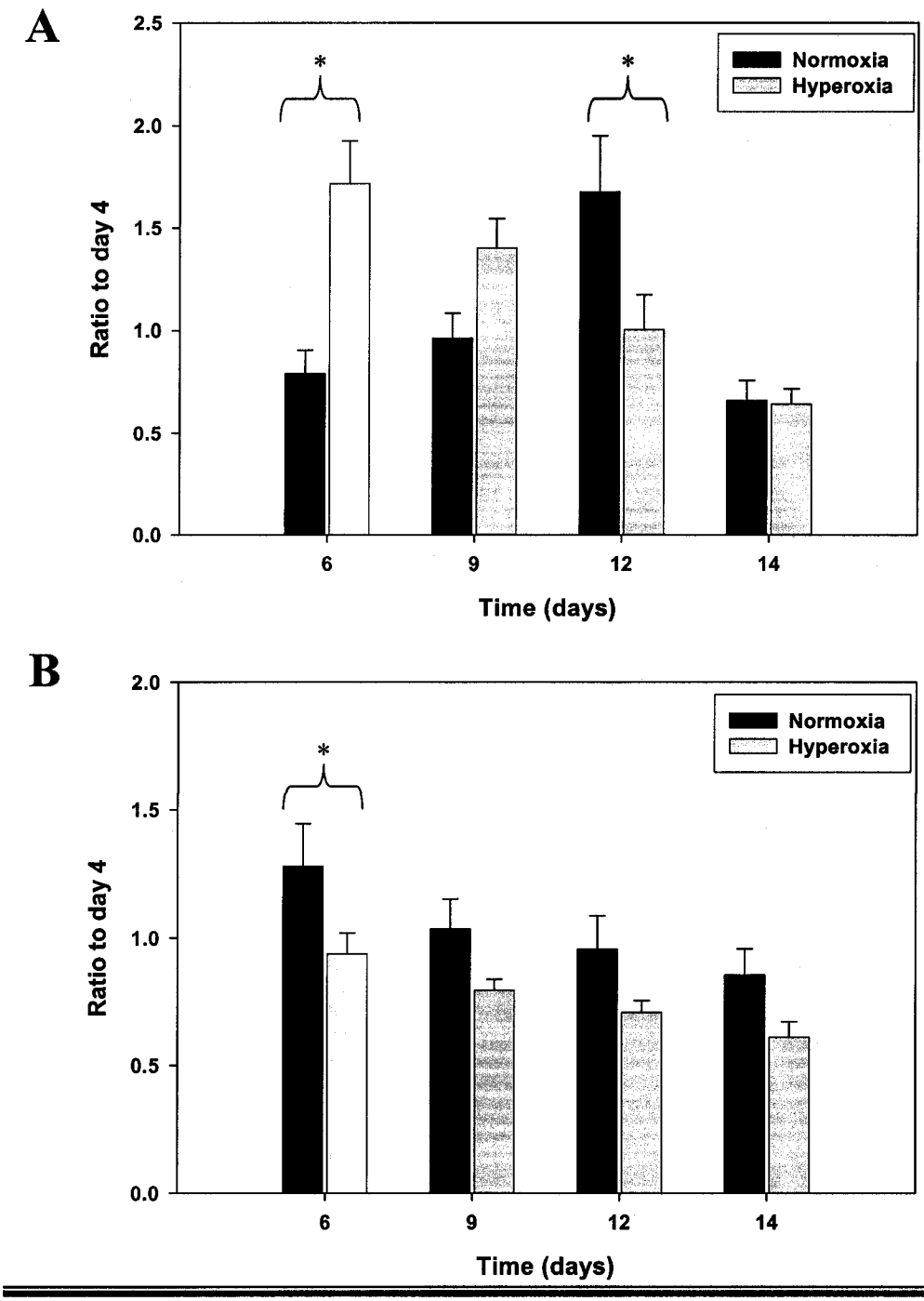

Figure 3.1: Effect of Hyperoxia on BLT_1 (A) and BLT_2 (B) mRNA Expression
Relative mRNA abundance was assessed using RT-PCR and compared to a d4 control sample. Data are expressed as means ± SEM and analyzed using two-way ANOVA and Holm-Sidak post hoc tests. * indicates significance between groups within each day ($p<0.05$). n=6 for all groups.

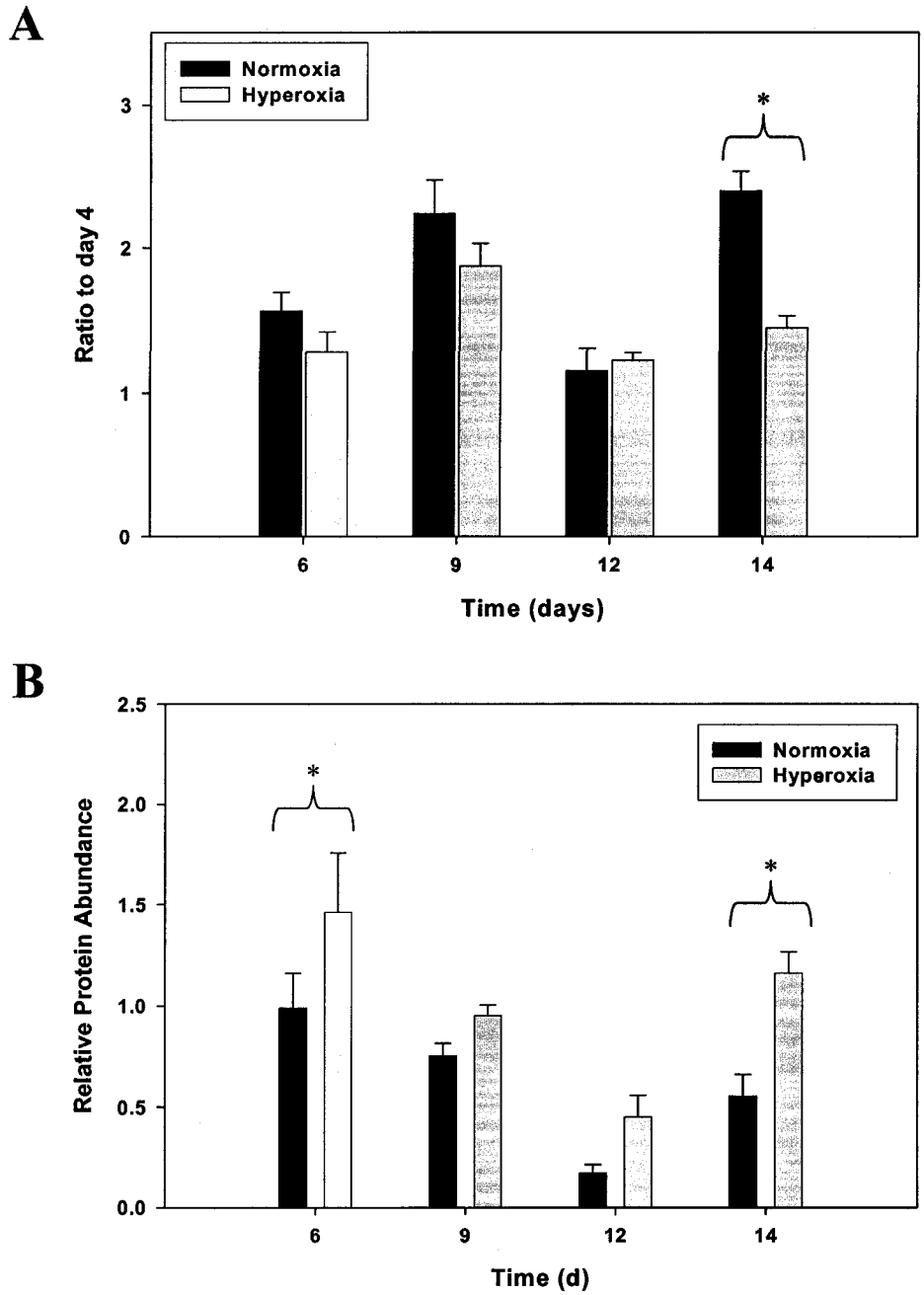

Figure 3.2: Effect of Hyperoxia on CysLT$_1$ mRNA Expression (A) and Protein Abundance (B)

Relative mRNA and protein abundance were assessed using RT-PCR and western immunoblotting, respectively, and compared to a d4 control sample. Data are expressed as means ± SEM and analyzed using two-way ANOVA and Holm-Sidak post hoc tests. * indicates significance between groups within each day ($p<0.05$). n=6 for all groups.

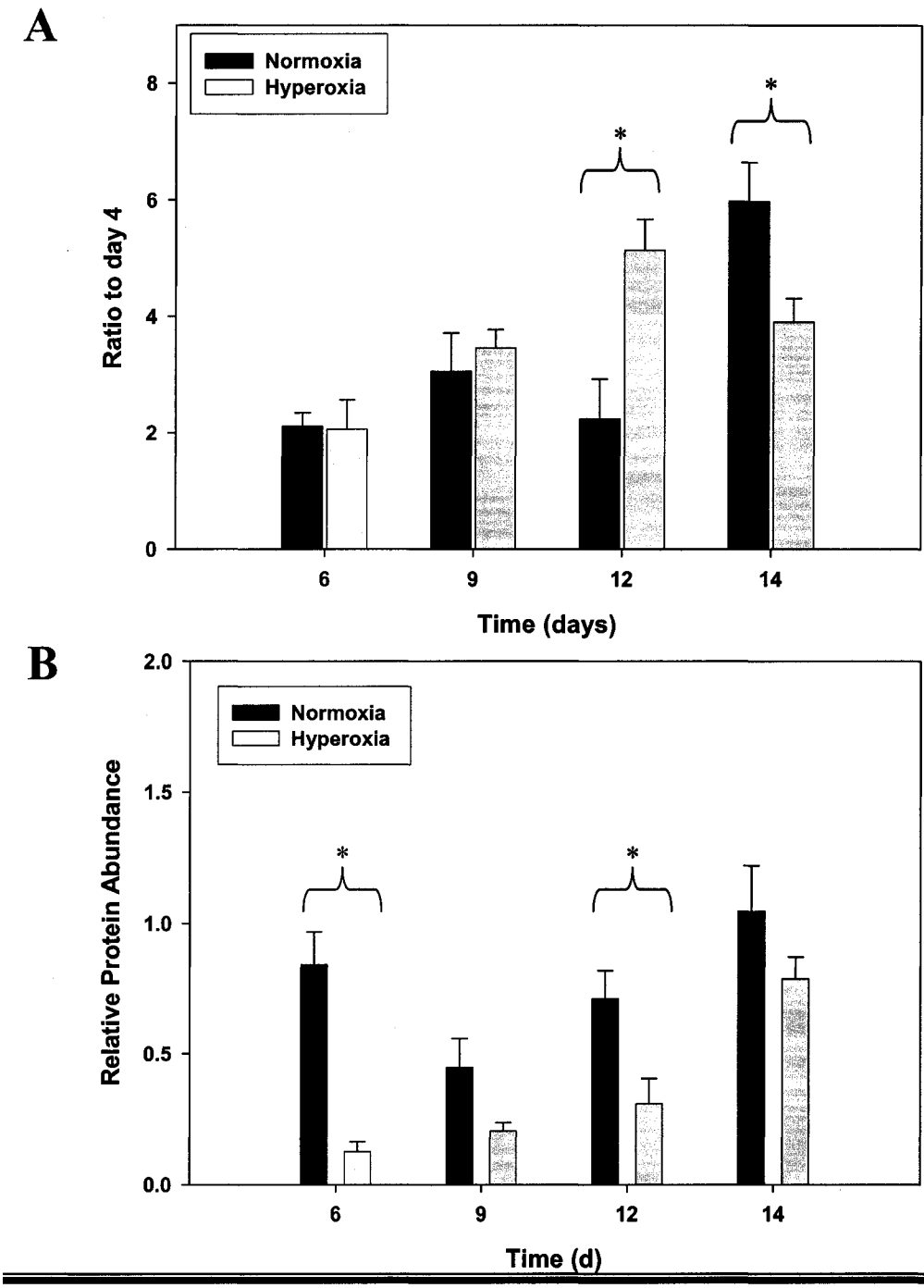

Figure 3.3: Effect of Hyperoxia on $CysLT_2$ mRNA Expression (A) and Protein Abundance (B)

Relative mRNA and protein abundance were assessed using RT-PCR and western immunoblotting, respectively, and compared to a d4 control sample. Data are expressed as means ± SEM and analyzed using two-way ANOVA and Holm-Sidak post hoc tests. * indicates significance between groups within each day ($p<0.05$). n=6 for all groups.

LT Analysis by EIA

We were interested in measuring LT content in developing rat lungs for two reasons. One was to examine the content of LTs present in the lungs at various times during development and to test for effects of hyperoxia on their expression. Also, we wanted to establish a baseline for comparison use in the adenoviral study.

LTB_4

LTB_4 levels were quantified during alveolarization. Extrapolating from previous data, we hypothesized that LTB_4 content would be increased in hyperoxic lungs [96, 140]. LTB_4 levels were measured on d4, d9, and d14 in pups exposed to either a normoxic or hyperoxic environment. There were no significant changes over time or as a result of exposure to oxygen at any of the time points tested. Although the amount of LTB_4 trended to a decrease in hyperoxic animals on d9, this reduction was not significant (Figure 3.4A).

CysLTs

CysLT levels were assessed as a group by EIA. We hypothesized that CysLT content would be increased by hyperoxia. As with LTB_4, the CysLTs were assessed on d4, d9, and d14. There were no significant changes over time or as a result of exposure to oxygen at any of the time points tested (Figure 3.4B).

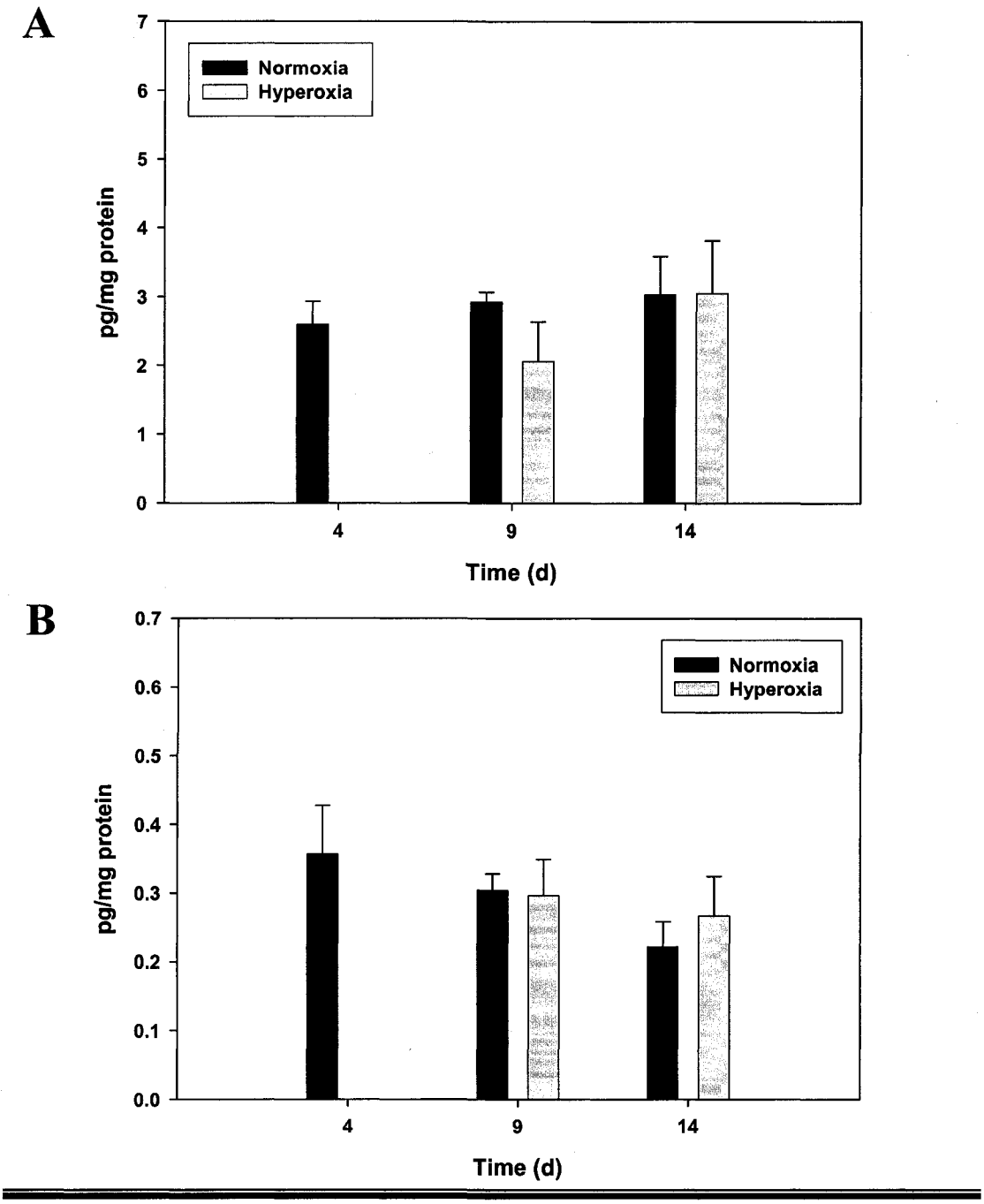

Figure 3.4: Effect of Hyperoxia on LTB_4 (A) and CysLT (B) Abundance
LT concentrations were measured from whole lung homogenates using EIA kits and normalized to protein content. The CysLTs were assessed as a group due to low kit specificity. Data are expressed as means ± SEM and analyzed using two-way ANOVA and Holm-Sidak post hoc tests. n number varies between groups (d4 = 5, d9 = 3, d14 = 6).

Study 2: 5-Lipoxygenase Adenoviral Over-expression

Adenoviral Infection

We tested 5LO adenoviral expression by RT-PCR from lung tissue and fluorescence of green fluorescent protein (GFP) in the distal lung to ensure that the virus was viable and that administration successfully reached the alveoli.

Viral Expression

Human 5LO

Human 5LO (h5LO) expression was measured by RT-PCR to ensure successful viral transfection and to confirm that h5LO would only be expressed in pups infected with Ad5LO. h5LO expression was only detected in Ad5LO animals, on both d9 and d14 with no other animals having detectable expression (Figure 3.5A).

GFP

GFP expression was also detected by RT-PCR to check for successful AdGFP viral transfection. GFP expression was detected in AdGFP animals, on both d9 and d14 (Figure 3.5B).

GFP Fluorescence

AdGFP

Lung sections were assessed for green fluorescence to ensure viral infection was successful and that virus was able to reach the distal parenchyma. Day 9 and d14 lobes were imaged at upper, middle, and lower portions to check for viral distribution. Green

fluorescence was visible throughout the lungs of AdGFP infected animals on both d9 and d14 (Figure 3.6A,B). A hematoxylin and eosin stain of a lung serial section near the section seen in Figure 3.6A is included to demonstrate viral administration reached the distal lung spaces (Figure 3.6E).

Ad5LO

Ad5LO treated animal lungs were also tested for fluorescence as a control. As Ad5LO does not fluoresce, we expected that the lungs should appear black under the microscope. Day 9 and d14 lobes were imaged at upper, middle, and lower portions to check for green fluorescence and for evidence of lung autofluorescence. No green fluorescence was visible at any level of the lung in these pups (Figure 3.6C).

Vehicle

Control animals treated with vehicle were also tested for fluorescence as a negative control. As expected, lungs did not show any fluorescence on either d9 or d14 at any level of the lung lobe (upper/middle/lower) (Figure 3.6D).

LT Analysis by EIA

To test the effect of the different viruses on LT synthesis, we measured LT content by EIA. We hypothesized that the Ad5LO treated animals would have increased LTB_4 and CysLT concentrations on d14 relative to AdGFP and controls.

LTB_4

Total lung LTB_4 levels were measured on d14 in vehicle, AdGFP, Ad5LO and No Treatment groups. There was a significant increase of LTB_4 in Ad5LO animals ($p < 0.05$) over all other treatments, in agreement with our hypothesis (Figure 3.7A). Levels increased by about 70-80% in Ad5LO animals over other treatment groups.

CysLTs

The CysLTs were quantified together as a group on d14 in vehicle, AdGFP, Ad5LO and No Treatment groups. In contrast to our hypothesis, the CysLTs were significantly decreased in Ad5LO animals ($p < 0.05$) over all other treatments (Figure 3.7B). The amount of CysLTs detected was reduced by about 50% in Ad5LO pups compared to other treatment groups.

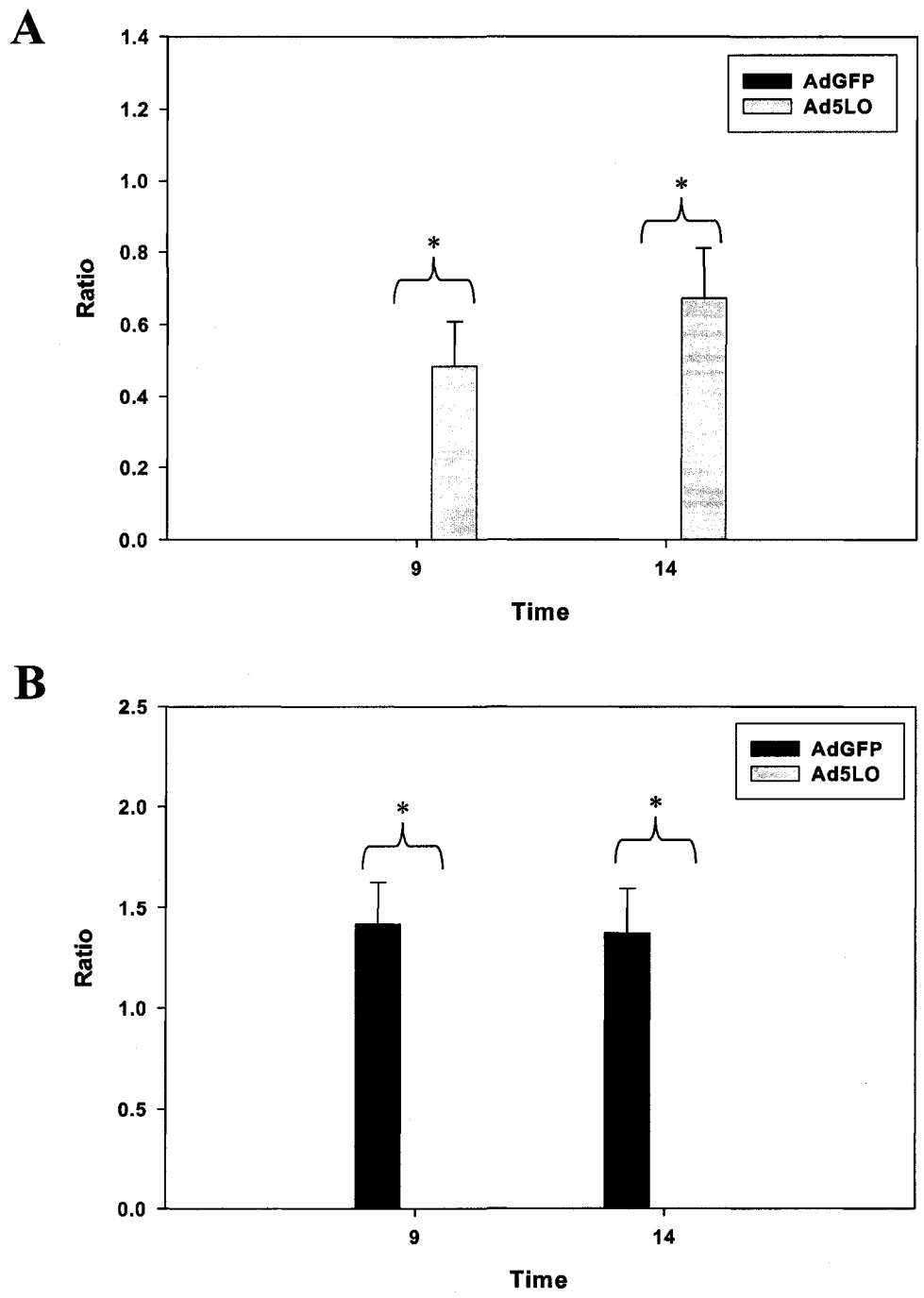

Figure 3.5: Adenoviral h5LO (A) and GFP (B) mRNA Expression
Relative mRNA abundance was measured using RT-PCR and standardized to control sample. Data are expressed as means ± SEM and analyzed using two-way ANOVA and Holm-Sidak post hoc tests. * indicate significance between groups within each day ($p<0.05$). n = 6 for all groups.

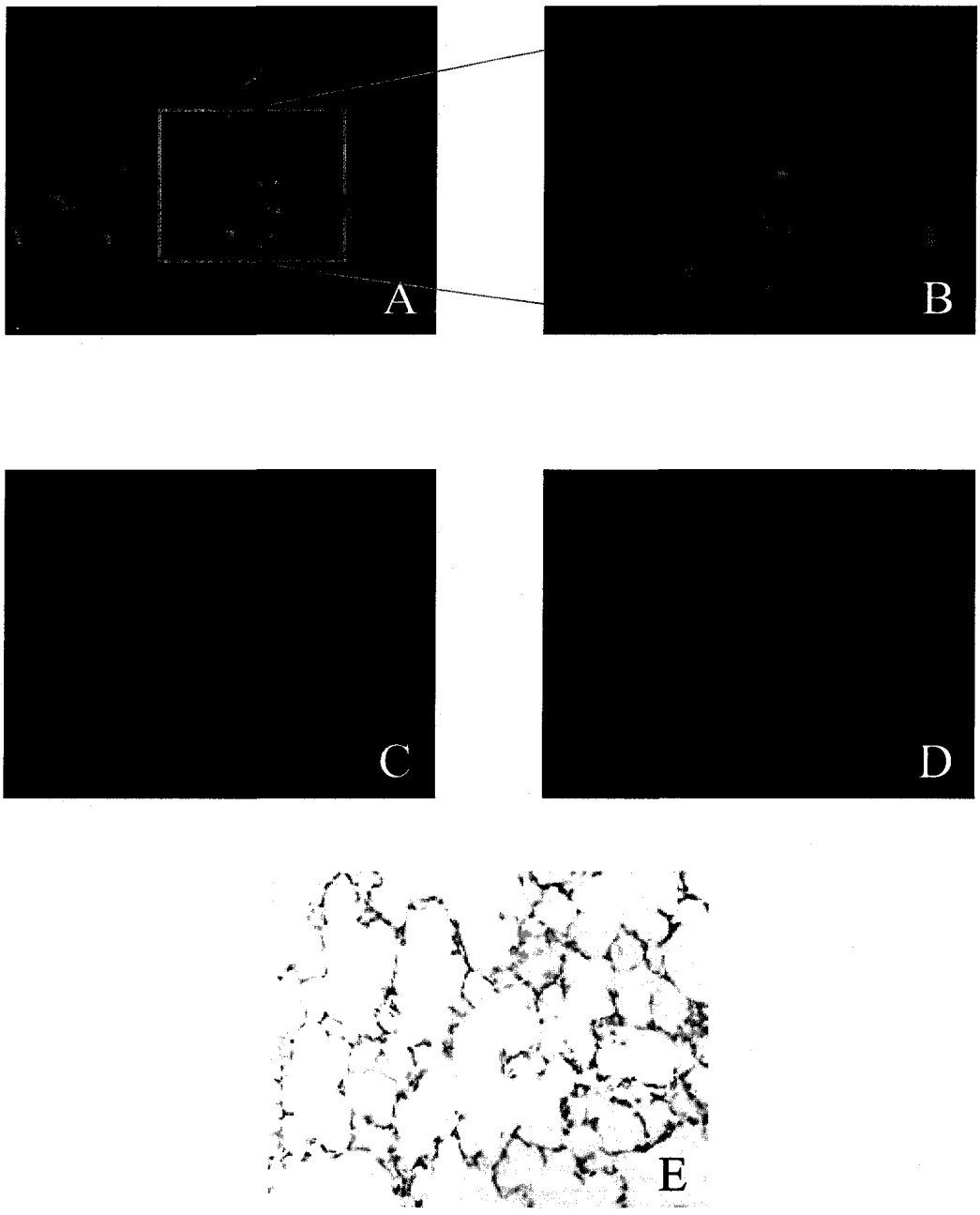

Figure 3.6: Adenoviral Lung Fluorescence (Day 14)
Sections (5μm thick) from lungs fixed and frozen in OTC. Fluorescence is seen in the sections from lungs of AdGFP infected animals (A) AdGFP 20X and (B) AdGFP 40X. The Ad5LO and vehicle control groups have no visible fluorescence (C) Ad5LO 20X and (D) Vehicle 20X. An H&E stain of distal lung (E) from approximately the same level (serial section) as seen in (A) is included, demonstrating virus reached alveoli.

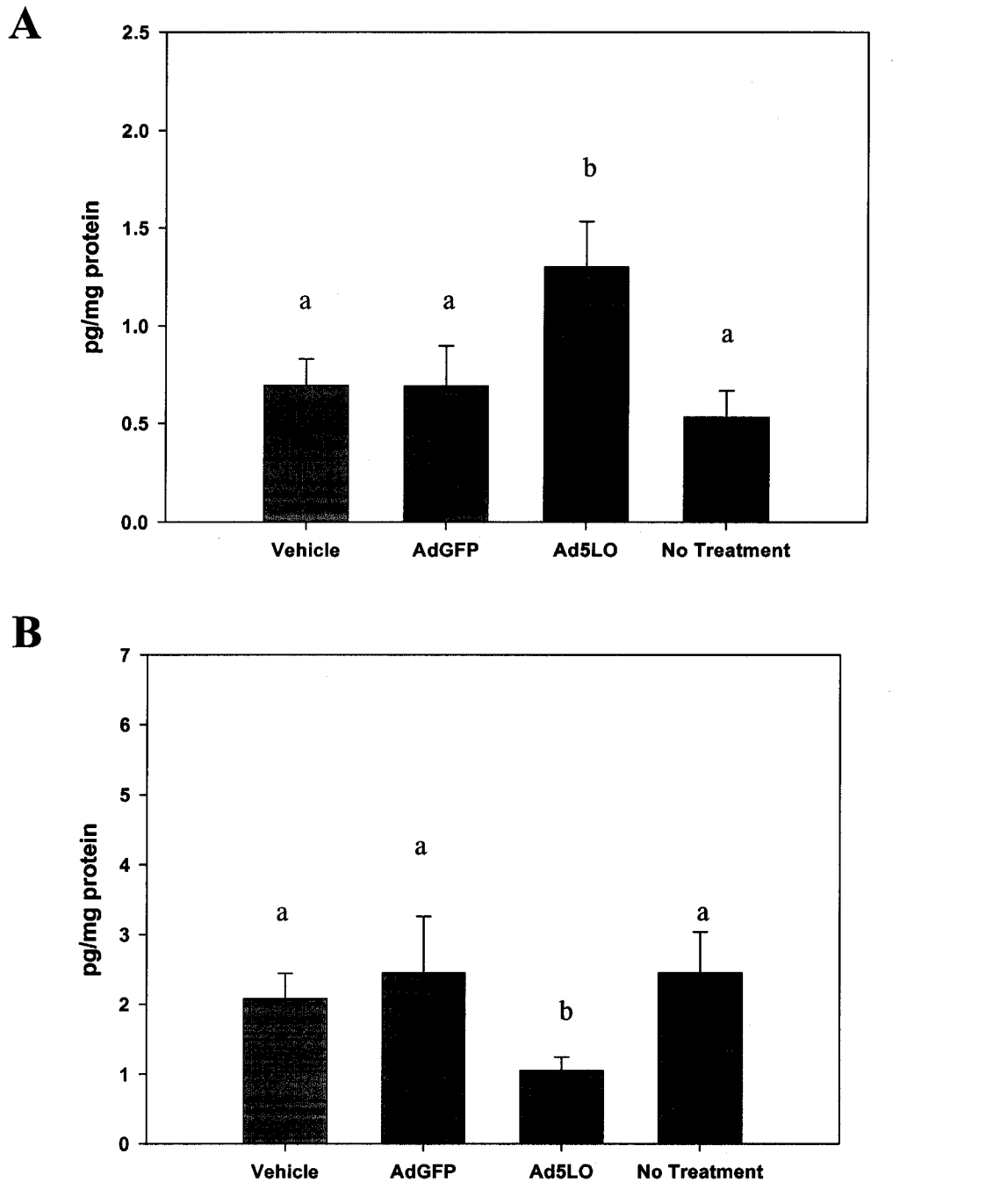

Figure 3.7: Adenoviral LTB_4 (A) and CysLT (B) Abundance (Day 14)
LT concentrations from whole lung extracts were assessed using EIA kits and normalized to protein content. Data are expressed as means ± SEM and analyzed using one-way ANOVA and Holm-Sidak post hoc tests. Superscripts indicate significance between groups within each day ($p<0.05$). n = 6 for all groups.

Endogenous Enzymes

The expression of rat 5LO and FLAP were tested to determine if up-regulation of 5LO activity had any effects on endogenous LT synthesis. We hypothesized that there would be no changes in rat 5LO or FLAP levels in pups infected with Ad5LO compared to AdGFP controls.

Rat 5LO and FLAP

Endogenous rat 5LO (r5LO) levels were assessed to determine if the Ad5LO transfection altered innate rat 5LO abundance. As expected, there was no significant difference between Ad5LO and AdGFP treatment groups on d9 or d14 (Figure 3.8A).

Changes in total lung FLAP mRNA abundance were assessed using Real-Time RT-PCR in order to determine whether Ad5LO transfection altered FLAP levels, as it is involved in LT synthesis. There were no significant differences over time or due to treatment (Ad5LO and AdGFP), as predicted (Figure 3.8B).

Pup and Lung Analysis

Pup and lung mass data were collected to test for differences between groups as well as a comparison to hyperoxic data. As Ad5LO was restricted to the lungs, we hypothesized that there would be no changes in pup mass between groups. Because we hypothesized that increasing 5LO would replicate the effects of high oxygen on lung development, we hypothesized that both lung weight and volume (when normalized to body weight) would be decreased in Ad5LO animals versus controls.

Pup Weights

Pup weights were monitored for systemic changes resulting from the treatments. Animals were weighed on d4, d9, and d14. On d14, pups in the Ad5LO, AdGFP, and vehicle groups weighed significantly less than pups in the No Treatment group ($p < 0.05$). This indicates the surgery and recovery processes may have inhibited pup development. There were no differences between AdGFP and Ad5LO groups (data not shown).

Lung Weights

Lung mass (blotted dry) was assessed as a measure of lung development. Lungs were weighed on d9 and d14 and compared to pup weights to normalize. Lungs in AdGFP treated animals weighed significantly more than those of vehicle control pups on d9 ($p < 0.05$). On d14, AdGFP exposed animals' lungs were significantly heavier than lungs from the No Treatment pups ($p < 0.05$). There were no differences between AdGFP and Ad5LO groups (data not shown).

Lung Volumes

Long volumes were gauged as another indicator of lung development. Lungs volumes were recorded on d9 and d14 and compared to pup weights to normalize. Lung volumes in AdGFP treated animals were significantly greater than those of vehicle control pups on both d9 ($p < 0.05$) and d14 ($p < 0.05$). There were no differences between AdGFP and Ad5LO groups (data not shown).

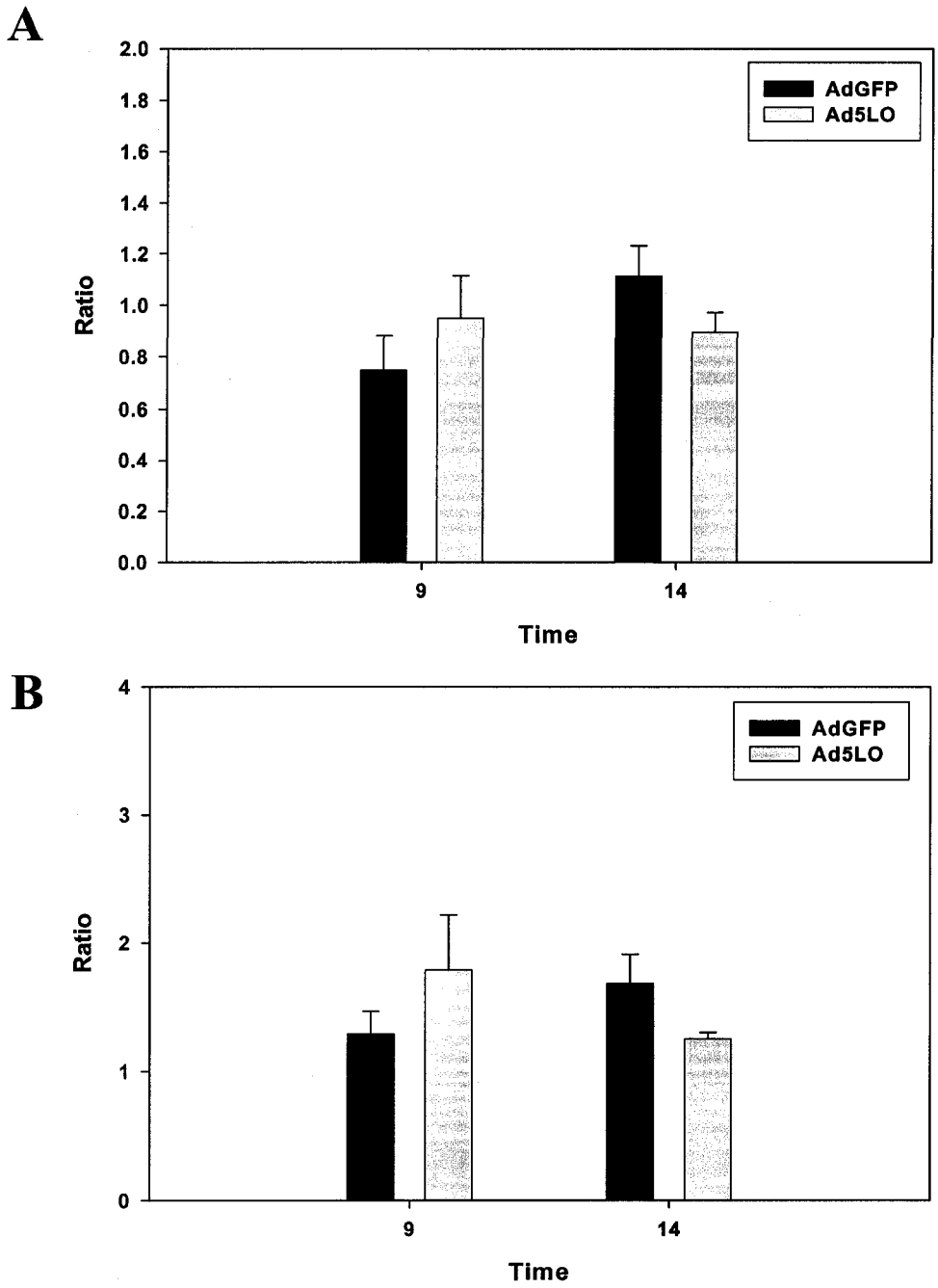

Figure 3.8: Adenoviral r5LO (A) and FLAP (B) mRNA Expression
The relative abundance of mRNA was measured using RT-PCR and standardized to a control sample. Data are expressed as means ± SEM and analyzed using two-way ANOVA and Holm-Sidak post hoc tests. n = 6 for all groups.

Lung mRNA & Protein

Data from mRNA and protein studies are presented here only from the Ad5LO and AdGFP groups. Due to the effects caused by the surgical procedure itself, the No Treatment group was not included below. The vehicle control group was also removed in the analysis as its effects were not clear and the variation was large between pups. The study was not robust enough to account for the interactions resulting from multiple variables, so only the main effects between adenoviral groups were evaluated. Therefore, the following data must be interpreted with the caveat that it is only a comparison between these two groups.

Since we thought that increasing 5LO expression would simulate many of the changes observed in hyperoxia, we hypothesized that (a) BLT_1 and BLT_2 levels would be increased in Ad5LO pups versus AdGFP; (b) that $CysLT_1$ would be decreased in Ad5LO treated animals; and (c) that $CysLT_2$ would be relatively unchanged between treatments (due to the opposite effects of LTC_4 and LTD_4). This study was developed prior to the LT receptor study and is based on previous data so the hypothesis may conflict with the results of study 1.

BLT1

Changes in total lung mRNA levels for BLT_1 were examined on d9 and d14 using Real-Time RT-PCR. There was a decrease in BLT_1 expression levels with time ($p < 0.05$). As predicted, on day 9 Ad5LO animals expressed significantly more receptor than the AdGFP group ($p < 0.05$); however, this difference was not found on d14 (Figure 3.9A).

BLT2

Lung mRNA levels for BLT_2 were examined on d9 and d14. There were no significant changes over time. In contrast to our hypothesis, no significant differences were seen between Ad5LO and AdGFP treated pups at either time point (Figure 3.9B).

CysLT1

Total lung mRNA expression levels for $CysLT_1$ were assessed in pups on d9 and d14. There were no significant differences over time or due to treatment (Ad5LO and AdGFP) (Figure 3.10A).

$CysLT_1$ protein mass was assessed on d9 and d14 using western immunoblotting and densitometry analysis. In contrast to $CysLT_1$ mRNA, there was an increase with time in AdGFP and Ad5LO treatment groups ($p < 0.001$). Treatment with Ad5LO also stimulated an overall increase in receptor protein levels ($p < 0.001$). Contrary to our hypothesis, $CysLT_1$ protein was significantly increased in the Ad5LO group on d9 over AdGFP ($p < 0.05$). $CysLT_1$ levels in Ad5LO pups were also increased over AdGFP controls on d14 ($p < 0.001$) (Figure 3.10B).

CysLT2

$CysLT_2$ mRNA levels in the lung were assessed using Real-Time RT-PCR. There was a decrease in expression in both groups over time from d9 to d14 ($p < 0.001$), but no differences between the treatment groups were observed (Figure 3.11A).

$CysLT_2$ protein levels were assessed on d9 and d14 using Western immunoblotting. Although there was no effect of time (in contrast to $CysLT_2$ mRNA), $CysLT_2$ protein was increased in the Ad5LO group over the AdGFP control group on d9 ($p < 0.05$). $CysLT_2$ levels were equal in Ad5LO and AdGFP treated animals on d14, as expected (Figure 3.11B).

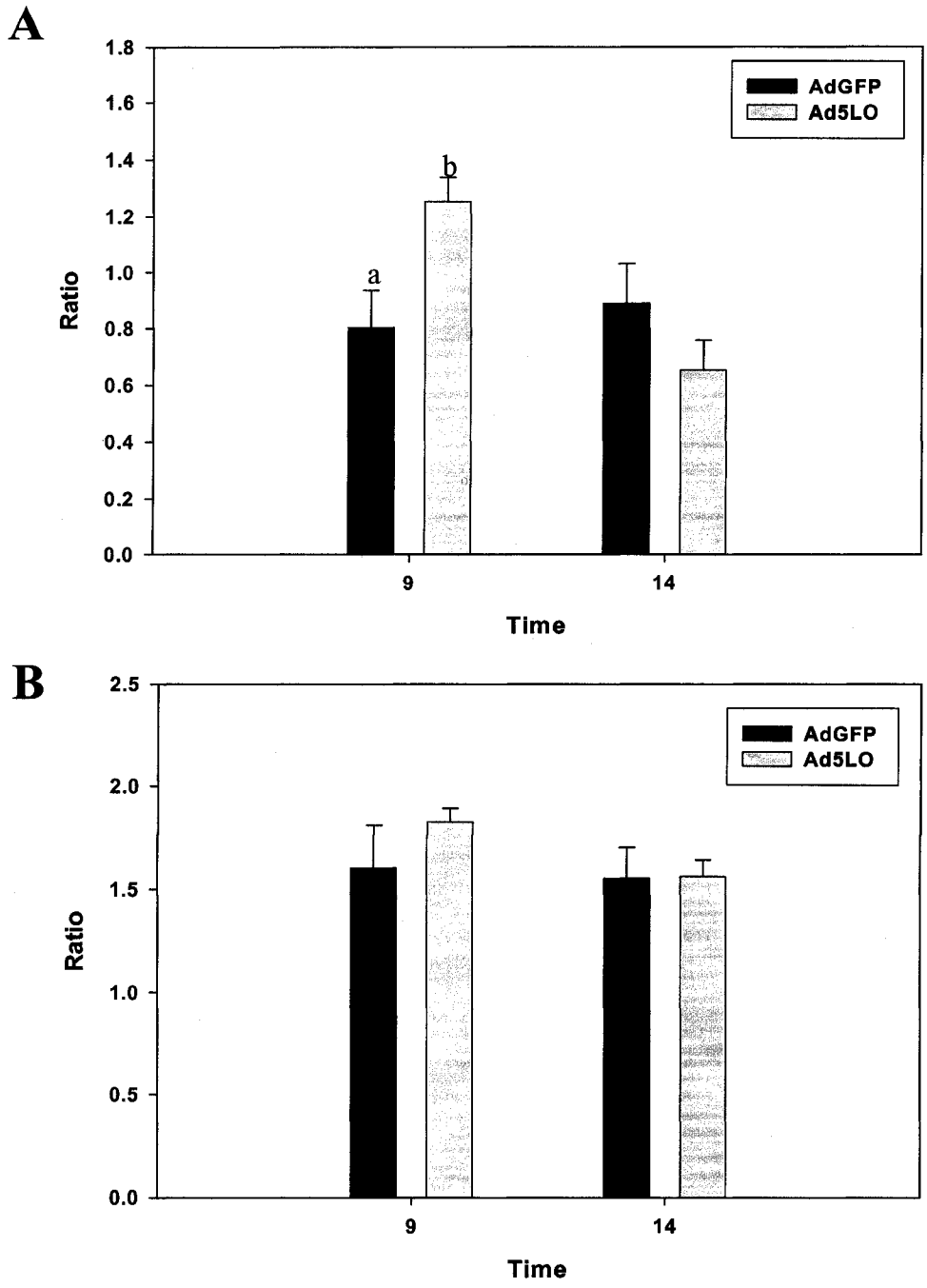

Figure 3.9: Adenoviral BLT_1 (A) and BLT_2 (B) mRNA Expression
Relative mRNA levels were assessed using RT-PCR and standardized to a control sample. Data are expressed as means ± SEM and analyzed using two-way ANOVA and Holm-Sidak post hoc tests. n = 6 for all groups. Superscripts indicate significance between groups within each day ($p<0.05$). n = 6 for all groups.

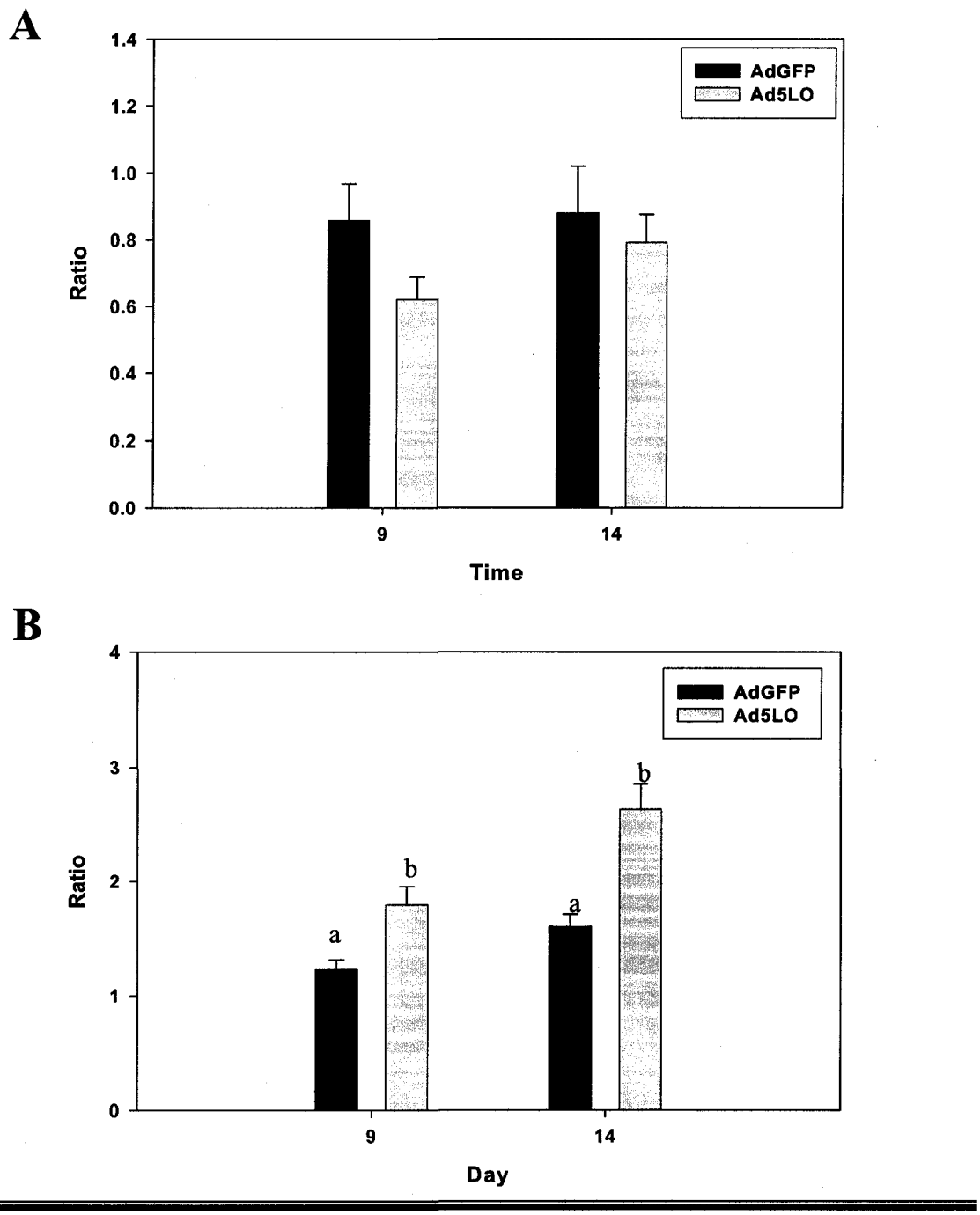

Figure 3.10: Adenoviral CysLT$_1$ mRNA (A) and Protein Abundance (B)
Relative mRNA and protein abundance were assessed using RT-PCR and western immunoblotting, respectively, and compared to a control sample. Data are expressed as means ± SEM and analyzed using two-way ANOVA and Holm-Sidak post hoc tests. Superscripts indicate significance between groups within each day ($p<0.05$). n = 6 for all groups.

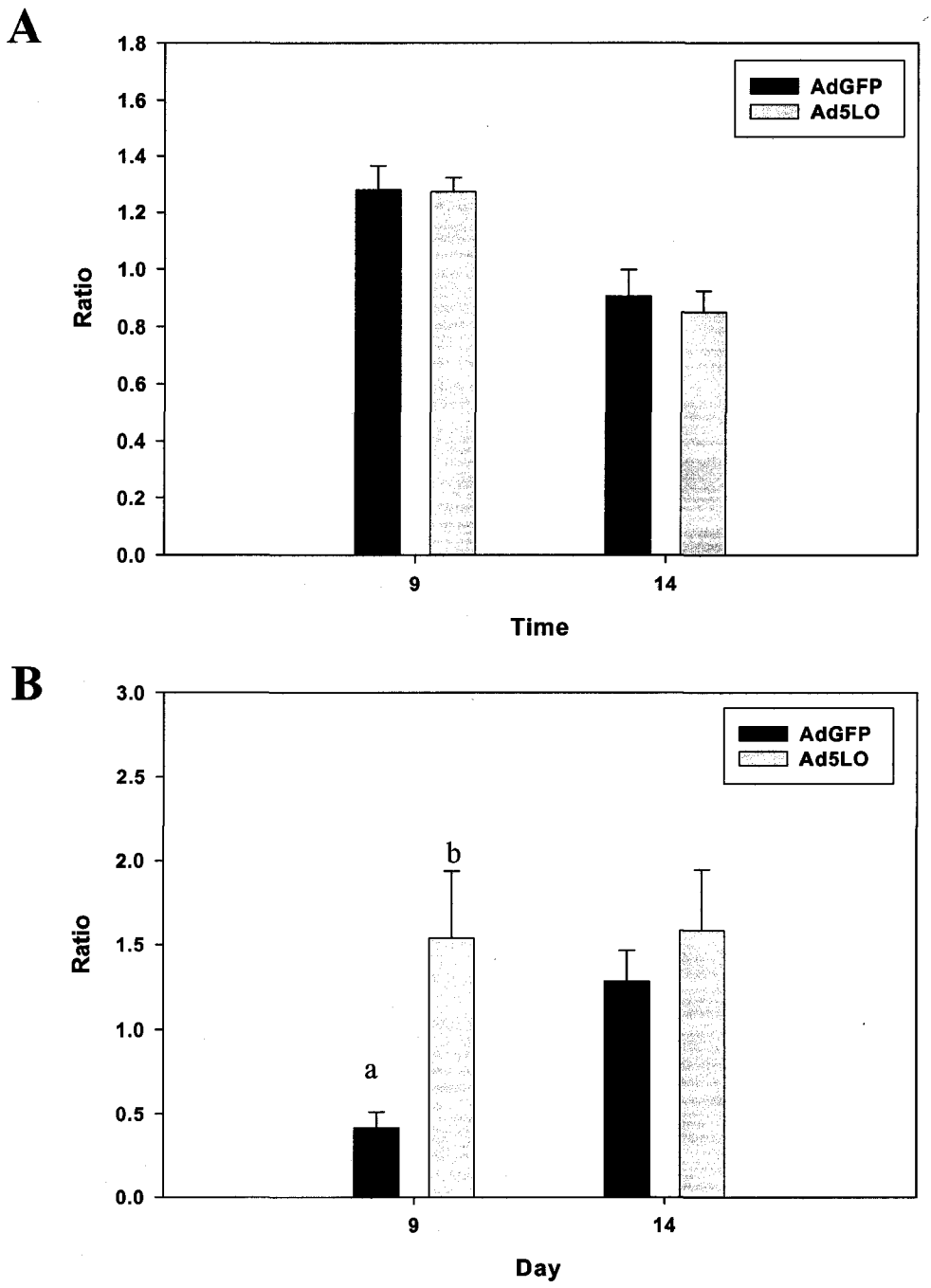

Figure 3.11: Adenoviral $CysLT_2$ mRNA (A) and Protein Abundance (B)
Relative mRNA and protein abundance were assessed using RT-PCR and western immunoblotting, respectively, and standardized to a control sample. Data are expressed as means ± SEM and analyzed using two-way ANOVA and Holm-Sidak post hoc tests. Superscripts indicate significance between groups within each day ($p<0.05$). n = 6 for all groups.

Markers of Lung Development

We were interested in whether Ad5LO had any effect on markers of lung maturation. We therefore determined the levels of tropoelastin mRNA and alveolar size using the mean linear intercept method.

Tropoelastin

Tropoelastin mRNA, which increases as septation occurs and is positively correlated with lung development, was assessed using RT-PCR as an indicator of changes in lung structure resulting from the treatments. We hypothesized that if 5LO was inhibiting lung development (via a mechanism similar to hyperoxia), then Ad5LO treated pups would show a decrease in tropoelastin mRNA expression. There was a significant increase in tropoelastin mRNA levels over time in both groups ($p < 0.001$) as would be expected in maturing lungs. However, Ad5LO treatment did not induce any change in tropoelastin mRNA expression at either time point (Figure 3.12).

Morphometric Analysis

Morphometric analysis was performed to test whether increasing 5LO levels resulted in an arrest of lung development. We hypothesized that if 5LO was an inhibitor of lung development, then Ad5LO-treated animals should demonstrate a decrease in mean linear intercept (MLI) versus AdGFP-treated and vehicle controls, thus indicating a less mature lung. Lung micrographs of d14 lungs were stained with hematoxylin and eosin and morphometrically analyzed using the MLI method [161]. Although a 9.2% decrease in

the mean of the MLI values induced by Ad5LO treatment over AdGFP animals was evident (n = 3), there were no significant differences between the groups on d14 (Figure 3.13).

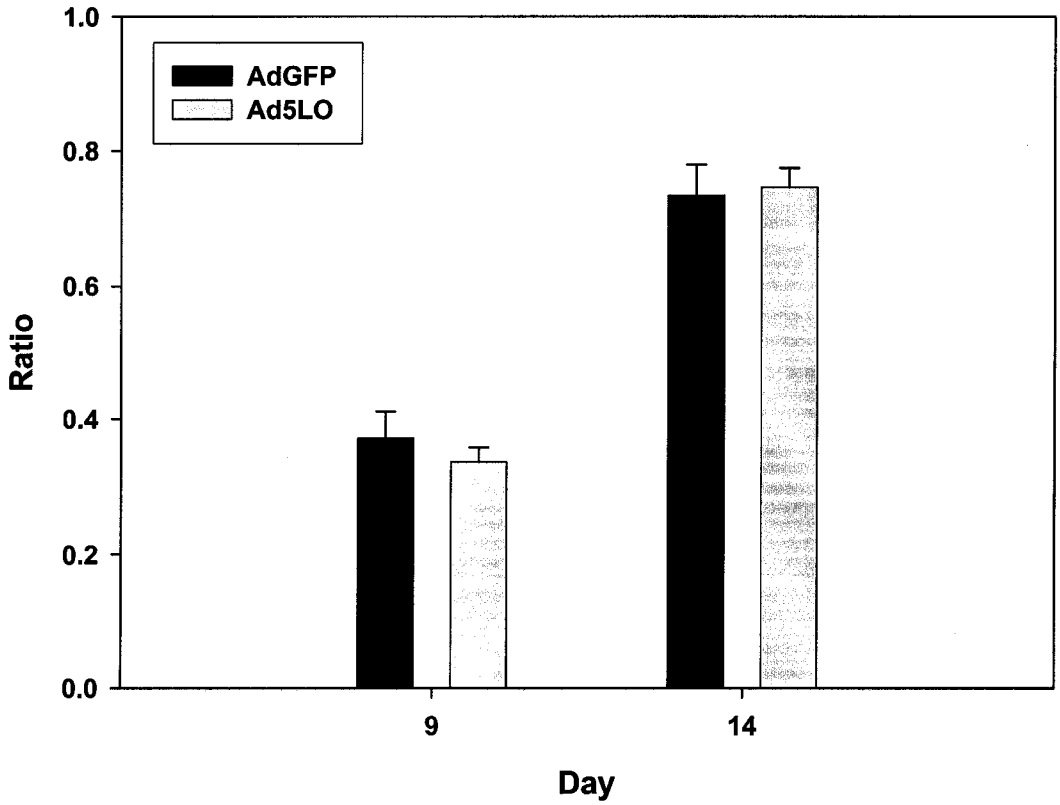

Figure 3.12: Adenoviral Tropoelastin mRNA Expression
The relative mRNA abundance was assessed using RT-PCR and standardized to a control sample. Data are expressed as means ± SEM and analyzed using two-way ANOVA and Holm-Sidak post hoc tests. n = 6 for all groups.

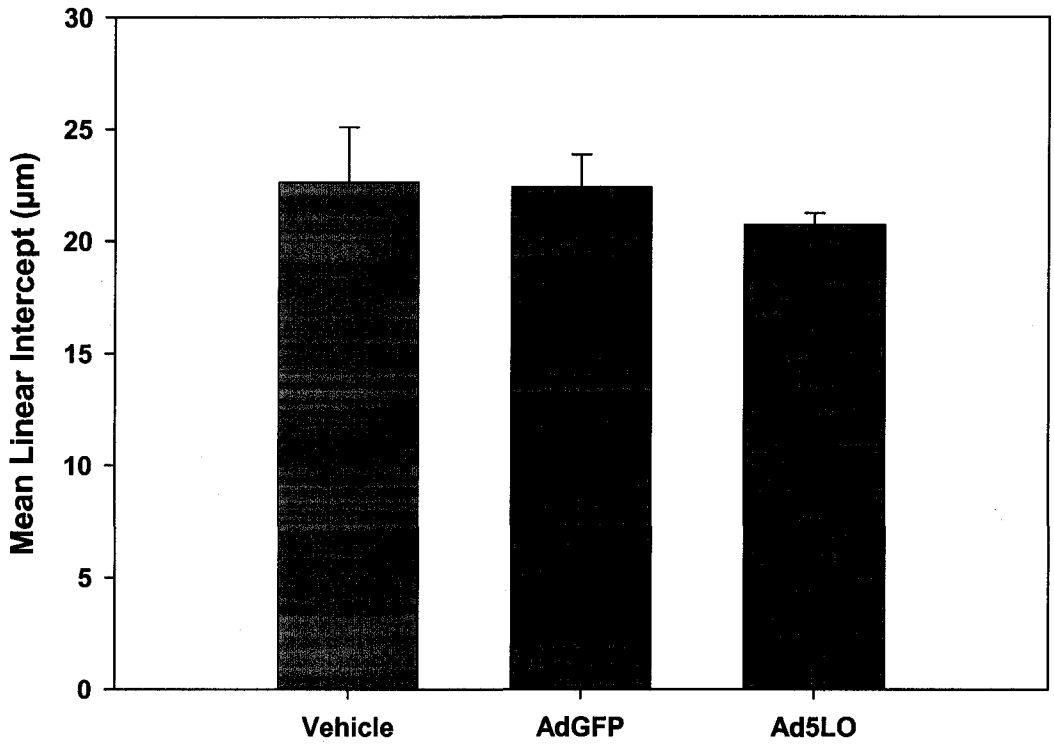

Figure 3.13: Adenoviral Morphometric Analysis (Day 14)
Serial sections (5 µm thick) from perfusion fixed lungs stained with H&E were analyzed using the MLI method. Data are expressed as means ± SEM and analyzed using one-way ANOVA. n = 3 for all groups.

CHAPTER 4 - DISCUSSION

Study 1: Effects of Hyperoxia on the Leukotrienes and Their Receptors

Hyperoxia has been shown to arrest lung alveolarization via exposure to ROS and their release from inflammatory cells, inflammatory mediators (e.g. LTs), and changes in growth factor (e.g. VEGF) and receptor expression. Previous studies in our laboratory demonstrated that the LTs as a group are involved in the arrest of lung development observed in response to exposure to hyperoxia. We have also shown that individual LTs can either arrest or accelerate alveolarization. We therefore were interested in extending these studies in a crucial direction: the elucidation of the normal and hyperoxic pattern of LT receptor expression in lung development to provide baseline information about the potential role of LT receptors in alveolarization. We observed changes in expression for all LT receptors in response to hyperoxia.

Effects of Hyperoxia on LT Receptors

This study assessed the level of BLT_1 mRNA expression in neonatal rat lungs, at different time points throughout alveolarization, in both normal and hyperoxic environments. In normal lung development, BLT_1 levels increased from days 6-12 and then decreased back to day 6 levels by day 14. In hyperoxia BLT_1 was initially increased, as predicted in our hypothesis. However, it then decreased towards the end of alveolarization. This effect appears to indicate a deceleration of BLT_1 mRNA expression versus normoxic animals. Overall, this pattern of expression would suggest that in hyperoxia, LTB_4 action via BLT_1 on day 6 would be the greatest early in alveolarization and becomes less important over time [141]. The initial phase of alveolarization, days 4-9, is the most sensitive to hyperoxia and so the fact that BLT_1 is increased during this

time period might partially explain the inhibitory effect of LTB_4 in lung development [140]. A compensatory mechanism may be acting to restore BLT_1 expression to normal levels following their initial increase in an attempt to ameliorate any undue effects. This could be in response to the increase in LTB_4 synthesis capacity documented in previous studies [96]. We were unable to assess BLT_1 protein expression due to the lack of a viable commercially available antibody for Western immunoblotting; however, this would be an important future study to perform to assess mRNA and protein correlation.

The ontogeny of BLT_2 mRNA expression in both normoxic and hyperoxic newborn rats was examined. BLT_2 levels steadily decreased over the period of alveolarization in normal lung development. Contrary to our hypothesis, BLT_2 levels were decreased by hyperoxia, although only significantly on day 6. Hyperoxic exposure resulted in an acceleration of the natural reduction in BLT_2 expression over the period of alveolarization. The reduction in BLT_2 seen in hyperoxia suggests that the receptor is down-regulated in response to increased LTB_4 and inflammation [96]. Therefore, it is likely that an increase in oxygen levels would not arrest lung development via a BLT_2 dependent pathway. We were unable to assess BLT_2 protein expression due to the lack of a viable commercially available antibody for western immunoblotting.

We were also interested in the expression of the CysLT receptors. We determined the mRNA and protein expression of $CysLT_1$ in both normoxic and hyperoxic neonatal rats. In normal alveolarization, $CysLT_1$ mRNA and protein were not well correlated. mRNA abundance increased from day 6 to 9, then decreased to day 12, and then increased to day

14. In contrast, protein levels decreased from day 6 to 12 and then rebounded slightly. In hyperoxia, $CysLT_1$ mRNA levels decreased in agreement with our hypothesis. This further supports the proposed pro-alveogenic role of LTD_4 in lung development [141]. Since $CysLT_1$ is viewed mainly as an LTD_4 receptor and LTD_4 was shown to accelerate alveolarization, it makes sense that hyperoxia would suppress its expression since oxygen arrests lung development [141].

In contrast, $CysLT_1$ protein was increased in the hyperoxic animals, contrary to our hypothesis. It is unknown why there is discordance between $CysLT_1$ mRNA and protein levels. Increased oxygen might cause the degradation of the mRNA disproportionately to the protein which is more stable in a high oxygen environment. This would lead to a build up of protein at certain time points despite a decrease in measured mRNA levels. There might also be post-translational regulation of the protein which slows its degradation, thus effectively increasing its levels in the tissue. Protein metabolism may be reduced to increase the proposed pro-alvegenic effects of LTD_4. Hyperoxia might also cause a decrease in mRNA gene transcription for $CysLT_1$ but also induce a stress response which up-regulates $CysLT_1$ protein translation and/or decreases protein degradation. Further studies are needed to examine the effects of oxygen on LT receptor mRNA and protein regulation.

$CysLT_2$ mRNA and protein expression in the lungs of normoxic and hyperoxic neonatal rat pups were also examined. In normal lung alveolarization, $CysLT_2$ mRNA abundance remained relatively stable from days 6-12 and then increased to day 14. $CysLT_2$ protein

expression in normal rat lung development did not mirror the mRNA data. Levels decreased from day 6 to 9, and then increased from 9 to 14. In hyperoxia, we found that $CysLT_2$ mRNA levels initially increased in lungs from days 6-12, but then decreased as alveolarization progressed to day 14. Our hypothesis that there would be little change in $CysLT_2$ expression in hyperoxia was incorrect; however, the expression pattern demonstrates that there is little net change in receptor levels during alveolarization. This reversal in expression might be due to the fluctuating levels of LTC_4 and LTD_4 seen in lung development, in both normoxia and hyperoxia. As the anti-alveogenic effects of LTC_4 and pro-alveogenic effects of LTD_4 occur in the developing lung, $CysLT_2$ levels are altered in an attempt to compensate and maintain a neutral effect [141]. Unfortunately, no data are available on individual CysLT expression patterns as they have so far only been measured as a group. The roles of $CysLT_2$ remain unclear because studies have been hampered by a lack of specific antagonists. A future study quantifying the individual CysLTs would be of significant importance in understanding their role in lung development. Since $CysLT_2$ mRNA is higher in hyperoxia than normoxia on day 12, it is possible that this might be responsible for inhibiting alveolarization via LTC_4; but, this effect is reduced on day 14 when $CysLT_2$ expression is less in hyperoxia than normoxia. Since the critical period for hyperoxic damage is days 4-9, the higher levels of $CysLT_2$ later in development will likely have less of an effect than if they were elevated earlier in the process. This might help explain why the rate of lung damage is lessened later in development [140].

As observed with $CysLT_1$, $CysLT_2$ protein levels did not correspond to mRNA expression. $CysLT_2$ protein was decreased during hyperoxic lung development, differing from our hypothesis. Again, it is unknown why there is this disagreement between mRNA and protein levels, but a compensatory mechanism is likely in play here too. The system could be trying to counter the effects of the shifting expression patterns of LTC_4 and LTD_4 in the lung; however, more studies are needed in order to determine if this is true. The reduction of $CysLT_2$ protein in hyperoxia suggests that if LTD_4 acts via this receptor to stimulate alveogenesis, this action is suppressed in hyperoxic animals [141].

Differences in mRNA and Protein

Differences in mRNA and proteins levels can be explained by differences in their synthesis and functions. There are three principal steps between mRNA and protein at which regulation can occur. The first is transcription where mRNA is synthesized in the nucleus and regulation can occur either at synthesis or degradation of RNA. This should not have caused any difference in our experiments. The second is splicing where introns are removed from the mRNA and regulation can occur either at splicing or movement out of the nucleus. Alternative splicing, the generation of multiple RNA transcript species from a common mRNA precursor, is one mechanism for the diversification and expansion of cellular proteins from a smaller set of genes [164]. This process may explain the difference between mRNA and protein observed in this study. The third is translation where protein is synthesized from the mRNA and regulation can occur at protein synthesis, protein breakdown, or protein secretion from the cell. In our experiments, the effects of cell secretion should not be an issue since cells are lysed and

total protein is extracted. Differing rates of mRNA and protein breakdown as well as differences in their metabolism and stability can also affect measurements. The stability of LT receptor mRNA or protein may have been reduced in the high oxygen environment [165]. The mRNA and protein samples determined in these studies represent the conditions at isolated time points and therefore may not accurately reflect the average receptor levels in the lungs. The variation in data may also suggest that oxygen is having an indirect affect, via inflammation, on LT receptor expression and is not directly regulating their synthesis. Future studies must be performed to identify the effects of alveolarization and hyperoxia on LT receptor mRNA and protein.

LT Receptors during the 'Critical Period'

A 'critical period' has been established, d4-9PN, during which hyperoxia, 5LO and LTs have their most significant effects on lung development [140, 153, 166]. In this period, the process of septation peaks and lung surface area increases dramatically [6, 78, 167]. Secondary trend analysis of LT receptor expression during this period was done. Hyperoxia caused a significant increase in BLT_1 mRNA and a decrease in BLT_2 mRNA on d6PN. Surprisingly, $CysLT_1$ protein levels were increased on d6PN, contrary to what we expected. $CysLT_2$ protein content was drastically (~85%) decreased on d6PN. Interestingly, there were no significant differences in any receptor on d9PN. Given these results, it would appear that the proposed anti-alveogenic BLT_1 mRNA is increased by hyperoxia, as predicted; but, pro-alveogenic $CysLT_1$ protein is also increased, although there is no significant difference in $CysLT_1$ mRNA expression. The large decrease in $CysLT_2$, which we did not expect, may explain why this increase in $CysLT_1$ is unable to

compensate for the effects of BLT_1. Future studies should examine the roles of LT receptors specifically during this 'critical period' and whether or not altering their expression is beneficial for lung development.

Effects of Hyperoxia on LT Levels

Although LT levels have been assessed previously in our laboratory, we were interested in determining them using a different technique and as a comparison for our LT adenoviral experiments. Previously, LTs were determined in developing rat lungs using an explant technique [96, 140]. Lung samples were removed from pups and stimulated to produce LTs, which were collected and measured. This technique assesses the ability of the lungs to synthesize LTs, and not the actual LT levels present in the lungs. They found that both LTB_4 and CysLT synthesis capacities were increased in hyperoxic animals during alveolarization [96, 140].

Our EIA protocol for this study was designed to determine the LT content of whole lungs at a certain time point. It is therefore a more accurate reflection of the *in vivo* conditions experienced by the lungs at a given time. However, since the samples were from whole lung homogenates, the accuracy can be affected by blood flow and diffusion. In contrast to previous studies, we found no differences between normoxic and hyperoxic lungs on days 9 or 14. This might be due to the increased breakdown of the LTs in a high oxygen environment. LTA_4 is known to be unstable in oxygen, which might explain the decrease measured in our experiment[168]. The differences between these data and earlier studies are likely due to the fact that there may be an increase in the capacity to synthesize LTs

(i.e. an increase in 5LO and FLAP expression); however, it is possible that there is no net increase in LT levels in the lungs of hyperoxic pups. Additional studies accurately tracking the LT content of lungs over multiple sample points must be performed to clarify this discrepancy.

Conclusions

This study is the first to examine the expression of the LT receptors in newborn rat pups during the period of alveolarization and their changes over time. It was also the first to show that hyperoxia affects pulmonary LT receptor levels. This further supports our original hypothesis that LTs are involved in the disruption of alveolarization caused by high oxygen concentrations and could be linked to newborn chronic lung disease. It builds on our previous work in identifying the roles of LTs in normal and pathological alveolarization. The increase in BLT_1 and decrease in $CysLT_1$ mRNA levels further supports the anti-alveogenic role for LTB_4 and pro-alveogenic action of LTD_4. This suggested 'yin and yang' relationship between LTB_4 and LTD_4, caused by hyperoxia, merits future study to identify the mechanism(s) involved.

Study 2: 5-Lipoxygenase Adenoviral Over-expression

Previous data from our laboratory employing multiple lines of evidence suggested that LTs affect lung development [96, 140]. The systemic (subcutaneous) administration of individual LTs during alveolarization demonstrated specific effects, especially for LTB_4 and LTD_4 [141]. However, there were no studies examining the effects of 5LO over-expression in the lungs during alveolarization. We were therefore interested in continuing

to explore the effects of LTs by developing a new model to study lung development in rat pups whereby 5LO activity was increased in newborn rat lungs. We achieved this by up-regulatung the expression of 5LO in the lungs using intratracheal administration of a 5LO adenovirus. This avoided multiple subcutaneous injections and the systemic effects of LTs, which are inflammatory mediators. However, we were sensitive to the possibility that adenovirus administration itself may be associated with inflammation and altered lung physiology. Waszak *et al.* showed that adenoviral expression caused no adverse effects in newborn rat lungs [169]. We were able to successfully administer the virus to neonatal rat pups and measure changes in LT expression during alveolarization. Future experiments should repeat these studies with a larger sample size to more clearly identify the effects of increasing 5LO and LTs during alveolarization.

Adenovirus Infection

Adenoviral Expression

The results of this study clearly show the transgenic expression of the human 5LO gene in the rat lung. The amount of human 5LO expressed was not quantified, but human 5LO cDNA was readily amplified by RT-PCR. The localized expression of the human 5LO gene in the rat lung demonstrates that this is an effective method for inducing targeted 5LO over-expression between 1 and 10 days after intratracheal administration of the adenoviruses [155-157, 170, 171]. Previous studies have shown that this technique limits the degree of expression of the introduced gene to the lungs; however, no previous studies have administered Ad5LO to neonatal rat pups for the purpose of studying lung development [155-157, 170, 171]. Intratracheal administration was found to be the best

experimental approach for the lung-specific over-expression of adenoviral encoded genes, with negligible effects on gene expression in other organs or on the serum concentration of the coded protein [155]. This technique has been shown to induce gene expression in all cell types of the airway epithelium, with little if any inflammation [155, 157, 169, 172]. These findings suggest that our model of adenoviral gene delivery limits expression to the lung and is a useful tool to study the role of 5LO gene expression in lung development, particularly in the postnatal alveolarization stage.

The first experiment following adenoviral infection tested for the expression of the administered gene in the lung. We assessed both the expression of human 5LO and GFP mRNA using RT-PCR as well as lung florescence as a control for GFP. Human 5LO was expressed only in the lungs of animals infected with Ad5LO, indicating successful uptake and function of the virus and that there was no pup-to-pup transmission of the virus. The expression of human 5LO was detected on both days 9 and 14 (the only days tested). Although no quantitative assessment was performed, the gene was readily amplified by RT-PCR. However, since we do not know the amount of viable virus that was present in the lungs, the data must be interpreted taking this into consideration. GFP mRNA expression was also examined and was detected only in pups administered AdGFP. It was found on both days 9 and 14. The gene amplified readily by RT-PCR; however, no quantitative analysis was performed. In order to assess the function of the GFP inserted, as well as the distribution of the virus (i.e. the level of infection), we performed lung fluorescence studies. Cells infected with AdGFP were expected to express GFP mRNA and synthesize GFP protein, which fluoresces. Fluorescence was detected in alveolar

epithelial cells in the lung slices of pups administered AdGFP on days 9 and 14. This demonstrates that the GFP transcript inserted was functional and reached the distal lung parenchyma. No fluorescence was observed in animals that were given Ad5LO or vehicle, indicating that GFP expression was limited to animals infected with AdGFP. It is interesting to note that the level of fluorescence is below what we expected. The concentration of virus administered should have been sufficient to infect all lung epithelial cells; however, it is evident that not all cells expressed GFP. It is impossible to know whether this is due to insufficient levels of virus, dilution with defective virus, or some other cause. It is also not clear whether or not this was limited to AdGFP or if Ad5LO was also not expressed in all cells (since it did not fluoresce). If this experiment is performed again, *in situ* hydridization should be performed to assess where human 5LO is being expressed and if the expression pattern observed for AdGFP is similar to Ad5LO.

Effects on LT Synthesis

Following assessment of viral expression, we examined whether the administered human 5LO affected endogenous LT synthesis. We determined LTB_4 and CysLT levels using EIA analysis. There were no differences in LTB_4 or CysLT levels between the vehicle, AdGFP, and No Treatment groups. The level of LTB_4 was increased, as expected, in the Ad5LO animals by about 85% over all other groups. Interestingly, CysLT levels did not increase as predicted in the Ad5LO group; they were actually decreased versus the other three groups by about 60%. This surprising finding suggests that the LTA_4 produced by the additional 5LO was shunted into the LTB_4 pathway at the expense of CysLTs. We

could find no published report of this occurring elsewhere and further investigations must be performed to ascertain the reasons for this result. Studies should be directed at the enzymes that synthesize LTB_4 and LTC_4 from their common precursor LTA_4, LTA_4 hydrolase and LTC_4 synthase, respectively [83, 88]. It is possible that 5LO or an increase in LTA_4 stimulates LTA_4 hydrolase and/or inhibits LTC_4 synthase. Previous studies using this 5LO adenovirus did not measure LT levels [143, 144]. Alternatively, this pattern of LT synthesis might be due to lack of substrate. AA, metabolized by 5LO to LTA_4, might not have been released from the membrane in sufficient amounts for the transfected 5LO to cause significant up-regulation of LT synthesis. The lack of an extracellular trigger to stimulate PLA_2 could explain this [147]. Additional cell signalling mechanisms, such as those found in hyperoxia, might be required for significant increases in AA release and LT synthesis [147]. Regardless of the cause, the importance of an increase in LTB_4 and a decrease in CysLT levels in the lung may be significant in terms of lung development, although the precise value of this observation remains to be determined. Interestingly, when compared to LT levels in the previous study, the quantity of LTB_4 per mg of protein is reduced in all groups in this experiment compared to normoxic animals; whereas, CysLT levels are about 10x higher in non-5LO animals compared to normoxic pups. This discrepancy might be due to variation between assay kits as the experiments were run over 1 year apart.

Endogenous Effects

We were also interested in determining what effects, if any, administering human 5LO had on endogenous rat 5LO and FLAP. These are the two enzymes involved in the first

step of LT synthesis (AA to LTA_4). We were concerned that by introducing human 5LO, we would inadvertently cause a corresponding decrease in rat 5LO; effectively nullifying the increase we were trying to achieve. We found that there was no significant difference between the Ad5LO and AdGFP animals at either of the time points assessed for both rat 5LO and FLAP. Therefore, we assumed there should be a similar level of LT synthesis occurring as a result of endogenous rat 5LO and FLAP in both groups. Hence, any changes observed would be a result of the human 5LO.

Effects on Lung & Pup Development

In order to assess other measures of adenoviral effects, we monitored pup mass throughout the course of the experiment as well as lung mass and volume on days 9 and 14. Expectedly, the pups gained weight over time; however, the three groups that were treated (Ad5LO, AdGFP, and vehicle) all weighed significantly less than the group that received no treatment. There was no significant difference between the Ad5LO and AdGFP pups. This suggests that the surgical procedure itself caused a reduction in growth, likely because the pain present after the analgesia wore off resulted in decreased suckling on the day of the operation. Because of this, we compared the effects of 5LO over-expression against only the AdGFP animals in the studies outlined below. To determine if this lack of nutrition or the administration of virus/vehicle had a disproportionate effect on the lungs, we determined both lung mass and volume as ratios to body mass. Neither lung mass nor volume, when normalized to body mass, was significantly different for either group of newborns. Therefore, we assumed that the effect of nutrition did not affect the lungs disproportionately. Interestingly, we found that the

vehicle treated animals had smaller and lighter lungs than the AdGFP treated group. The Ad5LO exposed pup lungs were not different from either AdGFP or vehicle groups. This might suggest that the exposure of the lungs to a virus stimulated their growth in the AdGFP group and that this effect was inhibited by increased LTB_4 levels in the Ad5LO group. In this experiment, we only examined the wet-weight of the lungs due to the limited tissues available; but, in future experiments an examination of lung dry-weights would be interesting as it would determine if the mass and/or volume changes were due to growth or to edema.

LT Receptor Expression – Preliminary Data

After determining the effectiveness of adenoviral administration, we generated preliminary data regarding 5LO's actions on the LT receptors. Data from mRNA and protein studies are presented here only from the Ad5LO and AdGFP groups. Because vehicle lungs were different from AdGFP, we only compared the two viral groups for the mRNA and protein studies below to remove another level of variation introduced. We were most interested in the effects of 5LO on the lungs and the critical thing to control for is the adenovirus itself. We realize that the results below are only interpretable in the narrow context of this study; but, our n-number is not high enough to properly control for the multiple levels of variation introduced by comparing the Ad5LO group to virus, vehicle, and surgical (no-treatment) control groups. Therefore, the following data must be interpreted with the caveat that it is only valid given these limiting conditions.

To examine the role of 5LO and LT levels in regulating LT receptor expression and to further elucidate the roles of the LT receptors in lung development, we investigated the expression of the four LT receptors. Based on the premise that 5LO inhibits lung development, we hypothesized that Ad5LO would cause an increase in BLT_1, BLT_2, and $CysLT_2$ and a decrease in $CysLT_1$ receptor levels. Ad5LO treatment stimulated a significant increase in BLT_1 on d9, but there were no other changes in the mRNA expression of the other receptors compared to AdGFP controls. The increase in BLT_1 on d9 in Ad5LO animals was in line with our hypothesis and suggests that an increase in 5LO activity or the increase in LTB_4 levels may have led to a feed forward increase in receptor expression. Due to the lack of sufficient pups, we were unable to quantify LTB_4 levels on d9 and therefore cannot make any conclusions about this increase in receptor expression.

In contrast to the mRNA data, when we determined protein levels of the CysLT receptors, we found that Ad5LO animals had significantly higher levels of $CysLT_1$ and $CysLT_2$ on both days 9 and 14. This increase in receptor protein may be in response to the decrease in CysLT levels observed in these animals [173]. These receptors are rapidly desensitized, and although their recovery is not as fast, the long time frame of our experimental paradigm would be sufficient to increase receptor protein levels in a low CysLT environment [173]. The fact that the protein data does not correspond to the mRNA data could be attributed to many reasons. Principal among these is that GPCRs are internalized upon desensitization and then returned to the cell membrane or resensitized [174]. This requires a completely different type of regulation than gene

transcription and translation, involving both homologous and heterologous regulators [173]. Regardless of the reasons, the changes in CysLT receptor protein levels do not correlate with changes in lung development.

Tropoelastin

As an initial test to determine if increased 5LO expression had an effect on lung development, we wanted to observe what, if any, changes occurred in the expression of tropoelastin. Tropoelastin, the subunits of elastin, have been shown to increase with alveolarization [46]. When we amplified tropoelastin mRNA by RT-PCR, we found no differences between Ad5LO and AdGFP groups. Analysis of mRNA was chosen over protein as the technique was established and there was no existing protocol for elastin protein IHC in our laboratory. We had hypothesized that if the LTs were inhibiting lung development, they would also cause a reduction in tropoelastin expression. It is possible that LTs do not have effects on tropoelastin or elastin; but, it may be that they alter the distribution of the elastin within the developing lung. We did not assess the effects of human 5LO on elastin levels or on tropoelastin or elastin distribution in the cells. Since it is the concentration of elastin at areas of secondary septa formation that is important in lung development, future studies involving immunohistochemistry should examine any changes in this pattern resulting from increased 5LO levels [175].

Morphometry

Following the tropoelastin study, we wanted to know if 5LO has an effect on lung structure and complexity. We conducted morphological experiments to assess the mean

linear intercept of the Ad5LO, AdGFP, and vehicle control groups. Unfortunately, no significant differences were found between the groups. This could be due to the low n-number for this part of the experiment. This was compounded by a high failure rate of lung perfusion. Since previous studies have shown changes resulting from increased or decreased LT levels [141], it is possibly a result of insufficient LT synthesis in this experiment. Future studies should repeat this experiment with a larger sample size and with different concentrations of adenovirus to determine the effects of increasing 5LO, using this technique, on lung development.

Conclusions

This study was the first to administer a 5LO adenovirus during rat lung development. It met our primary goal to successfully establish a model for delivering a 5LO adenovirus to rat lungs during alveolarization for the purpose of studying the roles of LTs in lung development. This experiment was also the first to investigate increased 5LO expression on alveolarization. As the expression of the adenovirus was confined to the lungs, its over-expression is likely to reflect the actions of endogenous 5LO produced solely in the lungs. Although no clear effects were seen on lung development, interesting changes were noted. Most significantly, the unexpected pattern of LT synthesis in animals infected with Ad5LO. Future work should focus on identifying the effects of 5LO on the LTB_4 and LTC_4 synthesis pathways to explain this observation. The observed differences between 5LO over-expression and hyperoxia on lung development are likely due to a failure of this experiment to adequately increase LT synthesis. However, these data provide a possible link between hyperoxia, 5LO, and decreased alveolarization. An

increase in oxygen stimulates an increase in 5LO expression, resulting in an increase in LTB_4 synthesis and a decrease in CysLT (most importantly LTD_4) production. A coincident increase in BLT_1 mediated by 5LO also occurs. Together, these effects would result in increased anti-alveogenic (LTB_4 and BLT_1) and decreased pro-alveogenic (LTD_4) processes, thus inhibiting lung development. This may explain one mechanism through which hyperoxia and 5LO affect alveolarization. More work is needed to adequately explain these phenomena and determine the effects of increased 5LO and LTs during alveolarization.

Summary

Previous studies from our laboratory have demonstrated that the LTs are mediators in hyperoxic lung injury [73, 96, 140, 141]. A model of BPD was established using newborn rats that demonstrated hyperoxia inhibits alveolarization. Then, lungs from these rats were shown to have elevated LT levels [73, 96, 140]. Inhibition of the LTs prevented the inhibition of alveolarization during hyperoxia [73, 140, 141]. Finally, it was shown that adding back certain LTs could either stimulate or inhibit septation [141]. Together, these data demonstrated a role for LTs as mediators in the hyperoxia-induced arrest of alveolarization.

The studies presented here sought to clarify the mechanisms involved and establish a new model to study the LTs in lung development. Study 1 explored LT receptor expression and the changes that occur in lung development. It was the first time LT receptor expression was determined during normoxic and hyperoxic alveolarization. It

demonstrated that hyperoxia not only influences LT expression, but alters LT receptor expression as well. It supported the findings that LTB_4 is anti-alveogenic and LTD_4 is pro-alveogenic.

The second study established a new model to explore the effects of 5LO up-regulation on alveolarization. It was the first time 5LO over-expression was examined during alveolarization. Unfortunately, the data were not robust enough to make definitive conclusions about the effects of this model in studying the role of LTs in lung development. However, the adenovirus did affect LT synthesis in the lung, demonstrating that the technique may be a viable means of exploring the role of LTs in lung development.

The implications of this research relate to its clinical applications in human BPD. Preterm infants delivered before 28 weeks of gestation are born before alveolarization has begun. Therefore, the lungs are not sufficiently developed to support the oxygen requirements *ex utero*. BPD is a clinical disease involving arrested alveolarization and permanent lung damage from ventilation with high oxygen concentrations. Therapies that stimulate lung development in the presence of the hyperoxia needed to support these babies would be of great importance. The receptor data from these studies will aid in the development of treatments for blocking anti-alveogenic LTB_4 activity while supporting pro-alveogenic LTD_4; thus, improving the potential outcomes in babies with BPD.

Future Studies

Future studies in this area should focus on answering the key remaining questions surrounding LTs in alveolarization. The distribution of LT receptors on epithelial cells and endothelial cells in the lungs during alveolarization must be examined. This will help elucidate the roles of LTs in both alveogenesis and angiogenesis. The concentrations of the CysLTs during normoxic and hyperoxic alveolarization must also be explored. This data will aid in the determination of the exact roles each LT is playing in lung development and whether or not LTD_4 is actually suppressed in hyperoxia as we predict. The adenoviral study should be repeated to work towards developing a new model for studying the LTs in alveolarization exclusively. Most importantly, a higher sample number for morphometry should be used. Higher doses and stimulating AA mobilization with the aim of increasing LT synthesis should be attempted. Linking the human 5LO gene to a fluorescent marker would also enhance the interpretation and validity of this new data. Finally, measurements of LTs and LT receptors during human BPD must be made to determine if there are differences between human and rat LT expression. If they are not significantly altered in humans in hyperoxia or BPD, then the relevance this research must be re-examined. However, if they are significantly increased in human BPD, as they are in rats exposed to hyperoxia, then the importance of an LT-related therapy for BPD should be further explored.

CHAPTER 5 - REFERENCES

References

1. Burri, P.H., *Fetal and postnatal development of the lung.* Annu Rev Physiol, 1984. **46**: p. 617-28.
2. Burri, P.H., *Morphology and respiratory function of the alveolar unit.* Int Arch Allergy Appl Immunol, 1985. **76**(Suppl 1): p. 2-12.
3. deMello, D.E. and L.M. Reid, *Embryonic and early fetal development of human lung vasculature and its functional implications.* Pediatr Dev Pathol, 2000. **3**(5): p. 439-49.
4. deMello, D.E., et al., *Early fetal development of lung vasculature.* Am J Respir Cell Mol Biol, 1997. **16**(5): p. 568-81.
5. Hislop, A., *Developmental biology of the pulmonary circulation.* Paediatr Respir Rev, 2005. **6**(1): p. 35-43.
6. Kauffman, S.L., *Cell proliferation in the mammalian lung.* Int Rev Exp Pathol, 1980. **22**: p. 131-91.
7. Le Cras, T.D., et al., *Treatment of newborn rats with a VEGF receptor inhibitor causes pulmonary hypertension and abnormal lung structure.* Am J Physiol Lung Cell Mol Physiol, 2002. **283**(3): p. L555-62.
8. Zeng, X., et al., *VEGF enhances pulmonary vasculogenesis and disrupts lung morphogenesis in vivo.* Dev Dyn, 1998. **211**(3): p. 215-27.
9. Warburton, D. and M.K. Lee, *Current concepts on lung development.* Curr Opin Pediatr, 1999. **11**(3): p. 188-92.

10. Warburton, D., et al., *The molecular basis of lung morphogenesis.* Mech Dev, 2000. **92**(1): p. 55-81.

11. Stenmark, K.R. and S.H. Abman, *Lung Vascular Development: Implications for the Pathogenesis of Bronchopulmonary Dysplasia.* Annu Rev Physiol, 2004.

12. Weinberger, B., et al., *Oxygen toxicity in premature infants.* Toxicol Appl Pharmacol, 2002. **181**(1): p. 60-7.

13. Jobe, A.J., *The new BPD: an arrest of lung development.* Pediatr Res, 1999. **46**(6): p. 641-3.

14. Maeda, S., et al., *Analysis of intrapulmonary vessels and epithelial-endothelial interactions in the human developing lung.* Lab Invest, 2002. **82**(3): p. 293-301.

15. Bhatt, A.J., et al., *Disrupted pulmonary vasculature and decreased vascular endothelial growth factor, Flt-1, and TIE-2 in human infants dying with bronchopulmonary dysplasia.* Am J Respir Crit Care Med, 2001. **164**(10 Pt 1): p. 1971-80.

16. Carmeliet, P. and D. Collen, *Molecular basis of angiogenesis. Role of VEGF and VE-cadherin.* Ann N Y Acad Sci, 2000. **902**: p. 249-62; discussion 262-4.

17. Bautch, V.L. and C.A. Ambler, *Assembly and patterning of vertebrate blood vessels.* Trends Cardiovasc Med, 2004. **14**(4): p. 138-43.

18. Blanco, L.N. and L. Frank, *The formation of alveoli in rat lung during the third and fourth postnatal weeks: effect of hyperoxia, dexamethasone, and deferoxamine.* Pediatr Res, 1993. **34**(3): p. 334-40.

19. Blanco, L.N. and L. Frank, *Development of gas-exchange surface area in rat lung. The effect of alveolar shape.* Am J Respir Crit Care Med, 1994. **149**(3 Pt 1): p. 759-66.

20. Abman, S.H., *Bronchopulmonary dysplasia: "a vascular hypothesis".* Am J Respir Crit Care Med, 2001. **164**(10 Pt 1): p. 1755-6.

21. Ferrara, N. and T. Davis-Smyth, *The biology of vascular endothelial growth factor.* Endocr Rev, 1997. **18**(1): p. 4-25.

22. Bhatt, A.J., et al., *Expression of vascular endothelial growth factor and Flk-1 in developing and glucocorticoid-treated mouse lung.* Pediatr Res, 2000. **47**(5): p. 606-13.

23. Maniscalco, W.M., et al., *Angiogenic factors and alveolar vasculature: development and alterations by injury in very premature baboons.* Am J Physiol Lung Cell Mol Physiol, 2002. **282**(4): p. L811-23.

24. Drake, C.J., J.E. Hungerford, and C.D. Little, *Morphogenesis of the first blood vessels.* Ann N Y Acad Sci, 1998. **857**: p. 155-79.

25. Burri, P.H. and V. Djonov, *Intussusceptive angiogenesis--the alternative to capillary sprouting.* Mol Aspects Med, 2002. **23**(6 Suppl): p. 1-27.

26. Risau, W., *Mechanisms of angiogenesis.* Nature, 1997. **386**(6626): p. 671-4.

27. Patan, S., et al., *Intussusceptive microvascular growth: a common alternative to capillary sprouting.* Arch Histol Cytol, 1992. **55 Suppl**: p. 65-75.

28. Patan, S., B. Haenni, and P.H. Burri, *Implementation of intussusceptive microvascular growth in the chicken chorioallantoic membrane (CAM): 1. pillar formation by folding of the capillary wall.* Microvasc Res, 1996. **51**(1): p. 80-98.

29. Burri, P.H. and M.R. Tarek, *A novel mechanism of capillary growth in the rat pulmonary microcirculation.* Anat Rec, 1990. **228**(1): p. 35-45.

30. Kurz, H., P.H. Burri, and V.G. Djonov, *Angiogenesis and vascular remodeling by intussusception: from form to function.* News Physiol Sci, 2003. **18**: p. 65-70.

31. Pardanaud, L., F. Yassine, and F. Dieterlen-Lievre, *Relationship between vasculogenesis, angiogenesis and haemopoiesis during avian ontogeny.* Development, 1989. **105**(3): p. 473-85.

32. Jakkula, M., et al., *Inhibition of angiogenesis decreases alveolarization in the developing rat lung.* Am J Physiol Lung Cell Mol Physiol, 2000. **279**(3): p. L600-7.

33. Flecknoe, S., et al., *Increased lung expansion alters the proportions of type I and type II alveolar epithelial cells in fetal sheep.* Am J Physiol Lung Cell Mol Physiol, 2000. **278**(6): p. L1180-5.

34. Shannon, J.M. and B.A. Hyatt, *Epithelial-mesenchymal interactions in the developing lung.* Annu Rev Physiol, 2004. **66**: p. 625-45.

35. Hall, S.M., A.A. Hislop, and S.G. Haworth, *Origin, differentiation, and maturation of human pulmonary veins.* Am J Respir Cell Mol Biol, 2002. **26**(3): p. 333-40.

36. Hall, S.M., et al., *Prenatal origins of human intrapulmonary arteries: formation and smooth muscle maturation.* Am J Respir Cell Mol Biol, 2000. **23**(2): p. 194-203.

37. Kasahara, Y., et al., *Inhibition of VEGF receptors causes lung cell apoptosis and emphysema.* J Clin Invest, 2000. **106**(11): p. 1311-9.

38. Kaner, R.J., et al., *Lung overexpression of the vascular endothelial growth factor gene induces pulmonary edema.* Am J Respir Cell Mol Biol, 2000. **22**(6): p. 657-64.

39. Parviz, M., *Transcriptional regulation of lung development: emergence of specificity.* Respir Res, 2000. **1**: p. 109-115.

40. Cole, T.J., J.A. Blendy, P. Monaghan, K. Kriegelstein, W. Schmid, G. Aguzzi, E. Hummler, K. Unsicker, & G. Schutz., *Targeted disruption of the glucocorticoid receptor gene blocks adrenergic chromaffin cell development and severely retards lung maturation.* Genes Dev., 1995. **9**: p. 1608-1621.

41. Yee, M., et al., *Type II epithelial cells are a critical target for hyperoxia-mediated impairment of postnatal lung development.* Am J Physiol Lung Cell Mol Physiol, 2006.

42. Maniscalco, W.M., et al., *Vascular endothelial growth factor mRNA increases in alveolar epithelial cells during recovery from oxygen injury.* Am J Respir Cell Mol Biol, 1995. **13**(4): p. 377-86.

43. Burri, P.H., *Structural aspects of prenatal and postnatal development and growth of the lung*, in *Lung Growth and Development*, J.A. McDonald, Editor. 1997, Marcel Dekker: New York. p. 740.

44. Burri, P.H., *Postnatal development and growth*, in *The Lung: Scientific Foundations*, R.G. Crystal, Editor. 1997, Lippincott-Raven Publishers: Philadelphia, Pennsylvania. p. 1013-1026.

45. Berk, J.L., Christine H.A., Shirley M., Phillip S.J., & Ronald G.H., *Hypoxia suppresses elastin repair by rat lung fibroblasts.* Am J Physiol Lung Cell Mol Physiol, 2005. **289**: p. L931-L936.

46. Bruce, M.C.C.E.H., *Transcriptional regulation of tropoelastin expression in rat lung fibroblasts: changes with age and hyperoxia.* Am J Physiol Lung Cell Mol Physiol, 1998. **274**: p. L940-L950.

47. Suri, C., et al., *Increased vascularization in mice overexpressing angiopoietin-1.* Science, 1998. **282**(5388): p. 468-71.

48. Northway, W.H., Jr., *Bronchopulmonary dysplasia: thirty-three years later.* Pediatr Pulmonol, 2001. **Suppl 23**: p. 5-7.

49. Northway, W.H., Jr., R.C. Rosan, and D.Y. Porter, *Pulmonary disease following respirator therapy of hyaline-membrane disease. Bronchopulmonary dysplasia.* N Engl J Med, 1967. **276**(7): p. 357-68.

50. Davis, P.G., et al., *Evaluating "old" definitions for the "new" bronchopulmonary dysplasia.* J Pediatr, 2002. **140**(5): p. 555-60.

51. Jobe, A.H. and E. Bancalari, *Bronchopulmonary dysplasia.* Am J Respir Crit Care Med, 2001. **163**(7): p. 1723-9.

52. Jobe, A.H. and M. Ikegami, *Mechanisms initiating lung injury in the preterm.* Early Hum Dev, 1998. **53**(1): p. 81-94.

53. Jobe, A.H. and M. Ikegami, *Antenatal infection/inflammation and postnatal lung maturation and injury.* Respir Res, 2001. **2**(1): p. 27-32.

54. Thomson, M.A., *Continuous positive airway pressure and surfactant; combined data from animal experiments and clinical trials.* Biol Neonate, 2002. **81 Suppl 1**: p. 16-9.

55. Luyet, C., P.H. Burri, and J.C. Schittny, *Suppression of cell proliferation and programmed cell death by dexamethasone during postnatal lung development.* Am J Physiol Lung Cell Mol Physiol, 2002. **282**(3): p. L477-83.

56. Compernolle, V., et al., *Loss of HIF-2alpha and inhibition of VEGF impair fetal lung maturation, whereas treatment with VEGF prevents fatal respiratory distress in premature mice.* Nat Med, 2002. **8**(7): p. 702-10.

57. Thebaud, B., et al., *Vascular endothelial growth factor gene therapy increases survival, promotes lung angiogenesis, and prevents alveolar damage in hyperoxia-induced lung injury: evidence that angiogenesis participates in alveolarization.* Circulation, 2005. **112**(16): p. 2477-86.

58. Massaro, G.D., et al., *Postnatal development of lung alveoli: suppression by 13% O2 and a critical period.* Am J Physiol, 1990. **258**(6 Pt 1): p. L321-7.

59. Randell, S.H., R.R. Mercer, and S.L. Young, *Neonatal hyperoxia alters the pulmonary alveolar and capillary structure of 40-day-old rats.* Am J Pathol, 1990. **136**(6): p. 1259-66.

60. Maniscalco, W.M., et al., *Hyperoxic injury decreases alveolar epithelial cell expression of vascular endothelial growth factor (VEGF) in neonatal rabbit lung.* Am J Respir Cell Mol Biol, 1997. **16**(5): p. 557-67.

61. Roberts, R.J., K.M. Weesner, and J.R. Bucher, *Oxygen-induced alterations in lung vascular development in the newborn rat.* Pediatr Res, 1983. **17**(5): p. 368-75.

62. Comhair, S.A. and S.C. Erzurum, *Antioxidant responses to oxidant-mediated lung diseases.* Am J Physiol Lung Cell Mol Physiol, 2002. **283**(2): p. L246-55.

63. Halliwell, B. and J.M. Gutteridge, *Role of free radicals and catalytic metal ions in human disease: an overview.* Methods Enzymol, 1990. **186**: p. 1-85.

64. Horowitz, S., et al., *Changes in gene expression in hyperoxia-induced neonatal lung injury.* Am J Physiol, 1990. **258**(2 Pt 1): p. L107-11.

65. Rozycki, H.J., P.G. Comber, and T.F. Huff, *Cytokines and oxygen radicals after hyperoxia in preterm and term alveolar macrophages.* Am J Physiol Lung Cell Mol Physiol, 2002. **282**(6): p. L1222-8.

66. Klekamp, J.G., K. Jarzecka, and E.A. Perkett, *Exposure to hyperoxia decreases the expression of vascular endothelial growth factor and its receptors in adult rat lungs.* Am J Pathol, 1999. **154**(3): p. 823-31.

67. Lassus, P., et al., *Pulmonary vascular endothelial growth factor and Flt-1 in fetuses, in acute and chronic lung disease, and in persistent pulmonary hypertension of the newborn.* Am J Respir Crit Care Med, 2001. **164**(10 Pt 1): p. 1981-7.

68. Thibeault, D.W., S. Mabry, and M. Rezaiekhaligh, *Neonatal pulmonary oxygen toxicity in the rat and lung changes with aging.* Pediatr Pulmonol, 1990. **9**(2): p. 96-108.

69. Bucher, J.R. and R.J. Roberts, *The development of the newborn rat lung in hyperoxia: a dose-response study of lung growth, maturation, and changes in antioxidant enzyme activities.* Pediatr Res, 1981. **15**(7): p. 999-1008.

70. Han, R.N., et al., *Changes in structure, mechanics, and insulin-like growth factor-related gene expression in the lungs of newborn rats exposed to air or 60% oxygen.* Pediatr Res, 1996. **39**(6): p. 921-9.

71. Wood, M.W., F. J. Seidler, and T. A. Slotkin., *Immediate decline in DNA synthesis in neonatal rat lung caused by exposure to 100% oxygen.* Res Commun Chem Pathol Pharmacol, 1993. **80**: p. 323-328.

72. McGrath-Morrow, S.A. and J. Stahl, *Apoptosis in neonatal murine lung exposed to hyperoxia.* Am J Respir Cell Mol Biol, 2001. **25**(2): p. 150-5.

73. Boros, V., et al., *Leukotrienes are indicated as mediators of hyperoxia-inhibited alveolarization in newborn rats.* Am J Physiol, 1997. **272**(3 Pt 1): p. L433-41.

74. Clark, J.M. and C.J. Lambertsen, *Pulmonary oxygen toxicity: a review.* Pharmacol Rev, 1971. **23**(2): p. 37-133.

75. Deng, H., S.N. Mason, and R.L. Auten, Jr., *Lung inflammation in hyperoxia can be prevented by antichemokine treatment in newborn rats.* Am J Respir Crit Care Med, 2000. **162**(6): p. 2316-23.

76. Tanswell, A.K. and B.A. Freeman, *Pulmonary antioxidant enzyme maturation in the fetal and neonatal rat. I. Developmental profiles.* Pediatr Res, 1984. **18**(7): p. 584-7.

77. Massaro, D. and G.D. Massaro, *Dexamethasone accelerates postnatal alveolar wall thinning and alters wall composition.* Am J Physiol, 1986. **251**(2 Pt 2): p. R218-24.

78. Massaro, D., et al., *Postnatal development of alveoli. Regulation and evidence for a critical period in rats.* J Clin Invest, 1985. **76**(4): p. 1297-305.

79. Massaro, D. and G.D. Massaro, *Invited Review: pulmonary alveoli: formation, the "call for oxygen," and other regulators.* Am J Physiol Lung Cell Mol Physiol, 2002. **282**(3): p. L345-58.

80. Massaro, G., et al., *Lung alveoli: endogenous programmed destruction and regeneration.* Am J Physiol Lung Cell Mol Physiol, 2002. **283**(2): p. L305-9.

81. Massaro, G.D. and D. Massaro, *Formation of alveoli in rats: postnatal effect of prenatal dexamethasone.* Am J Physiol, 1992. **263**(1 Pt 1): p. L37-41.

82. Massaro, G.D. and D. Massaro, *Postnatal lung growth: evidence that the gas-exchange region grows fastest at the periphery.* Am J Physiol, 1993. **265**(4 Pt 1): p. L319-22.

83. Funk, C.D., *Prostaglandins and leukotrienes: advances in eicosanoid biology.* Science, 2001. **294**(5548): p. 1871-5.

84. Leff, A.R., *Regulation of leukotrienes in the management of asthma: biology and clinical therapy.* Annu Rev Med, 2001. **52**: p. 1-14.

85. Leff, A.R., *Discovery of leukotrienes and development of antileukotriene agents.* Ann Allergy Asthma Immunol, 2001. **86**(6 Suppl 1): p. 4-8.

86. Woods, J.W., et al., *5-lipoxygenase and 5-lipoxygenase-activating protein are localized in the nuclear envelope of activated human leukocytes.* J Exp Med, 1993. **178**(6): p. 1935-46.

87. Samuelsson, B., *Leukotrienes: mediators of immediate hypersensitivity reactions and inflammation.* Science, 1983. **220**(4597): p. 568-75.

88. Yokomizo, T., T. Izumi, and T. Shimizu, *Leukotriene B4: metabolism and signal transduction.* Arch Biochem Biophys, 2001. **385**(2): p. 231-41.

89. Bisgaard, H., *Role of leukotrienes in asthma pathophysiology.* Pediatr Pulmonol, 2000. **30**(2): p. 166-76.

90. Ford-Hutchinson, A.W., *Leukotriene B4 in inflammation.* Crit Rev Immunol, 1990. **10**(1): p. 1-12.

91. Yokomizo, T., et al., *A second leukotriene B(4) receptor, BLT2. A new therapeutic target in inflammation and immunological disorders.* J Exp Med, 2000. **192**(3): p. 421-32.

92. Yokomizo, T., et al., *Leukotriene B4 receptor. Cloning and intracellular signaling.* Am J Respir Crit Care Med, 2000. **161**(2 Pt 2): p. S51-5.

93. Serhan, C.N. and S.M. Prescott, *The scent of a phagocyte: Advances on leukotriene b(4) receptors.* J Exp Med, 2000. **192**(3): p. F5-8.

94. Henderson, W.R., Jr., *Role of leukotrienes in asthma.* Ann Allergy, 1994. **72**(3): p. 272-8.

95. Heimburger, M. and J.E. Palmblad, *Effects of leukotriene C4 and D4, histamine and bradykinin on cytosolic calcium concentrations and adhesiveness of endothelial cells and neutrophils.* Clin Exp Immunol, 1996. **103**(3): p. 454-60.

96. Hosford, G.E., et al., *Hyperoxia increases protein mass of 5-lipoxygenase and its activating protein, flap, and leukotriene b(4) output in newborn rat lungs.* Exp Lung Res, 2002. **28**(8): p. 671-84.

97. Carter, B., et al., *gamma-glutamyl leukotrienase, a gamma-glutamyl transpeptidase gene family member, is expressed primarily in spleen.* J Biol Chem., 1998. **273**(43): p. 28277-85.

98. Orning, L. and S. Hammarstrom, *Inhibition of leukotriene C and leukotriene D biosynthesis.* J Biol Chem, 1980. **255**(17): p. 8023-6.

99. Drazen, J.M. and K.F. Austen, *Leukotrienes and airway responses.* Am Rev Respir Dis, 1987. **136**(4): p. 985-98.

100. Knickelbein, R.G., et al., *Hyperoxia enhances expression of gamma-glutamyl transpeptidase and increases protein S-glutathiolation in rat lung.* Am J Physiol., 1996. **270**: p. 115-122.

101. Laitinen, L.A., et al., *Leukotriene E4 and granulocytic infiltration into asthmatic airways.* Lancet, 1993. **341**(8851): p. 989-90.

102. Bouchelouche, K., et al., *Increased urinary leukotriene E4 and eosinophil protein X excretion in patients with interstitial cystitis.* J Urol, 2001. **166**(6): p. 2121-5.

103. Habib, G.M., et al., *Leukotriene D4 and cystinyl-bis-glycine metabolism in membrane-bound dipeptidase-deficient mice.* Proc Natl Acad Sci U S A, 1998. **95**(9): p. 4859-63.

104. Blain, J.F. and P. Sirois, *Involvement of LTD(4)in allergic pulmonary inflammation in mice: modulation by cysLT(1)antagonist MK-571.* Prostaglandins Leukot Essent Fatty Acids, 2000. **62**(6): p. 361-8.

105. Holgate, S.T., et al., *Roles of cysteinyl leukotrienes in airway inflammation, smooth muscle function, and remodeling.* J Allergy Clin Immunol, 2003. **111**(1 Suppl): p. S18-34; discussion S34-6.

106. Saegusa, S., H. Tsubone, and M. Kuwahara, *Leukotriene D(4)-induced Rho-mediated actin reorganization in human bronchial smooth muscle cells.* Eur J Pharmacol, 2001. **413**(2-3): p. 163-71.

107. Nicosia, S., et al., *Binding to cysteinyl-leukotriene receptors.* Am J Respir Crit Care Med, 2000. **161**(2 Pt 2): p. S46-50.

108. Back, M., *Functional characteristics of cysteinyl-leukotriene receptor subtypes.* Life Sci, 2002. **71**(6): p. 611-22.

109. Gorenne, I., X. Norel, and C. Brink, *Cysteinyl leukotriene receptors in the human lung: what's new?* Trends Pharmacol Sci, 1996. **17**(10): p. 342-5.

110. Heise, C.E., et al., *Characterization of the human cysteinyl leukotriene 2 receptor.* J Biol Chem, 2000. **275**(39): p. 30531-6.

111. Hui, Y. and C.D. Funk, *Cysteinyl leukotriene receptors.* Biochem Pharmacol, 2002. **64**(11): p. 1549-57.

112. Mancuso, P., P. Nana-Sinkam, and M. Peters-Golden, *Leukotriene B4 augments neutrophil phagocytosis of Klebsiella pneumoniae.* Infect Immun, 2001. **69**(4): p. 2011-6.

113. Norman, P., et al., *Characterisation of leukotriene receptors on rat lung strip.* Eur J Pharmacol, 1994. **271**(1): p. 73-8.

114. Sarau, H.M., et al., *Identification, molecular cloning, expression, and characterization of a cysteinyl leukotriene receptor.* Mol Pharmacol, 1999. **56**(3): p. 657-63.

115. Yokomizo, T., et al., *A G-protein-coupled receptor for leukotriene B4 that mediates chemotaxis.* Nature, 1997. **387**(6633): p. 620-4.

116. Huang, W.W., et al., *Molecular and biological characterization of the murine leukotriene B4 receptor expressed on eosinophils.* J Exp Med, 1998. **188**(6): p. 1063-74.

117. Devchand, P.R., et al., *The PPARalpha-leukotriene B4 pathway to inflammation control.* Nature, 1996. **384**(6604): p. 39-43.

118. Lynch, K.R., et al., *Characterization of the human cysteinyl leukotriene CysLT1 receptor.* Nature, 1999. **399**(6738): p. 789-93.

119. Parameswaran, K., et al., *Cysteinyl leukotrienes promote human airway smooth muscle migration.* Am J Respir Crit Care Med, 2002. **166**(5): p. 738-42.

120. Izumi, T., et al., *Leukotriene receptors: classification, gene expression, and signal transduction.* J Biochem (Tokyo), 2002. **132**(1): p. 1-6.

121. Ogasawara, H., et al., *Characterization of mouse cysteinyl leukotriene receptors mCysLT1 and mCysLT2: differential pharmacological properties and tissue distribution.* J Biol Chem, 2002. **277**(21): p. 18763-8.

122. Crooke, S.T., et al., *Signal transduction processes for the LTD4 receptor.* Adv Prostaglandin Thromboxane Leukot Res, 1990. **20**: p. 127-37.

123. Mong, S., et al., *Regulation of ligand binding to leukotriene D4 receptors: effects of cations and guanine nucleotides.* Eur J Pharmacol, 1984. **106**(2): p. 241-53.

124. Figueroa, D.J., et al., *Expression of the cysteinyl leukotriene 1 receptor in normal human lung and peripheral blood leukocytes.* Am J Respir Crit Care Med, 2001. **163**(1): p. 226-33.

125. Hoshino, M., T. Izumi, and T. Shimizu, *Leukotriene D4 activates mitogen-activated protein kinase through a protein kinase Calpha-Raf-1-dependent pathway in human monocytic leukemia THP-1 cells.* J Biol Chem, 1998. **273**(9): p. 4878-82.

126. Luttrell, L.M., et al., *G-protein-coupled receptors and their regulation: activation of the MAP kinase signaling pathway by G-protein-coupled receptors.* Adv Second Messenger Phosphoprotein Res, 1997. **31**: p. 263-77.

127. Ohishi, H., et al., *Molecular dynamics simulation of 1,2-dilauroyl-L-phosphatidylethanolamine binding to phospholipase A2: an attempt to explain the selective hydrolysis of substrate fatty acid ester at position 2.* J Biochem (Tokyo), 1993. **114**(2): p. 210-4.

128. Maekawa, A., K.F. Austen, and Y. Kanaoka, *Targeted gene disruption reveals the role of cysteinyl leukotriene 1 receptor in the enhanced vascular permeability of mice undergoing acute inflammatory responses.* J Biol Chem, 2002. **277**(23): p. 20820-4.

129. Hui, Y., et al., *The murine cysteinyl leukotriene 2 (CysLT2) receptor: cDNA and genomic cloning, alternative splicing, and in vitro characterization.* J Biol Chem, 2001. **8**: p. 8.

130. James, A.J. and A.P. Sampson, *A Tale of Two CysLTs.* Clin Exp Allergy, 2001. **31**(11): p. 1660-4.

131. Patry, C., et al., *Leukotriene receptors in HL-60 cells differentiated into eosinophils, monocytes and neutrophils.* Prostaglandins Leukot Essent Fatty Acids, 1996. **54**(5): p. 361-70.

132. Takasaki, J., et al., *The molecular characterization and tissue distribution of the human cysteinyl leukotriene CysLT(2) receptor.* Biochem Biophys Res Commun, 2000. **274**(2): p. 316-22.

133. Gauvreau, G.M., et al., *Inhaled leukotriene e(4), but not leukotriene d(4), increased airway inflammatory cells in subjects with atopic asthma.* Am J Respir Crit Care Med, 2001. **164**(8): p. 1495-500.

134. Israel, E., et al., *Effect of treatment with zileuton, a 5-lipoxygenase inhibitor, in patients with asthma. A randomized controlled trial. Zileuton Clinical Trial Group.* Jama, 1996. **275**(12): p. 931-6.

135. Israel, E., et al., *The effect of inhibition of 5-lipoxygenase by zileuton in mild-to-moderate asthma.* Ann Intern Med, 1993. **119**(11): p. 1059-66.

136. Reiss, T.F., et al., *Montelukast, a once-daily leukotriene receptor antagonist, in the treatment of chronic asthma: a multicenter, randomized, double-blind trial. Montelukast Clinical Research Study Group.* Arch Intern Med, 1998. **158**(11): p. 1213-20.

137. Knorr, B., et al., *Montelukast for chronic asthma in 6- to 14-year-old children: a randomized, double-blind trial. Pediatric Montelukast Study Group.* Jama, 1998. **279**(15): p. 1181-6.

138. Sorkness, C.A., *Leukotriene receptor antagonists in the treatment of asthma.* Pharmacotherapy, 2001. **21**(3 Pt 2): p. 34S-37S.

139. Virchow, J.C., Jr., et al., *Effect of a specific cysteinyl leukotriene-receptor 1-antagonist (montelukast) on the transmigration of eosinophils across human umbilical vein endothelial cells.* Clin Exp Allergy, 2001. **31**(6): p. 836-44.

140. Manji, J.S., et al., *Timing of hyperoxic exposure during alveolarization influences damage mediated by leukotrienes.* Am J Physiol Lung Cell Mol Physiol, 2001. **281**(4): p. L799-806.

141. McGill, S., *Effects of leukotrienes on lung development.* Thesis, 2004.

142. Jouvencel, P., et al., *Montelukast does not protect against hyperoxia-induced inhibition of alveolarization in newborn rats.* Pediatr Pulmonol, 2003. **35**(6): p. 446-51.

143. Zhang, Y.Y., et al., *Expression of 5-lipoxygenase in pulmonary artery endothelial cells.* Biochem J, 2002. **361**(Pt 2): p. 267-76.

144. Jones, J.E., et al., *Effect of 5-lipoxygenase on the development of pulmonary hypertension in rats.* Am J Physiol Heart Circ Physiol, 2004. **286**(5): p. H1775-84.

145. Caironi, P., et al., *5-Lipoxygenase deficiency prevents respiratory failure during ventilator-induced lung injury.* Am J Respir Crit Care Med, 2005. **172**(3): p. 334-43.

146. Jackson, R., D. Chandler, and J. Fulmer, *Production of arachidonic acid metabolites by endothelial cells in hyperoxia.* J Appl Physiol., 1986. **61**(2): p. 584-591.

147. Sporn, P., T. Murphy, and M. Peters-Golden, *Complex effects of in vitro hyperoxia on alveolar macrophage arachidonic acid metabolism.* Am J Respir Cell Mol Biol, 1990. **2**(2): p. 81-90.

148. Coalson, J.J., et al., *Diffuse alveolar damage in the evolution of bronchopulmonary dysplasia in the baboon.* Pediatr Res, 1988. **24**(3): p. 357-66.

149. Bonikos, D.S., et al., *Oxygen toxicity in the newborn. The effect of prolonged 100 per cent O2 exposure on the lungs of newborn mice.* Lab Invest, 1975. **32**(5): p. 619-35.

150. Carmeliet, P., et al., *Role of HIF-1alpha in hypoxia-mediated apoptosis, cell proliferation and tumour angiogenesis.* Nature, 1998. **394**(6692): p. 485-90.

151. Bailie, M.B., et al., *Leukotriene-deficient mice manifest enhanced lethality from Klebsiella pneumonia in association with decreased alveolar macrophage phagocytic and bactericidal activities.* J Immunol, 1996. **157**(12): p. 5221-4.

152. Burghardt, J.S., et al., *Lipid mediators in oxygen-induced airway remodeling and hyperresponsiveness in newborn rats.* Am J Respir Crit Care Med, 1996. **154**(4 Pt 1): p. 837-42.

153. Burghardt, J.S. and University of Alberta. Dept. of Physiology., *Leukotrienes mediate hyperoxia-induced lung damage in newborn rats.* 1998. [17], 165 leaves.

154. Zeltner, T.B. and P.H. Burri, *The postnatal development and growth of the human lung. II. Morphology.* Respir Physiol, 1987. **67**(3): p. 269-82.

155. Kanaan, S.A., et al., *Intratracheal adenovirus-mediated gene transfer is optimal in experimental lung transplantation.* J Thorac Cardiovasc Surg, 2002. **124**(6): p. 1130-6.

156. Chicoine, L.G., et al., *Intratracheal adenoviral-mediated delivery of iNOS decreases pulmonary vasoconstrictor responses in rats.* J Appl Physiol, 2004. **97**(5): p. 1814-22.

157. Pozeg, Z.I., et al., *In vivo gene transfer of the O2-sensitive potassium channel Kv1.5 reduces pulmonary hypertension and restores hypoxic pulmonary vasoconstriction in chronically hypoxic rats.* Circulation, 2003. **107**(15): p. 2037-44.

158. Tong-Chuan, H., S. Zhou, L., Costa, J. Yu, K. Kinzler, and B. Vogelstein, *A simplified system for generating recombinant adenoviruses.* Proc Natl Acad Sci USA, 1998. **95**: p. 2509-2514.

159. Burri, P.H. and E.R. Weibel, *Morphometric estimation of pulmonary diffusion capacity. II. Effect of Po2 on the growing lung, adaption of the growing rat lung to hypoxia and hyperoxia.* Respir Physiol, 1971. **11**(2): p. 247-64.

160. Zeltner, T.B., et al., *Morphometric estimation of regional differences in the rat lung.* Exp Lung Res, 1990. **16**(2): p. 145-58.

161. Tschanz, S.A., A.N. Makanya, B. Haenni, and P.H. Burri., *Effects of neonatal high-dose short-term glucocorticoid treatment on the lung: a morphologic and morphometric study in the rat.* Pediatric Research, 2003. **53**(1): p. 72-80.

162. Pfaffl, M.W., *A new mathematical model for relative quantification in real-time RT-PCR.* Nucleic Acids Res, 2001. **29**(9): p. e45.

163. Burnette, W.N., *"Western blotting": electrophoretic transfer of proteins from sodium dodecyl sulfate--polyacrylamide gels to unmodified nitrocellulose and*

radiographic detection with antibody and radioiodinated protein A. Anal Biochem, 1981. **112**(2): p. 195-203.

164. Cuperlovic-Culf, M., et al., *Microarray analysis of alternative splicing.* Omics, 2006. **10**(3): p. 344-57.

165. Paulding, W.R. and M.F. Czyzyk-Krzeska, *Hypoxia-induced regulation of mRNA stability.* Adv Exp Med Biol, 2000. **475**: p. 111-21.

166. Massaro, D. and G.D. Massaro, *Critical period for alveologenesis and early determinants of adult pulmonary disease.* Am J Physiol Lung Cell Mol Physiol, 2004. **287**(4): p. L715-7.

167. Kauffman, S.L., P.H. Burri, and E.R. Weibel, *The postnatal growth of the rat lung. II. Autoradiography.* Anat Rec, 1974. **180**(1): p. 63-76.

168. Zimmer, J., Voelker, D., Bernlohr, D., & Murphy, R., *Stabolization of leukotriene A4 by epithelial fatty acid binding protein in the rat basophilic leukemia cell.* J Biol Chem, 2004. **45**(11): p. 2138-2144.

169. Waszak, P., et al., *Effect of intratracheal adenoviral vector administration on lung development in newborn rats.* Hum Gene Ther, 2002. **13**(15): p. 1873-85.

170. Beyea, J.A., D.M. Olson, and S. Harvey, *Growth hormone expression in the perinatal and postnatal rat lung.* Dev Dyn, 2005. **232**(4): p. 1037-46.

171. Jayasankar, V., et al., *Targeted overexpression of growth hormone by adenoviral gene transfer preserves myocardial function and ventricular geometry in ischemic cardiomyopathy.* J Mol Cell Cardiol, 2004. **36**(4): p. 531-8.

172. Mastrangeli, A., et al., *Diversity of airway epithelial cell targets for in vivo recombinant adenovirus-mediated gene transfer.* J Clin Invest, 1993. **91**(1): p. 225-34.

173. Capra, V., et al., *CysLT1 receptor is a target for extracellular nucleotide-induced heterologous desensitization: a possible feedback mechanism in inflammation.* J Cell Sci, 2005. **118**(Pt 23): p. 5625-36.

174. Thompson, M.D., et al., *G-protein-coupled receptors and asthma endophenotypes: the cysteinyl leukotriene system in perspective.* Mol Diagn Ther, 2006. **10**(6): p. 353-66.

175. Joyce, B.J., et al., *Sustained changes in lung expansion alter tropoelastin mRNA levels and elastin content in fetal sheep lungs.* Am J Physiol Lung Cell Mol Physiol, 2003. **284**(4): p. L643-9.